Oscillatory Kinetics in Heterogeneous Catalysis

Ronald Imbihl and Gerhard Ertl*

Fritz-Haber-Institut der Max-Planck-Gesellschaft, Faradayweg 4-6, D-14195 Berlin (Dahlem), Germany

Received November 7, 1994 (Revised Manuscript Received March 9, 1995)

Contents

I. Introduction

Practically by definition, heterogeneous catalytic reactions represent systems far from thermodynamic equilibrium, and therefore one can observe in such systems rate oscillations, spatiotemporal patterns and chaos— a group of phenomena which has been denoted "dissipative structures" by Prigogine.[1] Although oscillatory kinetics in a heterogeneous chemical reaction system had been discovered quite early, namely by Fechner in 1828 in an electrochemical reaction,[2] it was only about 25 years ago that such phenomena were also found in heterogeneous catalysis by the group of Wicke, who observed rate oscillations in catalytic CO oxidation.[3,4] Since then, oscillatory surface reactions have developed into a field of very active research, while in the years before, studies of oscillating chemical reactions almost exclusively concentrated on the famous Belousov–Zhabotinskii reaction.[5]

After the discovery of rate oscillations in catalytic CO oxidation, numerous theoretical models were suggested to explain the origin of the kinetic instabilities, but it was soon realized that in situ investigations with surface sensitive techniques were required in order to verify the proposed mechanisms.[6] For this reason, experiments with single crystal surfaces were started, leading to experimentally verified mechanisms on the basis of which mathematical models could be formulated.[7,8] Due to this development, one can essentially distinguish between two types of experimental studies: experiments with polycrystalline catalysts conducted under nonisothermal high pressure conditions ($p > 1$ mbar), and single crystal experiments carried out under isothermal low pressure conditions ($p < 10^{-3}$ mbar).

While initially, the focus had almost entirely been on the phenomenology and on the mechanism which is responsible for the oscillatory behavior, with the development of spatially resolving techniques, the various aspects of spatiotemporal self-organization became the dominating theme.[9] A fascinating variety of different dynamical patterns were discovered in reactions on single crystal surfaces.[8–10] If compared with pattern formation in homogeneous systems, the surface studies introduced two principally new aspects, which are anisotropic diffusion, and the possibility of global synchronization via the gas phase. A third new aspect was opened up by the application of field electron and field ion microscopy to the study of oscillatory surface reactions, since these investigations demonstrated the capability of obtaining images with near-atomic resolution.[11,12]

The idea, which naturally followed these successful studies, was to control spatiotemporal pattern formation by using prepatterned surfaces. First experiments with lithograhic techniques have demonstrated that such an approach can be successful, and one can perhaps anticipate that further progress in this field may even lead to an improvement of the yield and selectivity of catalytic reactions.[13] Such attempts at exploiting the nonlinear characteristics of the kinetics have already been made, albeit with limited success, by periodically modulating the control parameters of the reaction.[14–17]

Following the first papers summarizing experimental reports of oscillatory catalytic reactions by Sheintuch and Schmitz in 1977, and by Slinko and Slinko in 1978, there have already been numerous reviews on oscillatory catalytic reactions.[6–10,18–23] In a paper focusing entirely on catalytic CO oxidation, Razon and Schmitz summarized the experimental and theoretical work of the high-pressure studies on this reaction.[6] A rather broad overview of the high-pressure studies, the theoretical modeling, as well as

0009-2665/95/0795-0697$15.50/0

Ronald Imbihl was born in Schwabmünchen, Germany, in 1953 and studied Chemistry at the Universität München where he received his Dr. degree in 1984. From 1984 to 1986 he worked as a postdoctoral fellow at the IBM research laboratory in Yorktown Heights, and subsequently he joined the Fritz Haber Institut in Berlin as a research associate. He received his Habilitation in Physical Chemistry from the Freie Universität Berlin in 1990, and in 1994 he was appointed as Professor of Physical Chemistry by the Universität Hannover. His research activities concentrate on experimental and theoretical studies of phenomena of nonlinear dynamics associated with reactions at well-defined surfaces.

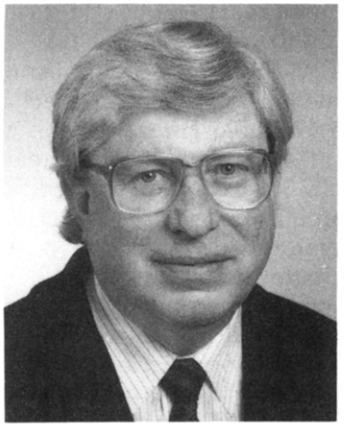

Gerhard Ertl was born in Stuttgart, Germany, in 1936 and received his Dr. degree in 1965 from the Technische Universität München, where, in 1967, he also became a Lecturer in Physical Chemistry. He served as Professor of Physical Chemistry at the Universities of Hannover (1968–1973) and München (1973–1986), and in 1986 he moved to Berlin where he was appointed as Director at the Fritz Haber Institute of the Max Planck Society as well as Honorary Professor at the Freie Universität and at the Technische Universität. His honors include the Japan Prize, the Hewlett Packard Europhysics Prize, the Leibniz Prize, the Emmett Award, as well as the Liebig, Bunsen, Gauss, and Mittasch Medals. He is a member of a number of societies and professional organizations, among them the American Academy of Arts and Sciences and the German Academy of Sciences "Leopoldina". His research interests cover various aspects of the chemistry and physics of solid surfaces, including the structure and dynamics on the atomic scale, phenomena of self-organization, as well as heterogeneous catalysis and electrochemistry.

the single crystal experiments, is given by Schüth et al.[19] A recently published review by Slinko and Jaeger also comprises the results of high-pressure and single crystal experiments.[18] The results of the single crystal experiments can be found in review papers by the authors of this report.[7,8,22] Finally, there have been two reviews dealing with the special topics of chaotic behavior and spatiotemporal self-organization.[10,23]

The purpose of the present paper is not to give a full account of all the experimental and theoretical work on oscillatory surface reactions, but to demonstrate the main lines in the development of the whole field. The paper is organized such that first the phenomenology and the mechanisms which give rise to oscillations are presented before the more complicated aspects of spatiotemporal self-organization and chaotic dynamics are discussed.

II. Observation of Rate Oscillations

A. Survey of Oscillatory Reactions

In their review paper, Schüth et al. list about 23 heterogeneously catalyzed reactions for which oscillatory behavior has been reported.[19] In Table 1, these reactions have been put into six different groups, which are then distinguished further by the type of catalyst, whether polycrystalline (poly) or single crystal (SC) catalysts were used, and by the pressure range in which the studies were conducted. By far the most extensively studied reaction is CO oxidation, which is catalyzed by group VIII noble metals and by some oxides such as CuO. Oscillations were also found in a number of other important oxidation reactions with O_2, i.e. in reactions with H_2, NH_3, hydrocarbons, methanol, and ethanol. Another large group of reactions in which rate oscillations occur is the catalytic reduction of NO with either CO, H_2, or NH_3 as reducing agent. These reactions, which are again catalyzed by noble metals group VIII are of particular importance in reducing air pollution.

While most of the above-mentioned reactions take place in the automotive catalytic converter, and involve oxidation reactions with O_2 or NO as oxidants, rate oscillations may also occur in reactions without oxygen, e.g. in hydrogenation reactions.[163–170] Rate oscillations have been observed in the reaction of CO with H_2 in the so-called Fischer–Tropsch synthesis and in the hydrogenation of ethylene and nitrobenzene ($PhNO_2$). Apart from the exothermic reactions listed in Table 1, there is also one example of an endothermic reaction exhibiting thermokinetic oscillations, namely the decomposition of methylamine (CH_3NH_2), on hot Ir, Pt, and Rh wires.[171,172] Finally, with the introduction of field electron microscopy (FEM) and field ion microscopy (FIM) as new tools for the study of oscillatory surface reactions, a new type of oscillatory behavior was found, in which oscillations may arise solely due to strong electric field gradients, without any net chemical reaction occurring. This type of field-induced oscillation occurred when a Pt tip was exposed to an environment of H_2 and H_2O.[173]

Studies of oscillatory reactions have been conducted with practically all types of catalysts, covering a pressure range from 10^{-9} mbar to atmospheric pressure. In what has been summarized as "polycrystalline" in Table 1, metallic catalysts have been used in the form of foils, ribbons, wires, evaporated films, and supported catalysts, with SiO_2 or Al_2O_3 being the support material in most cases. In some studies of rate oscillations in CO oxidation and methanol oxidation, Pd particles embedded in a zeolite matrix were used as catalyst.[27,28] This type of catalyst exhibits as a unique property, a very narrow size distribution of the metal particles.

Table 1. Oscillatory Reactions in Heterogeneous Catalysis

reaction	catalyst	catalyst type	orientation	p-range [mbar]
		CO Oxidation		
$CO + O_2$	Ir,[24] Pd[24-29]	poly		mbar to atm[a]
	Pt,[30-43] Rh[44,45]	poly		mbar to atm
	CuO[46]	poly		mbar to atm
	Pd	SC[b]	(110),[47-54] (111)[55]	10^{-3}–1
	Pt	SC	(100),[56-72] (110)[13,73-93]	10^{-5}–10^{-3}
	Pt	SC	(210)[94,95]	10^{-4}–10^{-1}
	Pt	SC[c]	[001] zone[96,97]	10^{-6}–10^{-4}
	Pt	SC	(111), (1311)[98]	atm
	Pt	SC	FET[d12,99,100]	10^{-6}–10^{-4}
		Other Oxidation Reactions with O_2		
$H_2 + O_2$	Ni,[101-104] Pd[105]	poly		atm
	Pt,[106-108] Rh[109]	poly		atm
	Pt	SC	FET[110,111]	10^{-4}
$NH_3 + O_2$	Pt[112-114]	poly		mbar to atm
$C_nH_m + O_2$	Ag,[115,116] Pd,[117] Pt[118-120]	poly		atm
	Rh,[44] CuO,[121]	poly		atm
	zeolites[122]	poly		atm
oxidative CH_4 coupling	La_2O_3–BaO–MgO[123]	poly		atm
$C_nH_mOH + O_2$	Pd,[124-126] Pt[127]	poly		atm
	V_2O_5,[128] zeolites[129]	poly		atm
		NO Reduction		
NO + CO	Pd,[42] Pt[42,130]	poly		10^{-4} to atm
	Pt	SC	(100),[131-143] [001] zone[136,144]	10^{-9}–10^{-5}
	Rh	SC	(110)[145]	10^{-6}
$NO + H_2$	Pt	SC	(100),[146-151] FET[152]	10^{-7}–10^{-5}
	Rh	SC	(110),[153,154] FET[11,155]	10^{-7}–10^{-5}
$NO + NH_3$	Pt[156,157]	poly		1 to atm
	Pt	SC	(100)[151,158-160]	10^{-6}
	Rh	SC	FET[11,155,161]	10^{-6}
NO + propene	Pt[162]	poly		atm
		Hydrogenation		
$CO + H_2$	Fe,[163,164] Pd[165]	poly		atm
$C_2H_4 + H_2$	Ni,[166] Pd,[167] Pt[168]	poly		atm
$PhNO_2 + H_2$	Cu,[169] Ni[169]	poly		atm
methanol to gasoline conversion	zeolite[170]	poly		atm
		Decomposition Reactions		
CH_3NH_2	Ir,[171] Pt,[171,172] Rh[171]	poly		1 to atm
		Field-Induced Reactions		
$H_2 + H_2O$	Pt	SC	FET[173]	10^{-6}

[a] Atmospheric pressure. [b] Single crystal. [c] Cylindrical Pt single crystal with axis parallel to [001]. [d] Field emitter tip.

With few exceptions, all of the above-mentioned experiments with polycrystalline material have been performed in the millibar to atmospheric pressure range. The reaction is therefore typically nonisothermal, and the rate oscillations are accompanied by temperature variations which usually comprise amplitudes between 1 and several ten degrees, and in extreme cases may reach several hundred degrees.[42,45,171] In a large number of studies, the reactor type which has been used can be described as a continuously stirred tank reactor (CSTR), i.e. in the ideal case, perfect mixing ensures that the concentration is everywhere the same. In the majority of the high-pressure studies, however, a concentration profile exists along the reactor, which means that the system represents a plug–flow reactor. With these premises, it is evident that heat and mass transfer limitations play an important role and that these factors have to be taken into account properly in an analysis of the experimental data.

Single crystal studies of oscillatory reactions have been almost exclusively conducted with only two types of reaction systems: catalytic CO oxidation on Pt and Pd surfaces, and catalytic NO reduction with CO, H_2 and NH_3 as reducing agent on Pt(100) and Rh(110). Experiments, in which several orientations of a metal catalyst are simultaneously exposed to the reacting gases, and where the behavior of the individual orientations was followed, have been conducted using a Pt single crystal of cylindrical shape (axis parallel to [001]),[96,97] and with a polycrystalline Pt foil.[174,175] In a new type of experiment, in which field emitter tips (FET's) were employed as catalysts, all orientations were simultaneously present on the tip surface.[11,12] By using field electron (FEM) and field ion microscopy (FIM), oscillatory reactions could be followed with near-atomic resolution. These FET studies comprise catalytic CO oxidation and the $H_2 + O_2$ reaction on Pt, and the reduction of NO with H_2 and NH_3 on Pt and Rh surfaces.

Almost all single crystal experiments have been carried out in a pressure range extending from 10^{-6} to 10^{-3} mbar, using UHV systems as a continuous flow reactor. The analysis of these experiments becomes appreciably simplified, since the reaction is practically isothermal under these conditions and since the molecular flow conditions eliminate concentration gradients rapidly in the UHV system. There exist only a few experiments, with catalytic CO oxidation on Pt(210) and Pd(110), where these

low-pressure experiments were extended up to ~1 mbar,[47,94] and there is in fact only one study in which single crystal experiments have also been conducted at atmospheric pressure.[98]

B. Experimental Techniques

1. Spatially Nonresolving Techniques

Under high-pressure conditions, only a few in situ techniques are available that allow one to monitor the state of the surface during rate oscillations. In most of these studies, only the oscillatory variations in the reaction rate were followed, either directly, via partial pressure measurements with a differentially pumped mass spectrometer, or via gas chromatography, or indirectly, by measuring the temperature variations caused by the exothermicity of the reaction, with a thermocouple or via the blackbody radiation.[176]

Changes in the adsorbate coverages can be detected by measuring the work function ($\Delta\varphi$) with a Kelvin probe. This method is nondestructive and highly sensitive (resolution $\approx$ 1 meV), but rather unspecific to the nature of the adsorbate.[59] Fourier transform infrared spectroscopy (FTIR) has frequently been applied in high-pressure studies because molecular adsorbates such CO or NO are easy to identify through characteristic vibrational losses, but on the other hand, the wavelength region for atomic adsorbates is typically obscured by experimental limitations. A method that has been introduced just recently to detect oscillatory changes in the state of the catalyst itself during rate oscillations on a supported Pt catalyst, is in situ X-ray diffractometry.[43] In that case the application of the method revealed that the catalyst undergoes a periodic oxidation and reduction in CO + O_2. Finally, there exist a number of other techniques which have been used only rarely, like ellipsometry[104] or solid state potentiometry.[119] The latter technique has been introduced by Vayenas et al. to monitor directly the activity of oxygen in the electrochemical oxidation of CO on the Pt electrode of a solid-state electrolyte.

Under the low-pressure conditions of the single crystal experiments, a number of powerful in situ techniques exist, but here also due to the destructive interaction of high-energy electrons with sensitive adsorbates, the use of techniques like auger electron spectroscopy is in general not feasible. At lower energies, however, the electrons interfere less destructively with adsorbates and this allows one to use low-energy electron diffraction (LEED) as an in situ technique to monitor structural changes of the catalyst surface during rate oscillations. The structural information one thus obtains was essential for clarifying the mechanism of the rate oscillations in catalytic CO oxidation on Pt single crystal surfaces.[59,75,95]

The potential of X-ray photoelectron spectroscopy (XPS), as an ex situ method to identify different states of atomic oxygen on the catalyst, has been demonstrated by Savchenko et al. with the system Pt(110)/CO + O_2.[80] Recently the range of in situ techniques for single crystal studies of rate oscillations has been expanded by the use of FTIR for Pt(100)/NO + CO[177] and Pt(210)/CO + O_2.[178]

2. Spatially Resolving Techniques

Usually all oscillatory reactions are accompanied by spatiotemporal pattern formation and, in order to make these patterns visible, different spatially resolving techniques have been developed for high- and for low-pressure studies. At high pressure (p > 1 mbar), when the reaction is nonisothermal, infrared thermography is a convenient way to image the heat/concentration wave patterns, with a temperature resolution of ~1 K and a spatial resolution of ~100 μm.[179] In the low-pressure experiments conducted with bulk single crystals, this technique is no longer feasible due to the isothermal reaction conditions, but here a number of different techniques have been developed covering different length scales, from macroscopic patterns to near atomic resolution.

In the first spatially resolved single crystal studies, the propagation of chemical waves in the system Pt(100)/CO + O_2 was detected by simply deflecting a LEED beam across the surface with a pair of Helmholtz coils and measuring the intensity variations of the diffraction spots.[57,59] The temporal and spatial resolution (~0.5 mm) of this method was of course rather limited, and scanning LEED was soon replaced by the technique which is commonly used today and which is known as photoemission electron microscopy (PEEM).[180] This technique had already been developed in the 1930, but it was almost forgotten in surface science until it found a renaissance with oscillatory surface reactions.

PEEM is based upon the principle that the yield of photoelectrons depends sensitively on the local work function, if one illuminates the sample with photons whose energy is just above the threshold for the excitation of photoelectrons. By imaging the lateral distribution of ejected photoelectrons, one thus obtains a picture of the locally varying work function. In the version which is in use today, and which was developed by W. Engel of the FHI, the PEEM instrument yields a typical spatial resolution of about 0.2 μm.[180]

A technique which in some respects is similar to the PEEM, but employs a LEED spot to image the surface, is the low-energy electron microscope (LEEM), developed by Bauer and Telieps.[181,182] The advantage of this technique is a higher resolution of ~100−1000 Å and its sensitivity to the surface structure and surface topography. A related technique that images the local work function variation, similar to PEEM, but with a higher resolution and a different contrast mechanism, is mirror electron microscopy (MEM).[69,70] All of these techniques have been applied as in situ methods to study details in the front propagation of chemical waves in Pt(100)/CO + O_2.[69-72] Of the different microscopic techniques, one should also mention reflection electron microscopy (REM). This technique has been used as an ex situ method to study reaction-induced substrate changes, which occur during oscillatory reactions on small Pt single crystal spheres (diameter ~0.2 mm).[183-185]

All of the above-mentioned techniques image structures that are still macroscopic, i.e. the length scale is of the order of micrometers and larger. The

introduction of field electron microscopy (FEM) and field ion microscopy (FIM), as in situ methods, enabled the study of oscillatory surface reactions on a microscopic level.[11,12] The resolution reaches ~10–20 Å in these experiments, but there are also a number of complications, as will be pointed out in more detail in section VI.E. Mainly due to limited temporal resolution, scanning tunneling microscopy (STM), has so far not been used as an in situ method to investigate oscillatory reactions. STM has only been applied "ex situ", to demonstrate reaction-induced substrate changes in catalytic CO oxidation on Pt(210).[186]

III. Mathematical Modeling

A. General Background

The formation of structures which are ordered in space and/or time, seems at first sight to be at variance with the second law of thermodynamics, stating that all spontaneous processes have to be associated with an increase in entropy. This contradiction is of course only apparent, since the above statement only applies to isolated systems, whereas kinetic oscillations and chemical waves occur in open systems, where a constant flow of energy and/or matter keeps the system far away from thermodynamic equilibrium.[1] It turned out that thermodynamic considerations are quite generally of little predictive power as one attempts to describe mathematically these dissipative structures but, instead, one has to analyze the kinetic equations which control the situation far away from thermodynamic equilibrium.

Chemical oscillators are just one subset of a huge and widespread field termed nonlinear dynamics, which comprises dissipative structures in physical and chemical systems, and which also contains the science of chaos and turbulence.[1,187–191] The name "nonlinear dynamics" already expresses the common origin of all these phenomena, which is that the underlying equations have to be nonlinear. In the chemical systems which are of interest here, the corresponding mathematical models have to be formulated as reaction–diffusion (RD) equations of the general form:

$$\frac{\partial c_i}{\partial t} = F_i(\lambda,\mathbf{c}) + D_i\frac{\partial^2 c_i}{\partial x^2}$$

In this equation $\mathbf{c}$ is a vector standing for the concentrations of the various chemical species and λ denotes a set of parameters such as temperature, pressure, etc. The kinetics of species i are contained in the term F_i, while the diffusion is treated in the usual Laplacian form in the second term, with D_i representing the diffusion coefficient. Very often one can simplify the situation by assuming spatial homogeneity. Then the second term vanishes, and the system of partial differential equations (PDE's) reduces to ordinary differential equations (ODE's):

$$\frac{dc_i}{dt} = F_i(\lambda,\mathbf{c})$$

If the right-hand side does not explicitly depend on time, the system is called autonomous, but of course one may easily generate nonautonomous behavior, e.g. by periodically modulating one of the parameters. For analyzing, in a systematic way, the possible solutions of equations of the type described above, one uses a mathematical tool called bifurcation theory. The term bifurcation just means a qualitative change in the behavior of the system as one varies one parameter such as, for example, a change from a stable steady state to oscillatory behavior, or a change from mono- to bistability. The theoretical background of this method and examples for practical applications can be found in many textbooks, and therefore, in the following, only a brief sketch of the main idea is given.[187–191]

Any realistic system requires in principle a large number of variables for its full description, but due to a separation of time and length scales, only a few of these many degrees of freedom are really important for the dynamics of the system.[189,190] Sometimes, even only two variables are sufficient. Then the system, after passing through the period of transient behavior, can only be either in a stable steady state, or it may exhibit sustained oscillations. Complex dynamical behavior, such as mixed-mode oscillations or chaos, is, however, not possible in two dimensions. In two variables, only a small number of bifurcation types are possible, and the most frequent bifurcation type through which oscillations arise in a dynamical system, namely a Hopf bifurcation, is illustrated in Figure 1. In this bifurcation type, oscillations are generated as a stable steady-state becomes unstable upon changing a parameter. The trajectories which represent the dynamical behavior of the system in a so-called phase–space representation are no longer attracted by the fixed point which represents the steady-state solution. Instead the trajectories circulate around this point, such that a stable limit cycle is generated, i.e. the system now exhibits sustained oscillations.

As one increases the number of variables from two to three, complex dynamical behavior is possible, and one may observe mixed-mode oscillations and deterministic chaos.[188,190] In a phase–space representation, i.e. a representation in which time has been eliminated by plotting the state variables (here concentrations of chemical species or adsorbate coverages) against each other, mixed-mode oscillations are visualized by motion on a torus and deterministic chaos by motion on a so-called "strange attractor".

So far we have neglected the spatial degrees of freedom, but in any spatially extended system, spatial pattern formation will play a role leading to chemical waves and stationary concentration patterns, known as Turing structures.[192] These types of dissipative structures will be discussed further in section VI.D. in connection with the experimental results.

B. Modeling Surface Reactions

1. General Remarks

In order to construct a realistic model for an oscillatory surface reaction, one first has to identify

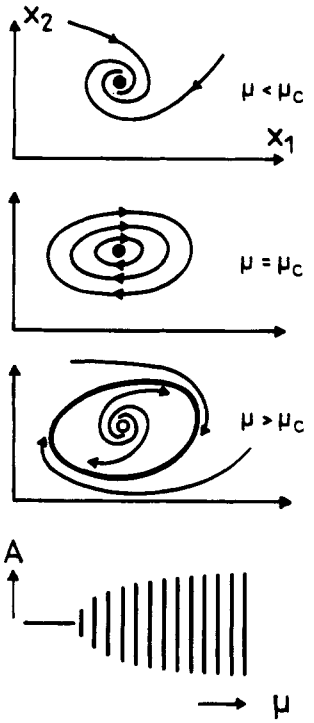

Figure 1. Development of a limit cycle in a so-called Hopf bifurcation as the bifurcation parameter is swept across the critical value μ_c at the bifurcation point. In the x_1,x_2 phase portraits, a stable steady state is represented by a filled circle; an unstable steady state by an open circle. Stable limit cycles ("kinetic oscillations") are indicated by bold lines. The experimentally observed behavior during a Hopf bifurcation is shown in the bottom part of the figure. The vertical lines denote here oscillation amplitudes of some signal *A*.

the relevant steps forming its mechanism. In the literature a large number of possible oscillation mechanisms have been proposed, but probably not more than a handful of these mathematical models can be regarded as representing a realistic situation.

Next, a suitable technique for modeling the surface reaction is required. If one wants to simulate the reaction on both a microscopic and a macroscopic level, then one is confronted with widely varying time and length scales, and there is no general concept on how these problems may be dealt with. A mean-field treatment with differential equations (DE's), neglects completely spatial correlations and fluctuations, but on the other hand, lattice–gas simulations based on a Monte Carlo algorithm or cellular automatons are strongly limited by the time and length scales these techniques can cover.[193-195] On the basis of a purely macroscopic description with DE's, there exist, of course, a number of mathematical models which often very nicely reproduce the experimental data, but on a more fundamental level the question of how to correctly model surface reactions is still unsolved.

The various mathematical models that have been developed to describe oscillatory surface reactions can be classified in different ways. One can first differentiate between general models, which do not refer to a particular experimental system, and realistic models. With respect to the experimental conditions, one can distinguish between pure surface reaction models, in which heat and mass transfer plays no role, and reactor models, which explicitly take into account the nonisothermality of the reaction and/or local or global variations in the educt partial pressures.[19] The latter arise due to mass balance in the reaction, and if the reactor is of the CSTR type no local pressure gradients exist, i.e. the pressure variations provide a global interaction. As will be discussed in more detail below, temperature and partial pressure variations are particularly important for understanding synchronization in oscillatory reactions, since the different local oscillators are coupled together via these variations.

Typically, mathematical models are formulated with ODE's, and only in cases when spatiotemporal pattern formation is considered are the ODE's extended to PDE's, by taking the spatial degrees of freedom into account. The underlying picture of a local oscillation mechanism might, however, be misleading, since in certain cases only the coupling of spatial nonuniformities may lead to oscillatory behavior, while the uncoupled systems display simple steady-state kinetics.[196,197]

2. Isothermal General Models

General models are important for classifying oscillation mechanisms, and practically all realistic models can be traced back to one or several types of these general mechanisms. General models have been reviewed in the papers by Schmidt et al.[19] and by Sheintuch,[198] and therefore, they are discussed here only briefly. One of the earliest models for obtaining kinetic oscillations in a surface reaction is that of a slow buffer step, which is not in equilibrium with the fast steps of the mechanism. Such a model was originally proposed by Eigenberger,[199] and as physical representations of this buffer step, one may consider the transition between various forms of oxygen with different reactivities in catalytic CO oxidation (the "oxide" model), or the conversion of a linear-bonded CO species into a bridge-bonded species.[200,201]

In a second class of oscillation schemes, coverage-dependent activation energies generate oscillatory behavior. This idea was introduced by Belyaev[101,202] and then further analyzed by Pikios and Luss,[203] Tambe et al.,[204] and Ivanov et al.[205] An interesting interpretation of these coverage-dependent activation energies was given by Pikios and Luss, who associated such a dependence with surface heterogeneity.[203] In general, coverage-dependent activation energies arise if energetic interactions between adparticles exist. This is practically always the case, but it remains to be shown whether the oscillations in any real system can in fact be traced back to such a mechanism.

A very simple scheme illustrating the main idea was proposed by Kevrekidis et al.[206] and then further studied by Vlachos et al.[207] They considered a unimolecular decomposition reaction of the form

$$A + * \rightleftarrows A_{ad}$$

$$A_{ad} \rightarrow P + Q + *$$

(An asterisk denotes a vacant adsorption site here and in all following equations.) Introducing attrac-

tive interactions between the adparticles leads to condensation, and a van der Waals-like loop in the adsorption isotherm is generated along which an oscillation cycle can proceed if, in addition, mass balance in the gas phase is taken into account, i.e. if a reactor model is used.

A third class of oscillation mechanism comprises the so-called vacancy models. A vacant site requirement may arise in a surface reaction, if either a decomposition step with more than a single product is involved or if a structural rearrangement of an adsorbed molecule has to precede the reaction step. Such a surface reaction step may, for example, be formulated as

$$A_{ad} + B_{ad} + 2^* \rightarrow P + 4^*$$

The increase in the number of vacant sites implies strongly autocatalytic behavior, which may cause oscillations.[208,209] In its general form vacancy models were introduced by Takoudis et al.,[208] and they are discussed here in more detail using the example of the NO reducing reactions on Pt(100) (see section V.B).

Finally, one should add that some of the realistic models that had been proposed for specific systems can easily be generalized. Such mechanisms are, for example, the island model for catalytic CO oxidation by Cutlip et al.,[210] suggesting that reaction only takes place at the perimeter of adsorbate islands, or the phase transition (reconstruction) model developed to describe oscillations in CO oxidation on Pt single crystal surfaces.[7,8]

For determining whether a proposed reaction scheme yields oscillatory solutions, one can always either directly integrate the DE's of the kinetic model, or more elegantly use bifurcation theory. For isothermal reaction models, however, a more general method exists called stoichiometric network analysis (SNA), which examines the feedback mechanism inherent in a chemical reaction scheme. This method was developed originally by Clarke to examine the stability of complex chemical reaction networks.[211] It was shown by Eiswirth et al.[212] that SNA is also applicable to oscillatory surface reaction models, if one translates surface phase transitions, subsurface oxygen formation etc. into a "chemical" language.

An important aspect with experimental observations concerns the role of heat and mass transfer, since these limitations alone might generate oscillatory behavior. For the isothermal reactions obeying a Langmuir–Hinshelwood scheme, the role of mass balance was investigated by Morton and Goodman.[213] They demonstrated that including mass balance can lead to oscillations in systems that exhibit merely bistability without mass balance. The amplitude of the oscillations was, however, rather small and the period of the oscillations was comparable to the residence time of the reactor. The problem of mass balance was also treated by several other authors, mostly in connection with heat transfer as will be outlined in the following section.

3. Nonisothermal Models

Due to the exponential dependence of rate constants on temperature, nonisothermal conditions can be expected to have a very strong influence on the dynamic properties of a catalytic reaction system and possibly generate oscillatory behavior. For example, oscillations in the decomposition of N_2O on CuO already reported in 1968[214] were demonstrated later to be solely generated by heat and mass transport limitations.

The influence of nonisothermal reaction conditions on reactions obeying an Eley–Rideal [ER], or a Langmuir–Hinshelwood (LH) scheme, was investigated by Dagonnier et al.[215] and by Sheintuch.[198] It was found that an ER mechanism stabilizes the system, whereas an LH scheme easily leads to oscillatory behavior. In addition, Sheintuch demonstrated, that nonisothermality leads to qualitatively new features in the dynamical behavior, such as quasiperiodicity and multiple peak time series.

A very simple model demonstrating the influence of spatial inhomogeneities of the catalyst surface on the dynamical behavior was analyzed by Ray and Hastings[216] and by Jensen and Ray.[217,218] They considered a catalytic reaction consisting of a single adsorption and reaction step:

$$A + * \rightarrow A_{ad}$$

$$A_{ad} \rightarrow P + *$$

and included mass and heat balance. It was shown that oscillations occurred on a porous catalyst surface described by the "fuzzy wire model", while a nonporous catalyst exhibited simple steady-state behavior.

In reaction schemes of the LH type, a simple mechanism for thermokinetic oscillations is possible, in which catalytic sites at low temperature are blocked by some species, A. These sites are then reactivated, as with increasing temperature, and either due to desorption or reaction, the blocking species is removed. Such blocking/reactivation schemes have been analyzed in general form,[198,215] and they have also been applied to specific oscillatory reactions; the NO + CO reaction on Pd,[25] the H_2 + O_2 reaction on Pt,[31] the methanol to gasoline process on a ZSM-5 zeolite catalyst,[170] and the hydrogenation of ethylene on Pt and Pd.[168]

An extensive theoretical treatment of nonisothermal oscillations can be found in the papers of Aluko and Chang,[219–221] who modeled the oscillations in catalytic CO oxidation on the basis of the oxide model developed originally by Sales, Turner, and Maple.[200] A methodology for a systematic analysis of the bifurcation types and multiplicity features one may encounter in nonisothermal reactions of the LH type is presented by Harold, Sheintuch, and Luss.[222–224] This analysis has been applied to catalytic CO oxidation on Pt/Al_2O_3 by the same authors.

A nonisothermal reaction which could be modeled very successfully with a thermokinetic blocking/reactivation scheme is the endothermic decomposition of methylamine on electrically heated Pt, Rh, and Ir wires.[171] The oscillation mechanism for this violent oscillator, displaying temperature amplitudes up to 500 K and frequencies up to 10 Hz, is very simple. In the reactive state, the temperature decreases due to the endothermic reaction, but in the inactive low-T state, when the surface is covered by some blocking

species, the temperature rises again by electric heating, leading to desorption of the blocking species.

4. Limitations of Mean-Field Treatment

In the formulation of surface reaction models with ODE's, it is implicitly assumed that the adparticles are uniformly distributed like in an ideal 2D gas. Such a mean-field treatment, is strictly justified if the mobility of the adparticles is infinitely high and if no repulsive or attractive interactions are operating.[193,375] For any realistic system, however, spatial correlations exist, and in order to take these into account, lattice–gas models have been formulated, which typically employ a Monte Carlo algorithm.[193] In the field of statistical physics, such lattice–gas models have found widespread interest, mainly because the kinetic transitions observed in these systems bear many analogies to phase transitions in classical thermodynamics. One of the most popular models of this type has been introduced by Ziff, Gulari, and Barshed to describe catalytic CO oxidation.[225]

Although simulations with lattice–gas models are in principle exact, such models suffer from the fact that, due to computational limitations, they have to use unrealistically low-surface mobilities. High-surface mobilities, on the other hand, tend to restore the validity of the mean-field equations. There is, however, a clear need to develop models which correctly take into account energetic interactions between the adparticles, and provide a valid microscopic picture. This need stems from the increased spatial resolution of in situ techniques, reaching near atomic level (~10 Å) in the FEM and FIM experiments.[11,12,100] Recently, there has been considerable progress in this direction. Starting from first principles, macroscopic equations have been derived, which in principle correctly take adsorbate–adsorbate interactions into account. These so-called kinetic lattice–gas models, have so far, however, only successfully been applied to simulate complicated thermal desorption spectra, while the application to systems far from equilibrium, still needs to be worked out.[194,195,226]

IV. Catalytic CO Oxidation

A. Reaction Scheme and Bistability

The catalytic effect of Pt wires on the reaction of CO with oxygen had already been observed by Faraday, and since then catalytic CO oxidation has been the subject of numerous papers including the "classical" work of Langmuir.[227,228] Meanwhile, it has been well established that the mechanism of this reaction follows a Langmuir–Hinshelwood scheme, described by the following three equations:[229]

$$CO + * \rightleftharpoons CO_{ad}$$

$$O_2 + 2* \rightarrow O_{ad}$$

$$O_{ad} + CO_{ad} \rightarrow CO_2 + 2*$$

Rate oscillations in catalytic CO oxidation were discovered in the group of Wicke,[3,4] who used a supported Pt catalyst. These early works were followed by numerous reports of oscillatory kinetics observed mostly in the atmospheric pressure range with Pt, Pd, and Ir catalysts, either in the form of wires, foils, ribbons, or in the form of supported catalysts and small metal particles (nanometer) embedded in a zeolite matrix.[6,19] Very different types of oscillations were found: sinusoidal or harmonic oscillations, relaxation-type oscillations involving different times scales, and chaotic behavior. Examples of these different types are displayed in Figure 2.

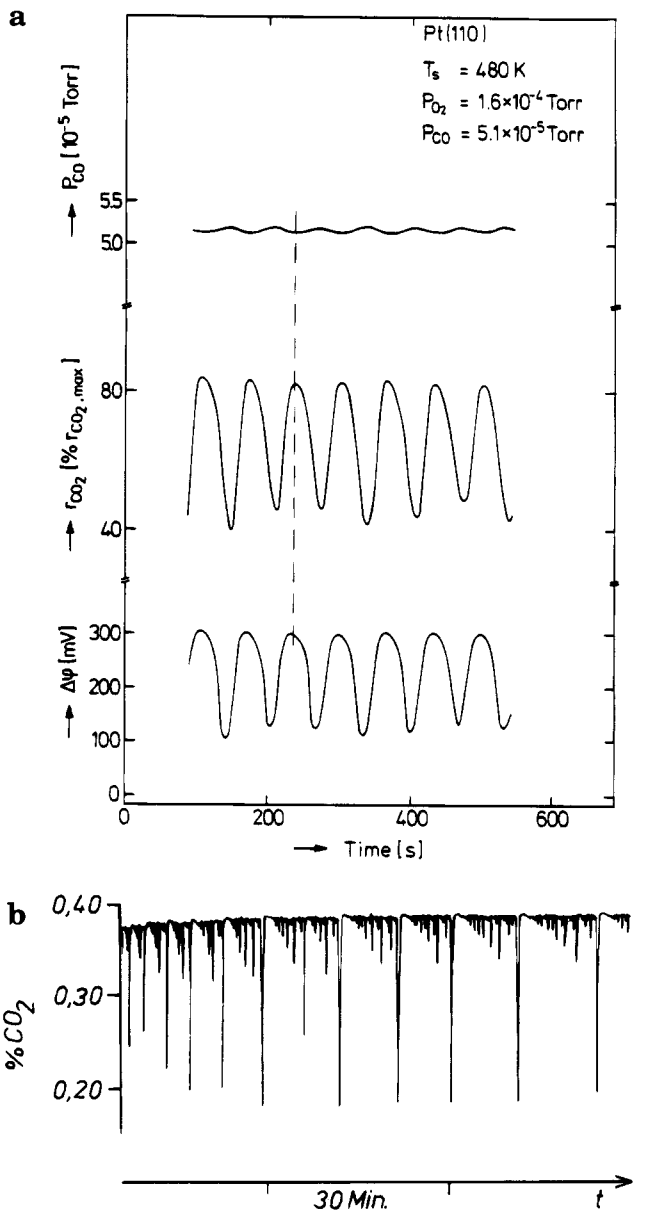

Figure 2. Some examples of different wave-forms of rate oscillations in catalytic CO oxidation: (a) kinetic oscillations in catalytic CO oxidation on Pt(110) measured via the variation of the CO_2 partial pressure p_{CO_2} and the work function variation $\Delta\varphi$ and (b) self-similar pattern observed in catalytic CO oxidation at atmospheric pressure and T = 453 K with a Pd/zeolite catalyst. (a: Reprinted from ref 78. Copyright 1990 American Institute of Physics. b: Reprinted from ref 28. Copyright 1986 Chemical Society of London.)

For determining the existence range for oscillations one typically only varies one or two parameters, corresponding to a cut through a multidimensional

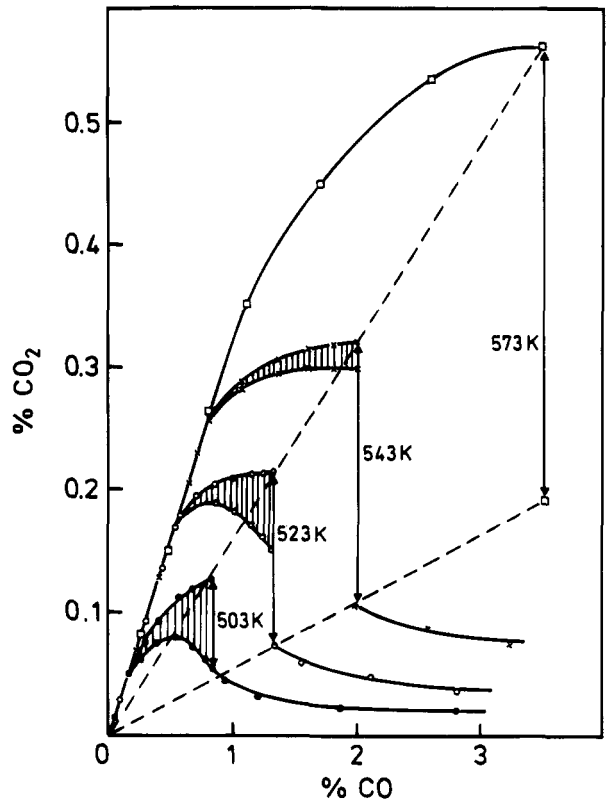

Figure 3. Bifurcation diagram showing the steady state behavior and the development of rate oscillations (hatched areas) at various temperatures in catalytic CO oxidation on a Pt/Al_2O_3, SiO_2 supported catalyst at atmospheric pressure. Shown is the CO_2 production rate while the CO partial pressure p_{CO} is varied as bifurcation parameter. (Reprinted from ref 31. Copyright 1980 VCH Publishers, Inc.)

parameter space. By plotting the steady states and the oscillation amplitude vs the parameter which is varied, one obtains so-called bifurcation diagrams, a typical example of which is shown in Figure 3. In this example, the transition from a steady-state to oscillatory behavior occurs continuously at the low p_{CO} side, and discontinuously at the high p_{CO} side.

Similar bifurcation diagrams have been found in almost all other high- and low-pressure studies of catalytic CO oxidation. The kinetics are characterized by two different branches: a high-rate branch at low p_{CO}, in which the CO_2 production at low p_{CO} rises linearly with p_{CO}, and a low-rate branch at high p_{CO}, in which the reaction rate decreases with increasing p_{CO}. The existence of the two rate branches can be traced back to an asymmetric inhibition of the reaction by the reactants.[7,8,229] With oxygen forming a very open adlayer structure, CO can still adsorb and react, while a fully CO covered surface completely inhibits the adsorption of oxygen and, hence, poisons the reaction.

Under conditions under which no oscillations occur, the existence of the two kinetic branches leads to hysteresis effects, i.e. one observes a clockwise hysteresis in the reaction rate upon variation of p_{CO}.[31,85,230] At high enough temperatures (T > 600 K for atmospheric pressure), the CO coverage does not reach the coverage necessary for complete inhibition of the reaction, and hence the range of bistability vanishes in a so-called cusp point. Multistability and hysteresis effects in catalytic CO oxidation have been observed both in high-, as well as in low-, pressure experiments with a Pt(111) surface.[31,231] The occurrence of multistability could be modeled quite successfully with a two-variable system derived from the above LH scheme.[85,230]

B. Rate Oscillations at High Pressure

While the LH scheme suffices to describe bistability, an additional mechanistic step is required in order to explain the rate oscillations, which typically occur in the vicinity of the rate maximum (see Figure 3). Since differing mechanisms are operating, the high-pressure experiments are discussed separately from the single crystal experiments. For the former, a large number of possible oscillation mechanisms have been suggested, which can be found listed in the review paper by Razon and Schmitz.[6] However, if merely hypothetical mechanisms are eliminated, only a small number of models remain: the oxide model introduced by Sales, Turner, and Maple,[200] the carbon model by Chabal et al.,[38,232] and finally the reconstruction (phase transition) model, which has been shown to be the valid mechanism for Pt single crystal surfaces at low pressure.[56,59,73,85]

In the oxide model, it is assumed that part of the active surface covered by chemisorbed oxygen is transformed into an inactive state, as oxide is formed. A slow reduction of the oxide by chemisorbed CO then leads back to the initial active state of a metallic surface. In contrast to the oxide model, the carbon model assumes a deactivation of the surface by carbon atoms. The source of the carbon atoms, however, is not clear and therefore the general applicability of this model remains doubtful.

The metals Pd and Ir, and (with reduced tendency) also Pt, form oxides at high p_{O_2} ($\geq$1 mbar). The time scale on which these oxides are reduced by CO was shown to be not too far from the period of the oscillations.[233] Therefore, these reduction experiments were considered as support for the validity of the oxide model. Direct confirmation of this mechanism was sought in in situ FTIR experiments.[34,35,232] These experiments, however, demonstrated essentially that the active state of the surface correlates with a low CO coverage and vice versa, in agreement with the well-known inhibition effect of adsorbed CO for catalytic CO oxidation.

Indirect evidence for the oxide model was obtained in solid-state potentiometry by Vayenas et al.,[234] who showed that the conditions under which rate oscillations occur coincide with those under which Pt oxide forms. A direct proof for the validity of the oxide model was provided only recently in in situ X-ray diffraction experiments with a supported Pt catalyst illustrated in Figure 4.[43] By applying a Debye function analysis to angular diffraction profiles measured at the two extrema, it was demonstrated that the X-ray intensity variations are caused by the formation and reduction of PtO and Pt_3O_4 reaching a maximum oxidation degree of ~20−30%.

The Pt particles in the above experiment only have an average diameter of ~10−15 Å, and small noble metal clusters are known to exhibit a higher tendency for oxidation than bulk material.[235] It therefore

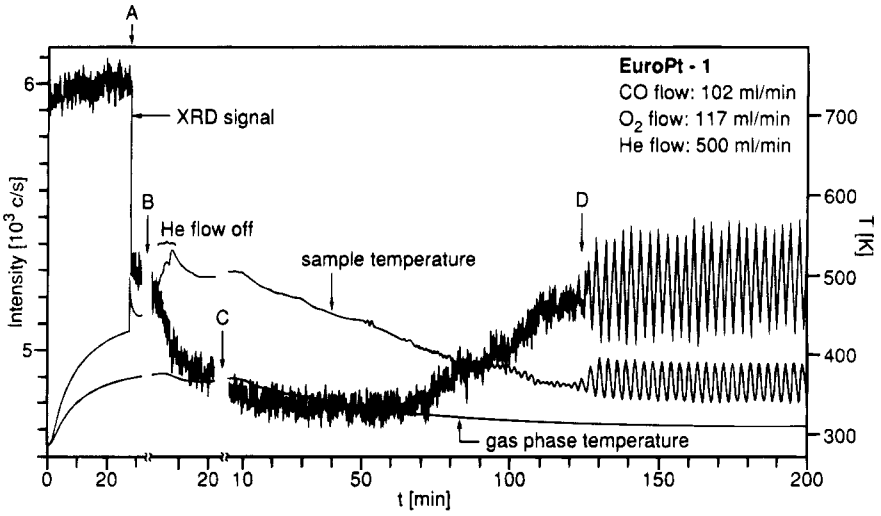

Figure 4. In situ X-ray diffraction (XRD) experiment showing that a periodic oxidation and reduction of Pt metal takes place during rate oscillations in catalytic CO oxidation on a supported Pt catalyst. The diagram shows the variations in the sample temperature which indicate the changes in catalytic activity, i.e. in the CO_2 production rate and the intensity variations of a Bragg peak of the metal catalyst. The diagram displays the whole experiment starting with the adjustment of the parameters which then leads to sustained rate oscillations. The experiment was conducted at atmospheric pressure. (Reprinted from ref 43. Copyright 1994 J. C. Baltzer AG.)

remains to be shown whether the oxide model also applies for the oscillations observed on Pt wires and foils. For this type of catalyst, the reconstruction model derived from single crystal studies appears to be a realistic possibility; the more so as grains with (100) and (110) orientation on a polycrystalline Pt foil exhibited the same behavior as the single crystal orientations.[174] These experiments had, however, been conducted with well-cleaned surfaces at low pressure ($p < 10^{-3}$ mbar). With Pt samples which have not undergone extensive cleaning cylces, Si impurities are present leading to partial oxidation.[236] Further experimental work is therefore required in order to finally resolve the mechanistic details of such systems.

C. Pt Single Crystal Experiments

1. The Reconstruction Model

Structural models of the three low-index planes of Pt are displayed in Figure 5. Of the three low-index planes only the close-packed Pt(111) surface is stable in its bulklike 1 × 1 termination, while the more open (100) and (110) surfaces reconstruct into a quasi hexagonal ("hex")[237-240] and a 1 × 2 "missing row" geometry,[241-245] respectively. The reconstruction of both Pt(100) and Pt(110), can reversibly be lifted by certain adsorbates, such as CO, NO, etc. This constitutes an adsorbate-induced phase transition, which is controlled by critical adsorbate coverages.[246]

The geometries of the reconstructed surfaces, as well as the properties of the 1 × 1 ⇄ hex phase transition of Pt(100) and 1 × 1 ⇄ 1 × 2 phase transition of Pt(110), have been the aim of numerous investigations conducted with LEED,[246-248] Rutherford back-scattering,[241,249,250] vibrational spectroscopy,[251,252] STM,[253-255] and molecular beam experiments.[256,257]

The driving force for adsorbate-induced surface phase transitions can be rationalized on the basis of simple thermodynamic considerations, as first pointed

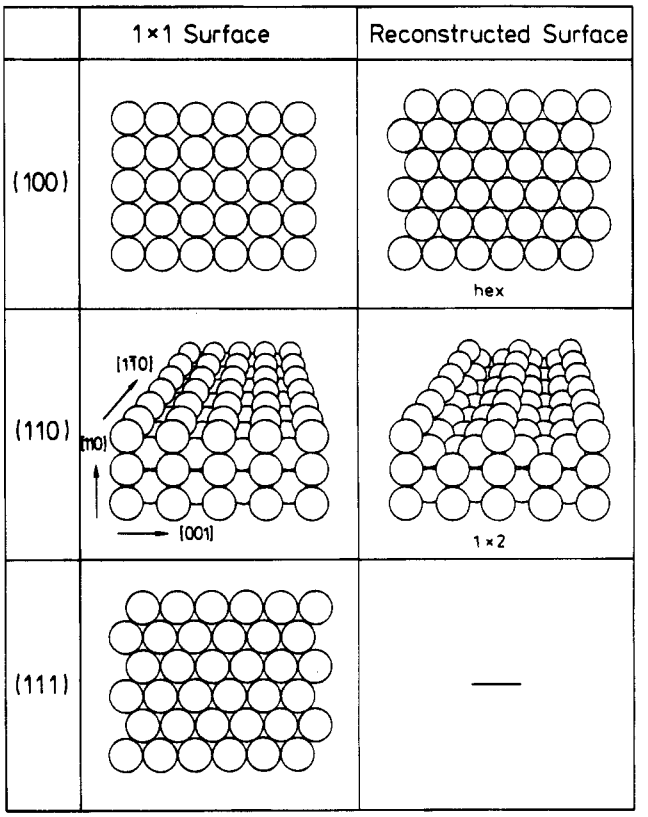

Figure 5. Reconstructed and nonreconstructed surfaces for the three low-index planes of Pt.

out by Behm et al.[246] with the CO-induced 1 × 1 ⇄ hex phase transition of Pt(100). The clean Pt(100) surface is reconstructed because of the lower surface energy of the hex phase as compared to the 1 × 1 phase. The relative stability of the two phases may, however, switch if an adsorbate is more strongly bound on the 1 × 1 phase than on the hex phase. As soon as the gain in adsorption energy overcompensates the loss in reconstruction energy, the reconstruction is lifted by the adsorbate. The difference in adsorption energy was shown to be quite substan-

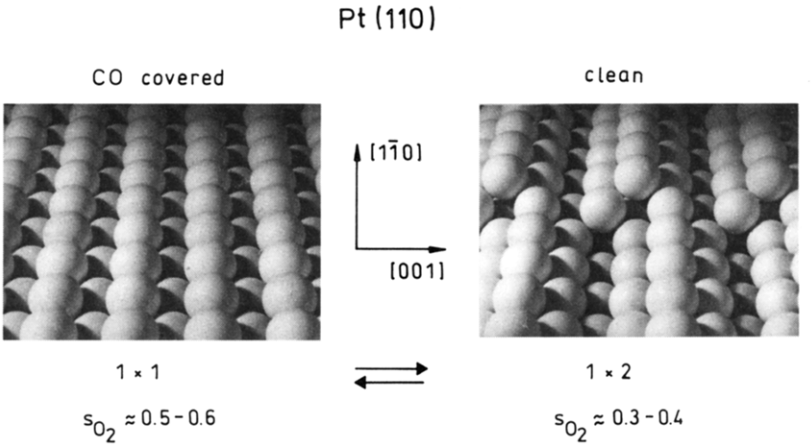

Figure 6. Ball model illustrating the CO induced $1 \times 1 \rightleftarrows 1 \times 2$ surface phase transition of Pt(110). The different oxygen-sticking coefficients, s_{O_2}'s, of the two phases are responsible for rate oscillations during catalytic CO oxidation. The model also demonstrates how the necessary mass transport of Pt atoms creates an atomic step on the surface.

tial for Pt(100)/CO, where values of 37 and 27 kcal/mol have been determined for the 1×1 and hex phase, respectively.

The microscopic details of the $1 \times 1 \rightleftarrows$ hex and the $1 \times 1 \rightleftarrows 1 \times 2$ phase transition, have been investigated with STM, showing how the mass transport of Pt atoms occurs.[253-255] The growth kinetics of the 1×1 phase in the CO-induced lifting of the hex reconstruction of Pt(100), have been the subject of a molecular beam investigation by King et al.[256,257] It was demonstrated, that the growth kinetics of the 1×1 phase obey a power law of order 4.5 with respect of the CO coverage on the hex phase.

The key observation leading to the reconstruction model for oscillations on Pt surfaces was that it was only those orientations displaying oscillatory behavior, that were structurally unstable, while the stable Pt(111) surface merely exhibited bistability in catalytic CO oxidation.[59,73,231] Rate oscillations occur under conditions where oxygen adsorption is rate limiting, and since the oxygen sticking coefficient, s_{O_2}, is structure sensitive on Pt surfaces, the phase transition can cause a periodic switching between two states of different catalytic activity. On Pt(100), s_{O_2} differs drastically between the 1×1 and the hex phase, with $s_{O_2}^{1\times1} \approx 0.3$ and $s_{O_2}^{hex} \approx 10^{-4}-10^{-3}$,[258,259] while the corresponding difference for Pt(110) is much smaller with $s_{O_2}^{1\times2} \approx 0.3-0.4$ and $s_{O_2}^{1\times1} \approx 0.6$.[260]

The oscillation mechanism is illustrated in Figure 6 for the case of Pt(110). Starting with a CO covered 1×1 phase, the adsorption rate of oxygen, and hence the catalytic activity, will be high. As a consequence, more adsorbed CO will be consumed by reaction and desorption than supplied by adsorption, and its coverage decreases until, below a critical value $\theta_{CO,crit} \approx 0.2$, the surface will reconstruct into the 1×2 phase. On this surface, s_{O_2} is low and consequently the CO coverage will rise. Above $\theta_{CO,crit}$, the reconstruction is lifted, and the initial situation of a CO covered 1×1 surface is established again.

Direct evidence for the validity of the reconstruction mechanism sketched above was obtained in in situ LEED experiments that demonstrated that the oscillations of the reaction rate were in fact accompanied by periodic structural changes of the substrate. Such experiments have been conducted for both Pt(100) and Pt(110) surfaces, and Figure 7a displays the corresponding LEED measurement for Pt(100).[59,73,75]

Although the basic mechanism is identical, the two surfaces, Pt(100) and Pt(110), differ quite strongly in their oscillation properties. With Pt(100), one typically finds only irregular oscillations,[58,59] whereas Pt(110) exhibits very regular oscillations with a variety of different waveforms, ranging from rapid harmonic oscillations (period τ of the order of seconds) at high temperature ($T > 500$ K) and mixed-mode oscillations at intermediate temperature, to slow ($\tau > 1$ min) harmonic oscillations at low temperature ($T < 450$ K).[73,75] As will be shown below (see section VI.C.1), the differing regularity of the oscillations reflects different levels of spatiotemporal self-organization on the oscillating surface, which in turn are essentially a consequence of differently wide existence ranges for oscillations in parameter space.[78] The corresponding diagram for $T = 480$ K, displayed in Figure 8, reveals that Pt(110) exhibits an extremely narrow parameter space for oscillations in p_{CO}, while Pt(100) displays oscillatory behavior over a much larger range of p_{CO}.[58,73,78] As was demonstrated by mathematical modeling, the different width of the oscillatory range for Pt(100) and Pt(110) is a consequence of how strongly s_{O_2} differs between the 1×1 and the reconstructed surface.[78] On Pt(100), s_{O_2} differs by 2-3 orders of magnitude, between the two surface phases while the corresponding ratio for Pt(110) is only about 1.5.

2. Faceting and Oscillations on the High-Index Planes of Pt

An at first puzzling phenomenon was the appearance of an induction period in the development of rate oscillations on Pt(110) at lower temperature.[73,75] In situ LEED experiments, however, revealed that this induction period is due to a faceting process. The initially flat Pt(110) surface facets under the influence of the catalytic reaction into new orientations that almost exclusively belong to the [001] zone.[74,75] The faceting process, which in LEED can be observed as a continuous splitting of the integral order beams, takes place in the 10^{-4} mbar range on a time scale

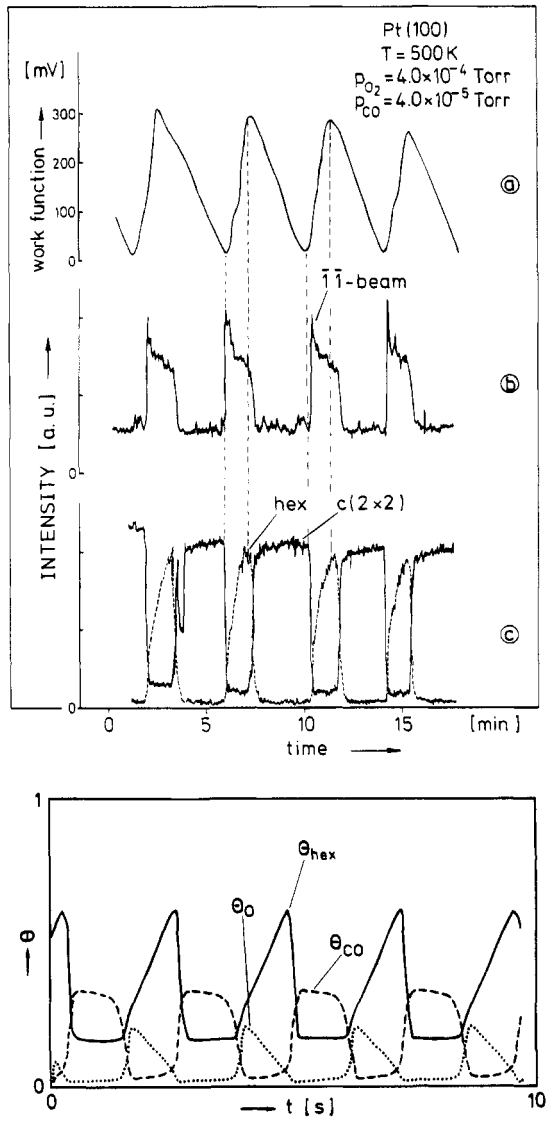

Figure 7. Experimental and simulated oscillations in catalytic CO oxidation on Pt(100): (a) Experiment. In situ LEED measurements showing the coupling between the oscillations in the reaction rate and periodic structural changes via the $1 \times 1 \rightleftarrows$ hex phase transition of Pt(100). The reaction rate, r_{CO_2}, has been measured here via the work function variation, which is proportional to r_{CO_2} under oscillatory conditions. The amount of hex reconstruction is given by the intensity of one of the hex spots, while the half-order spot of the $c(2 \times 2)$-CO structure represents the amount of nonreconstructed 1×1 phase. (b) Simulation. A four-variable model described in ref 56 served to model the reaction. θ_{CO} should be compared with the $c(2 \times 2)$ intensity in a and θ_O with the intensity of the $\bar{1}\bar{1}$ beam in a. (a: Reprinted from ref 59. Copyright 1986 American Institute of Physics. b: Reprinted from ref 56. Copyright 1985 American Institute of Physics.)

of ~10−30 min. The facets that are formed are actually microfacets, since their size is of the order of ~100 Å.[261]

The kinetics and the conditions for faceting have been investigated in detail.[74,75,261-266] It was shown that faceting only occurs at $T < 530$ K (for $p_{O_2} = 1.5 \times 10^{-4}$ mbar); above this temperature a thermal reordering process keeps the (110) surface flat. Associated with the faceting of Pt(110) is an increase in catalytic activity, which in a reaction rate vs p_{CO} diagram, shows up as a shift of the rate maximum toward higher p_{CO}, as displayed in Figure 9. The

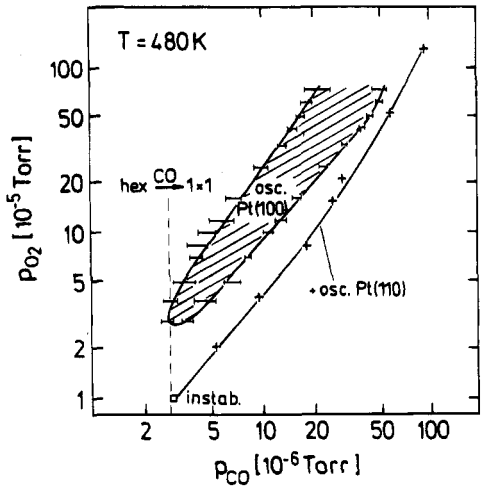

Figure 8. Existence diagram for the occurrence of kinetic oscillations on Pt(100) and Pt(110) at $T = 480$ K. The dashed line marks the minimum p_{CO} which is required for the CO-induced lifting of the hex reconstruction on Pt(100). (From refs 58 and 78. Copyright 1989 American Institute of Physics.)

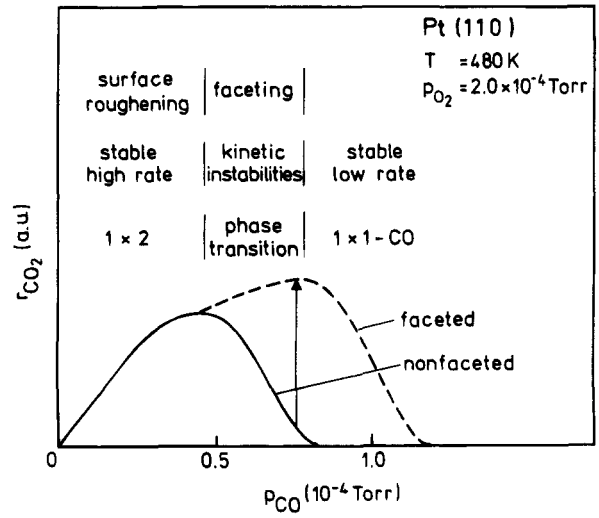

Figure 9. Relation between the conditions for faceting and the kinetics of catalytic CO oxidation on Pt(110). The solid line indicates the rate curve for the nonfaceted surface, while the dashed curve indicates the increase in catalytic activity after strong faceting of the surface. The different regions indicated on top of the rate curve all refer to the nonfaceted Pt(110) surface. The arrow denotes the increase of the reaction rate during faceting. (Reprinted from ref 261. Copyright 1990 American Institute of Physics.)

increase in catalytic activity was traced back to a higher oxygen sticking coefficient on the faceted surface. As was demonstrated by measurements with a cylindrically shaped Pt single crystal, whose surface exhibits all orientations of the [001] zone, s_{O_2} is highly structure sensitive.[96] The resulting diagram, displayed in Figure 10, shows that the orientational variation of s_{O_2} is exactly anticorrelated with the work function variation of the clean surface. The work function in turn correlates with the density of (100) steps thus explaining the increase is s_{O_2} with progressive faceting. The highest s_{O_2} is found at,[210] and this orientation also represents the limiting case in the faceting of Pt(110).

One can show with the ball model of the Pt(110) surface displayed in Figure 6, that the mass transport of 50% of the surface atoms that is associated

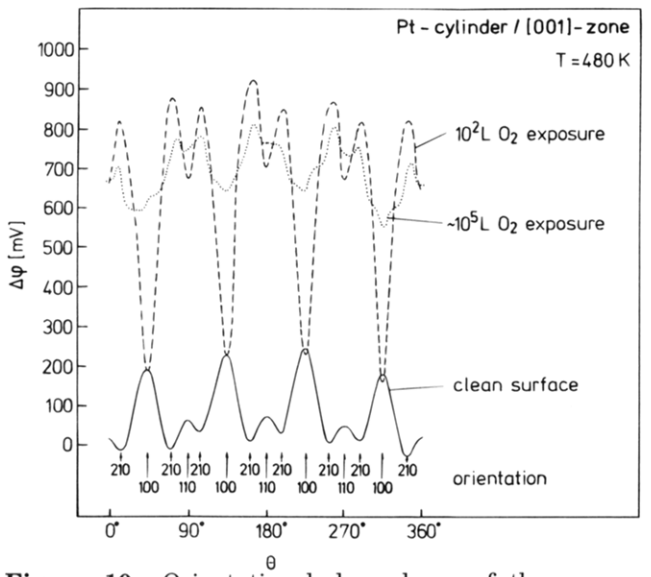

Figure 10. Orientational dependence of the oxygen-sticking coefficient, s_{O_2}, on a cylindrical Pt surface exhibiting all orientations of the [001] zone. The work function change after 100 L of O_2 desorption has been shown to be proportional to the oxygen-sticking coefficient s_{O_2}. (Reprinted from ref 96. Copyright 1985 J. C. Baltzer AG.)

with the $1 \times 1 \rightleftarrows 1 \times 2$ transition necessarily creates steps.[74] By accumulating steps of (100) orientation, all planes of the [001] zone can be constructed, but in order to create faceting, evidently a driving force is required too. As will be pointed out in more detail in section VI.D, this cannot be traced back to a principle of equilibrium thermodynamics, but the faceting has to be discussed within the framework of a dissipative structure of the Turing type.[263,265] Experimentally, this interpretation is reflected by the fact that faceting only occurs under reaction conditions, while adsorbed CO and oxygen alone do not cause such a restructuring of the Pt(110) surface.[74,75]

The appearance of an induction period for the oscillations on Pt(110) (at low T) is due to faceting causing the oscillatory window in p_{CO} to shift toward the chosen parameter values.[74,75,264] In addition, one observes that faceting causes a strong increase of the oscillation period, up to a factor of 100, compared to the unfaceted surface.[75] In terms of the dynamics, the faceting process induces a second, slower time scale, besides the fast $1 \times 1 \rightleftarrows 1 \times 2$ phase transition, leading to mixed-mode oscillations in an intermediate T range.[73] The faceting process itself is reversible, as demonstrated by the observation of oscillations, in which the degree of faceting (more precisely the inclination angle of the facets), underwent periodic changes parallel to the variations of the reaction rate.[75]

Kinetic oscillations in catalytic CO oxidation have also been found on high-index planes of Pt, namely on Pt(210) by Ehsasi et al.[94] and on the cylindrical Pt surface that comprises all orientations of the [001] zone by Sander et al.[96] Since the clean Pt(210) surface does not reconstruct, the simple reconstruction model at first sight seems not to be applicable to the oscillations on this surface. Subsequent LEED investigations by Sander et al.,[95] however, demonstrated that the Pt(210) surface facets into (110) and (310) orientations under reaction conditions. On the

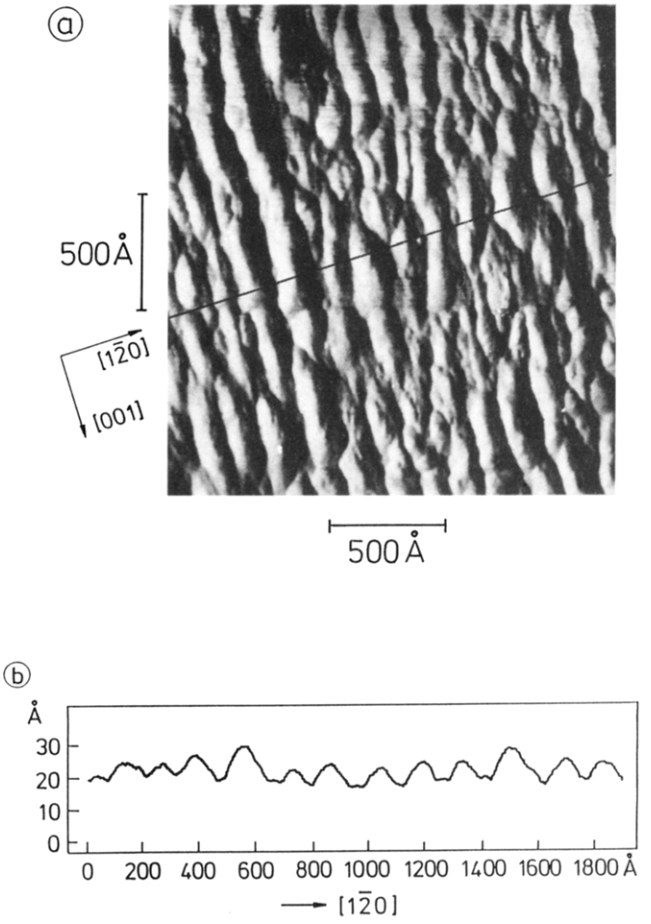

Figure 11. STM image (a) of a Pt(210) surface which had been faceted during catalytic CO oxidation. The surface had been exposed for 1 h at $T = 480$ K to CO and O_2 at 10^{-4} mbar. A profile cut in the (120) direction is shown in b. (Reprinted from ref 186. Copyright 1992 J. C. Baltzer AG.)

low-index planes, which are thus created, the same phase transition mechanism can then operate which has been shown to be valid for the low-index planes of Pt. The involvement of faceting explained the appearance of an induction period for the oscillations on Pt(210), and the restricted parameter space for oscillations to $T < 500$ K and $p_{O_2} \geq 10^{-4}$ mbar.

A real-space image obtained by scanning tunneling microscopy (STM) of the faceted Pt(210) surface is shown in Figure 11.[186] In contrast to Pt(110), the faceting of Pt(210) is associated with a decrease in catalytic activity. As one can expect from the structural relations, the conditions for faceting and the faceting behavior of Pt(210) are almost exactly complementary to that of Pt(110).[95]

3. Subsurface Oxygen

Thermodynamical considerations demonstrate that Pt oxide does not form under the low-pressure conditions employed in single crystal experiments.[236,267] There is, however, strong experimental evidence that, under certain conditions, an oxygen species below the surface forms, whose existence is not linked to impurities like Si or Ca. Thermal desorption experiments from a Pt(110) surface, which had been strongly faceted during catalytic CO oxidation, revealed an oxygen state more strongly bound than the chemisorbed species.[80,262] In XPS, this state was

characterized by a broad O1s peak at 530 eV.[80] Mechanistically, the formation of this subsurface species had been linked to structural rearrangements of the surface during faceting that facilitate penetration of oxygen into deeper layers.[262]

In recent experiments with photoemission electron microscopy (PEEM) on catalytic CO oxidation on Pt(100) and Pt(110), it was observed, that under certain conditions, the reaction fronts were followed by a region of reduced work function.[67,68,174] For Pt(100), a procedure had been developed to prepare this state and to characterize it by TDS, AES, and work function measurements.[67,68] It was shown that this state exhibits a work function about 1 eV lower than that of the clean surface and that the formation of this state can be associated with the population of oxygen subsurface sites, similar to the subsurface state that has been found in catalytic CO oxidation on Pd(110).[48] With respect to the oscillation mechanism, the subsurface oxygen species does not alter the principle validity of the reconstruction model. It provides, however, an additional interesting feature to the mechanism.

4. Mathematical Modeling

The starting point for mathematical modeling of the oscillations on Pt single crystal surfaces is the LH scheme for catalytic CO oxidation, as outlined above. This scheme alone predicts bistability and quite a number of studies conducted mainly with the ZGB model focus on the kinetic phase transitions between the reactive and the CO-poisoned state of the surface.[85,193,225,230] In order to obtain oscillatory solutions, the equations of the LH scheme have to be complemented by additional terms describing the switching of the adsorption properties through the mechanism of an adsorbate-induced surface phase transition. Mathematical models of this reconstruction mechanism, describing the oscillations on Pt(100) and Pt(110), have been formulated both with DE's and with cellular automatons (CA's).

The mathematical model which was developed first comprises a set of four coupled DE's describing the variation of the adsorbate coverages on the hex and 1 × 1 phase of Pt(100) and the phase transition between the two substrate phases.[56] As demonstrated by Figure 7, the model reproduces the experimentally observed sequence of adsorbate and substrate structures. The four-variable model was modified by Andradé et al., who used a Landau functional to describe the kinetics of the phase transition.[62] Models based on cellular automata were formulated for the oscillations on Pt(100) by Möller et al.[60] and by Kapral et al.[66] The influence of stochastic events was studied by Rosé et al., who used a description derived from a master equation.[268]

A somewhat different three-variable model for oscillations on Pt(110) was developed by Krischer et al.[85] Due to its simpler structure it is more suitable for further mathematical analysis. Denoting the fraction of the surface which is in the 1 × 1 state by $\theta_{1\times1}$, with the amount of 1 × 2 then given by $1 - \theta_{1\times1}$, one obtains the following set of equations in which θ_{CO} and θ_O represent the CO and the oxygen coverages, respectively:

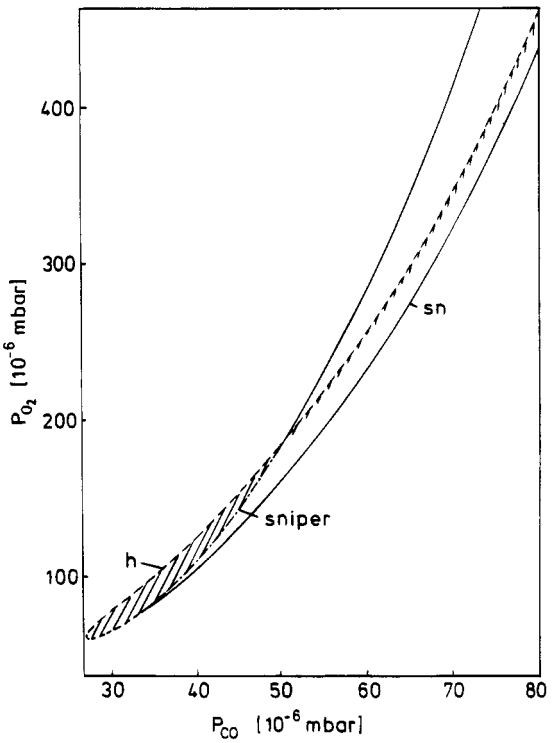

Figure 12. Skeleton bifurcation model for catalytic CO oxidation on Pt(110) at T = 540 K. The hatched region marks the parameter space in which oscillations occur. Left of this region a stable state corresponding to a predominantly oxygen-covered surface can be found and right of it a stable state corresponding to a CO-covered surface is present. sn, sniper, and h denote bifurcations of the type saddle node, saddle node of infinite period and Hopf, respectively.[187,188] At $p_{CO} > 10^{-5}$ mbar the oscillation range (hatched area) becomes extremely narrow in parameter space. (Reprinted from ref 85. Copyright 1992 American Institute of Physics.)

$$\frac{d\theta_{CO}}{dt} = k_1 p_{CO}[1 - (\theta_{CO}/\theta_{CO,sat})^3] - k_2\theta_{CO} - k_3\theta_{CO}\theta_O \quad (1)$$

$$\frac{d\theta_O}{dt} = s_{O_2} k_4 p_{O_2}(1 - \theta_{CO}/\theta_{CO,sat} - \theta_O/\theta_{O,sat})^2 - k_3\theta_{CO}\theta_O \quad (2)$$

with $s_{O_2} = \theta_{1\times1} s_{O_2}^{1\times2} + \theta_{1\times2}$

$$\frac{d\theta_{1\times1}}{dt} = \begin{cases} -k_5\theta_{1\times1} & \text{for } \theta_{CO} \le 0.2 \\ k_5\left(\sum_{i=0}^{3} q_i{}^3\theta^i{}_{CO} - \theta_{1\times1}\right) & \text{for } 0.2 \le \theta_{CO} \le 0.5 \\ k_5(1 - \theta_{1\times1}) & \text{for } \theta_{CO} > 0.5 \end{cases} \quad (3)$$

In these equations the terms with k_1 and k_2 describe CO adsorption and desorption, respectively; oxygen adsorption is modeled by the k_4 term, and the reaction between CO and O is in the term containing k_3. The kinetics of the 1 × 1 ⇄ 1 × 2 phase transitions are described in eq 3 as an activated process, in which the surface structure relaxes to that amount of 1 × 1 phase that is stabilized by the CO coverage. A polynomial expression is used here to

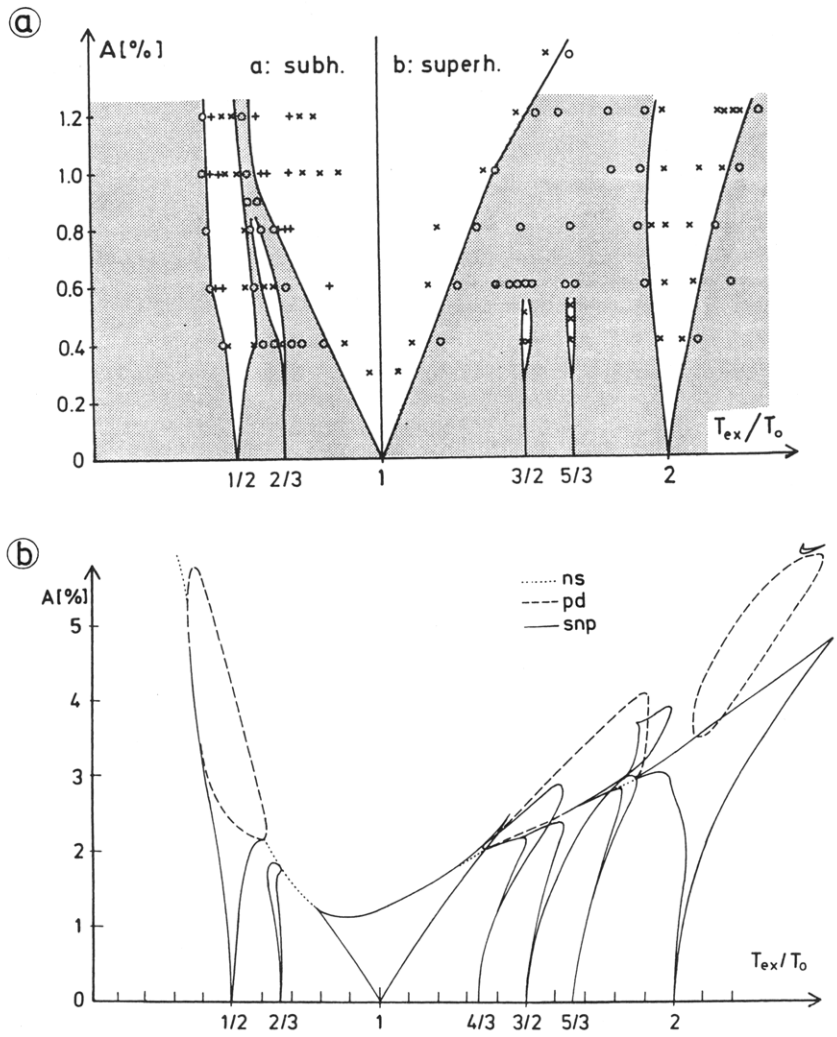

Figure 13. Dynamic phase diagram for periodically forced oscillations in CO oxidation on Pt(110): (a) Experimental data recorded at $T = 525$ K and $T = 530$ K in the 10^{-5} mbar range. The axes A and T_{ex}/T_0 denote the amplitude with which p_{O_2} was modulated, and the period length of the modulation T_{ex} expressed with respect to the period T_0 of the autonomous oscillations. The shaded areas in the diagram indicate regions of quasi periodic behavior in between the entrainment bands. And (b) simulated dynamical phase diagram which has been calculated using the three-variable model for catalytic CO oxidation on Pt(110). Shown is only the skeleton bifurcation structure with ns denoting a Neimark−Sacker[187] and pd a period doubling bifurcation. (a: Reprinted from ref 76. Copyright 1988 American Institute of Physics. b: Reprinted from ref 86. Copyright 1992 American Institute of Physics.)

reproduce the experimentally observed coverage dependence of the phase transition. 1×1 nuclei only form beyond a critical CO coverage of 0.2 on the 1×2 phase and completion of the lifting of the reconstruction is achieved at $\theta_{CO} = 0.5$.

Integration of this set of differential equations reproduces the experimentally observed behavior, and the resulting bifurcation diagram, whose skeleton is displayed in Figure 12, reproduces the narrow existence range for oscillations seen in the experiments (see Figure 8). By taking into account the slow structural changes caused by faceting, this model was extended to a four-variable model, which successfully simulated the mixed-mode oscillations observed experimentally.[73,85]

An alternative model for the oscillations in Pt(110)/CO + O_2 has been formulated by Elokhin et al.,[269,270] on the basis of the experimental result of Savchenko et al.[80] that an oxide-like species is formed under oscillatory conditions. In this model it is assumed that a subsurface oxygen species is formed, whose reactivity is lower than that of chemisorbed oxygen and which modifies the adsorption properties of the Pt layer on top.

5. Periodic Forcing

The response of a surface reaction to external periodic modulation of one of the control parameters is of considerable importance for two reasons. First, due to heat and mass transfer limitations, each oscillating reaction generates periodic variations in the educt partial pressures and in the temperature (at high p), which can very efficiently synchronize different local oscillators. Second, by applying periodic forcing externally, one can potentially increase the yield and selectivity of catalytic reactions.[14−17]

The response of a system that oscillates autonomously with period T_0, to a periodic modulation of a system parameter with amplitude A and period T_{ex}, can be characterized in the following way.[271−273] The system may be entrained, in which case the phase difference between perturbation and response is fixed, or alternatively the system may exhibit quasi periodic behavior, characterized by a continuously

varying phase difference between perturbation and response. In the case of entrainment, one can use the ratio between the response period, T_r, and the perturbation period, T_{per}, and express this ratio with two small integer numbers, k and l, as $T_r/T_{per} = k/l$. One then obtains three cases, with $k/l = 1$ representing harmonic entrainment, $k/l > 1$ superharmonic entrainment and $k/l < 1$ subharmonic entrainment.

In heterogeneous catalysis, periodic forcing has mostly been applied to reactions which play a role in the automotive catalytic converter, and in some cases substantial increases of the yield have been reported.[14-17] A number of forcing experiments have been conducted in catalytic CO oxidation under high-pressure conditions ($p > 1$ mbar).[15,274,275] Single crystal experiments have been performed for catalytic CO oxidation on Pt(100) and Pt(110).[61,76] A very rich dynamical behavior was found on Pt(110), as demonstrated by the "dynamical" phase diagram in Figure 13, exhibiting a number of different entrainment bands separated by regions of quasi periodic behavior.[76]

The phase diagram, displayed in Figure 13a, was reproduced theoretically by Krischer et al.,[86] by mapping out the bifurcation diagram for the forced three-variable model. As was shown quite generally by Vance, Tsarouhas, and Ross,[272,273] the skeleton bifurcation diagram of a forced system does not depend on the specific characteristics of a reaction system, but only on the type of bifurcation (of the autonomous system) around which the system is perturbed.

D. Pd Single Crystal Experiments

Kinetic oscillations in catalytic CO oxidation have been investigated on Pd(110) and Pd(111) in the pressure range from 10^{-3} to 1 mbar, with most of the studies concentrating on Pd(110).[47-49,52,55] Characteristic for the oscillations on Pd(110) is that they require a minimum p_{O_2} of the order of 10^{-3} mbar and that they occur at relatively low temperature at $T <$ 450 K, with a large excess of oxygen in the gas phase ($p_{O_2}/p_{CO} > 1{:}100$).

Since clean Pd surfaces do not reconstruct, the operation of a reconstruction mechanism similar to Pt surfaces at first seemed to be excluded. This possibility appeared to be realistic again, when it was shown that CO at high coverages ($0.75 < \theta_{CO} < 1.0$) induces a 1×2 reconstruction of the missing row type.[276,277] In contrast to oxygen adsorption on Pt surfaces, oxygen adsorption on Pd surfaces is not structure sensitive and therefore a reconstruction mechanism still cannot work in the same way as on Pt surfaces. It turned out that the oscillation mechanism for Pd(110) is in fact based on a different principle, namely the ability of Pd catalysts to incorporate oxygen, such that a subsurface oxygen species is formed.[48]

The key feature that illustrates the role of subsurface oxygen in the oscillation mechanism, is the reversal of the usual clockwise (cw) hysteresis in the CO_2 production rate (upon variation of p_{CO}), into a counterclockwise (ccw) hysteresis under conditions where rate oscillations occur.[48] The existence range for oscillations and the corresponding ccw hysteresis are depicted in Figure 14. The usual cw hysteresis is observed at low p_{O_2}, but with increasing p_{O_2}, the hysteresis loop first becomes narrower until finally a switching of the branches occurs. One therefore obtains a cross-shaped stability diagram if one plots the transition points of the cw/ccw hysteresis into a p_{O_2},p_{CO} diagram.[52] In the experimental diagram which is displayed for $T = 350$ K in Figure 15a, the crossing point of the branches at $p_{O_2} \approx 9 \times 10^{-3}$ mbar marks the lower pressure limit for oscillations.

The existence of a ccw hysteresis in the reaction rate can be attributed to the filling and depletion of the subsurface oxygen reservoir associated with deactivation and activation of the catalyst, respectively.[48] At low p_{CO} with an oxygen-covered surface oxygen atoms will penetrate into the deeper layers of the Pd catalyst. The reverse process takes place at high p_{CO}, when oxygen from the subsurface region diffuses back to the surface and reacts with CO to form CO_2, leading to a depletion of the subsurface oxygen reservoir. One can therefore complement the LH scheme for catalytic CO oxidation on Pd surfaces by adding a fourth equation

$$O_{ad} \rightleftarrows O_{sub}$$

that describes the reversible conversion of the chemisorbed oxygen species into a subsurface species. The oscillation mechanism can be rationalized in the same way as the reversal of the hysteresis.[48] Starting with an active oxygen-covered surface oxygen starts to penetrate into the subsurface region, leading to a deactivation of the surface, i.e. the oxygen-sticking coefficient becomes small. The surface therefore becomes CO-covered, but as O_{sub} now diffuses back to the surface and reacts with CO, the decreasing subsurface oxygen concentration leads to a reactivation of the surface and the initial situation is established again.

Experimental evidence for the existence of an oxygen subsurface state on Pd(110) was obtained in (i) TDS experiments showing an adsorption state that does not saturate at high O_2 exposures and (ii) in work function measurements demonstrating a $\Delta\varphi$ decrease at high O_2 exposure, which is attributed to oxygen sites located underneath the surface layer and therefore being associated with an inverse dipole moment.[278-280] On Rh(210), the existence of a subsurface state was proven by the difference in the oxygen signal from techniques with different depth resolution, i.e., XPS and ion scattering.[281] Finally, in titration experiments with CO, it was shown that after an initial very high O_2 exposure, oxygen from deeper layers continuously segregates to the surface.[48] Therefore, in these experiments, a total CO_2 yield was obtained that corresponds to more than two monolayers of oxygen.

On the basis of the LH scheme of catalytic CO oxidation to which the reversible formation of subsurface oxygen has been added as a fourth step, a mathematical model was developed by Bassett et al.[50] that could qualitatively reproduce the oscillations in Pd(110)/CO + O_2 very well. In this model, the subsurface oxygen concentration modified the cata-

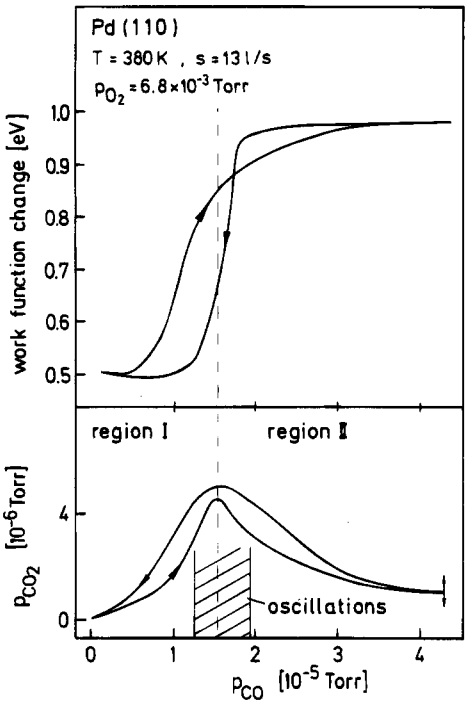

Figure 14. Connection between the occurrence of a ccw hysteresis in the dependence of the reaction rate (p_{CO_2}) on p_{CO} and the existence of kinetic oscillations in catalytic CO oxidation on Pd(110). Included in the diagram is the variation in $\Delta\varphi$ marking the transition between a CO covered ($\Delta\varphi$ = 0.9 eV) and an oxygen covered surface ($\Delta\varphi$ = 0.5 eV). (Reprinted from ref 48. Copyright 1989 J. C. Baltzer AG.)

lytic activity via the oxygen sticking coefficient, assuming an exponential dependence of s_{O_2} on the subsurface oxygen concentration. Although the model reproduced a number of features, it failed to simulate the experimentally observed stability diagram shown in Figure 15a.

This discrepancy could be removed by taking repulsive interactions between adsorbed CO and oxygen into account.[53] These interactions lower the activation barrier for penetration of chemisorbed oxygen into the subsurface region, thus facilitating subsurface oxygen formation at higher coverages. The stability diagram one thus obtains is shown in Figure 15b.

V. Catalytic NO Reduction and the $H_2 + O_2$ Reaction

A. Introduction

Catalytic reduction of NO with CO, H_2, NH_3, or hydrocarbons has been intensively investigated on Pt and Rh surfaces, which are the noble metals used in the automotive catalytic converter.[282] Dynamical effects, such as multistability and rate oscillations, have been studied with polycrystalline catalysts, with Pt(100) and Rh(110) single crystal surfaces, as well as with Pt and Rh field emitter tips (FET's) (see Table 1).

Among the various reaction systems, the catalytic reduction of NO with CO, H_3 or NH_3 on Pt(100) is understood best. Therefore, we focus mainly on these reactions here. All three reactions exhibit very

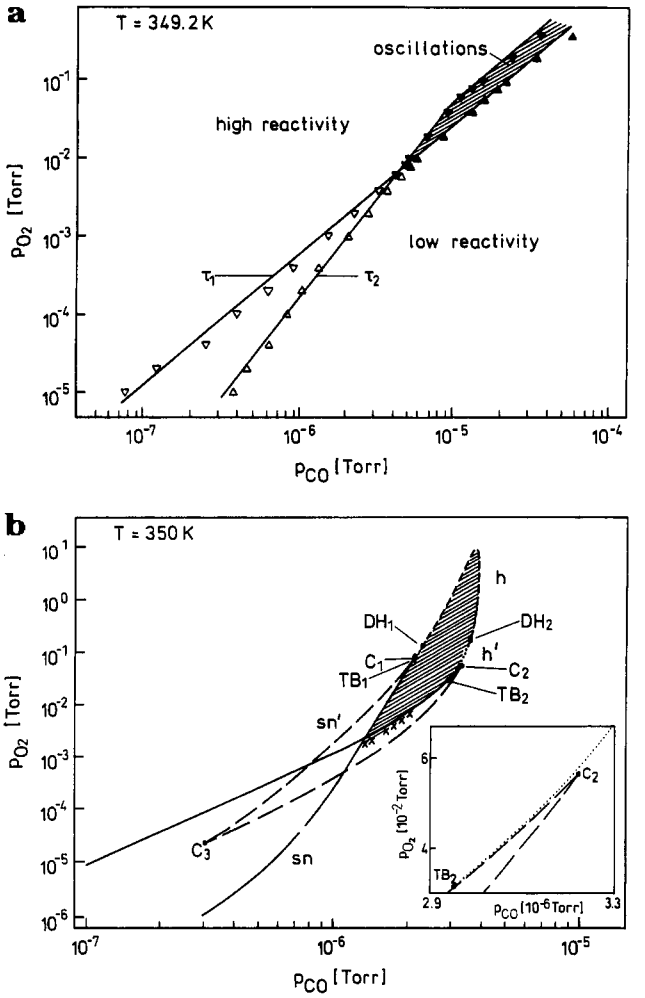

Figure 15. Cross-shaped bifurcation diagram for catalytic CO oxidation on Pd(110) showing the various regions of monostability, bistability, and oscillatory behavior in p_{CO},p_{O_2} parameter space at T = 350 K: (a) Experimental bifurcation diagram for catalytic CO oxidation on Pd(110) at T = 349.2 K. τ_1 and τ_2 represent the boundaries of the bistable region. And (b) calculated bifurcation diagram using the three-variable subsurface oxygen model described in ref 53. The hatched area denotes the oscillatory range. In between the sn bifurcations the system exhibits bistability. For a detailed explanation of the various bifurcation types in the plot see ref 53. (a: Reprinted from ref 52. Copyright 1993 American Institute of Physics. b: Reprinted from ref 53. Copyright 1993 American Institute of Physics.)

similar dynamical behavior, whose origin can be traced back to the autocatalysis inherent to the vacant-site requirement for NO dissociation.

B. The NO + CO Reaction

Kinetic oscillations in the NO + CO reaction on Pt were first reported by Lintz et al., who studied the reaction under isothermal conditions in the 10^{-4} mbar range, using a Pt ribbon as catalyst.[130] In an FTIR investigation conducted by Schüth and Wicke at atmospheric pressure with supported Pt and Pd catalysts, the rate oscillations were accompanied by temperature excursions of up to 25 K, i.e. the oscillations were thermokinetic.[42]

On single crystal surfaces, rate oscillations in the NO + CO reaction were discovered by King et al., at extremely low pressure, in the 10^{-9} mbar range on Pt(100).[131] The oscillations on Pt(100) then became

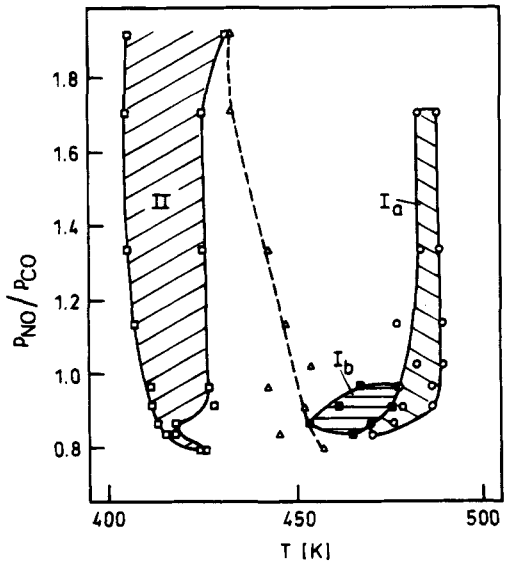

Figure 16. Existence ranges for oscillatory behavior in the NO + CO reaction on Pt(100) for fixed $p_{NO} = 4 \times 10^{-6}$ mbar. Range Ia denotes the occurrence of sustained rate oscillations, while range Ib and range II mark spatiotemporal pattern formation, i.e. unsynchronized local oscillations, without the occurrence of oscillations in the reaction rate. (Reprinted from ref 141. Copyright 1994 American Institute of Physics.)

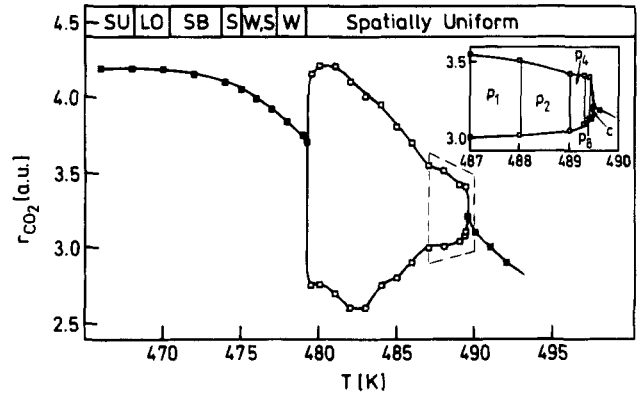

Figure 17. Bifurcation diagram for the NO + CO reaction on Pt(100) showing the occurrence of sustained rate oscillations at elevated temperature (ranges Ia and Ib in Figure 16). The diagram shows the range where the CO_2 production, r_{CO_2}, is stationary (filled squares) and where the reaction rate exhibits kinetic oscillations. The oscillation amplitude, i.e. the upper and lower turning points, are marked by open squares. The inset shows the Feigenbaum scenario, which is found at the upper temperature boundary of the oscillatory range. The different abbreviations on top, refer to different types of spatiotemporal patterns, which can be observed below the oscillatory range. Experimental conditions: $p_{NO} = p_{CO} = 4 \times 10^{-6}$ mbar. (Reprinted from ref 140. Copyright 1993 American Institute of Physics.)

the subject of a number of detailed studies conducted in the 10^{-7} to 10^{-5} mbar range both with laterally integrating techniques, such as reaction rate, $\Delta\varphi$, LEED, and FTIR measurements,[131-135,177] as well as with spatially resolved measurements with PEEM.[136,140-144] No oscillations were found on Pt(111) and Pt(110). This latter result has been traced back to the relatively low dissociation probability for NO of ~1% on Pt(111) and ~10% on Pt(110), as compared to ca. 60% for Pt(100).[283-285] A study of the NO + CO reaction on the cylindrically shaped Pt single crystal (axis parallel to [001] demonstrated that oscillatory behavior only occurs in a narrow orientational range from (100) to (310), which is also the most active one in NO dissociation.[136]

Oscillatory behavior in the NO + CO reaction on Pt(100) occurs in two separate T windows, depicted in Figure 16, which differ with respect to the structure of the underlying substrate, and with respect to the level of synchronization.[134,141] In the lower-lying T window, no sustained rate oscillations exist, but the surface is only oscillating on a local scale (a few micrometers), as was demonstrated by PEEM[141] (see also section VI.C.2). By applying a small synchronizing T jump (~1−5 K), however, one can excite rate oscillations, which then decay within a small number of periods. Sustained rate oscillations can be obtained by periodic T forcing.[135]

In contrast to the lower-lying T window, where the oscillations proceed on a pure 1 × 1 substrate, the oscillations in the upper T window, take place on a largely hex-reconstructed surface and the oscillations are coupled to periodic structural changes via the 1 × 1 ⇄ hex phase transition.[134,142] One observes sustained rate oscillations, which proceed spatially uniformly.

At both ends of the oscillatory T window, one finds interesting transitions to a stationary reaction rate, as demonstrated by the bifurcation diagram displayed in Figure 17.[140,142] At the upper T boundary the oscillations develop via a Feigenbaum scenario, starting from small amplitude chaotic oscillations, while the discontinuous transition to a stationary reaction rate at the lower T boundary is associated with the onset of spatiotemporal pattern formation (see also section VI.C.2).

Neglecting N_2O formation, the mechanism of the NO + CO reaction can be described by the following sequence of steps:[134]

$$CO + * \rightleftarrows CO_{ad} \quad \text{(R1)}$$

$$NO + * \rightleftarrows NO_{ad} \quad \text{(R2)}$$

$$NO_{ad} + * \rightarrow N_{ad} + O_{ad} \quad \text{(R3)}$$

$$2N_{ad} \rightarrow N_2 + 2* \quad \text{(R4)}$$

$$CO_{ad} + O_{ad} \rightarrow CO_2 + 2* \quad \text{(R5)}$$

The slow rate-determining step in this sequence is the dissociation of NO in R3, which requires an additional vacant site in order to proceed. Since more vacant sites are liberated in subsequent product-forming steps than are consumed by the dissociation of NO, an autocatalytic behavior with respect to the production of vacant sites results. This autocatalysis explains the existence of a so-called "surface explosion", i.e. the formation of extremely narrow product peaks (FWHM ≈ 2−5 K) in temperature-programmed reaction (TPR) experiments with NO and CO coadsorbed on Pt(100).[286,287]

The autocatalysis in the above scheme is also the main driving force for the rate oscillations, as was shown by formulating a three-variable model based on steps R1−R5.[134,137] Structural transformations

play no role in this model and therefore, it describes the oscillations in the lower-lying T window in Figure 16. For the three-variable model, a detailed bifurcation analysis has been conducted.[137]

By incorporating the adsorbate-driven $1 \times 1 \rightleftarrows$ hex phase transition, the three-variable model has been extended to six variables.[134] The resulting model reproduces qualitatively well the occurrence of rate oscillations in the upper T window, which are coupled to the phase transitions. Since the hex phase is inefficient with respect to NO dissociation, the catalytic activity is determined by the amount of 1×1 substrate. A modified model for the NO + CO reaction on Pt(100)-hex was proposed by Hopkinson and King, who incorporated the recently determined growth kinetics for the 1×1 phase in the CO/NO-induced lifting of the hex reconstruction.[288] Despite qualitative agreement, this modified model also displayed shortcomings with respect to a quantitative description of the oscillations in the upper T window.

One of the main difficulties in reaching a quantitative description of the NO + CO reaction in the upper T window can be attributed to the role of structural defects. Due to the structural sensitivity of NO dissociation, defects contribute strongly to the catalytic activity of Pt(100)-hex.[134] How the defect properties of a Pt surface are modified by the NO + CO reaction itself has been demonstrated in a reflection electron microscopy (REM) study by Uchida et al., showing a meandering of initially straight step edges under the influence of the reaction.[185]

C. The NO + H_2 and NO + NH_3 Reactions

The two reactions NO + H_2 and NO + NH_3 introduce a new aspect into the study of oscillatory surface reactions, since they involve complex chemical networks with several reactions pathways. Therefore, not only the reaction rates, but also the selectivity, may undergo oscillatory changes.[147,149,151] The main product channels in the NO + NH_3 reaction are described by the two equations:

$$6NO + 4NH_3 \rightarrow 5N_2 + 6H_2O$$

$$8NO + 2NH_3 \rightarrow 5N_2O + 3H_2O$$

In the NO + H_2 reaction, both N_2 and NH_3 are formed according to

$$2NO + 2H_2 \rightarrow N_2 + 2H_2O$$

$$2NO + 5H_2 \rightarrow 2NH_3 + 2H_2O$$

and with a much smaller yield, N_2O also appears as reaction product.[147] Rate oscillations in the NO + NH_3 reaction on Pt have been studied at high pressure, in the millibar range, by Takoudis and Schmidt on a Pt wire, and by Katona and Somorjai on a Pt foil.[156,157]

On a Pt(100) surface, kinetic oscillations in the NO + NH_3 reaction were investigated at low pressure between 10^{-7} and 10^{-5} mbar in rate, $\Delta\varphi$, LEED, and PEEM measurements.[158-160] The system Pt(100)/NO + H_2 was studied by Slinko et al.[149] and in the group of Nieuwenhuys.[147,150] The comparison of the oscillatory reactions revealed, that both systems exhibit almost identical dynamical behavior. In the NO + H_2 reaction on Pt(100), deterministic chaos was identified by Cobden et al.[150] PEEM investigations of this reaction system conducted by Mundschau and Rausenberger[148] showed the existence of propagating reaction fronts.

Mechanistically, the oscillatory NO + H_2 and NO + NH_3 reactions are apparently very similar to the system Pt(100)/NO + CO at elevated temperatures, since all three systems exhibit similar hysteresis effects and display rate oscillations, which proceed on a largely hex-reconstructed surface. Consequently, a mathematical model was formulated analogous to the one for Pt(100)-hex/NO + CO.[151] This model describes rather well the oscillations and the rate hysteresis for both systems. The involvement of the $1 \times 1 \rightleftarrows$ hex phase transition in the oscillation mechanism of the NO + NH_3 reaction was demonstrated by LEED and in the PEEM measurements displayed in Figure 18.[158,159] The three distinct gray levels seen in the PEEM image were identified with a cyclic transformation of the surface structure, involving the $1 \times 1 \rightleftarrows$ hex phase transition.

Compared to Pt surfaces, Rh exhibits a much higher efficiency in dissociating NO. Oscillatory behavior in the NO + H_2 and NO + NH_3 reactions on Rh were first found in field electron microscopic studies by Nieuwenhuys et al., in the 10^{-6} mbar range.[11,155,161] On a Rh(110) surface oscillatory behavior in the NO + H_2 reaction was detected in the 10^{-6}–10^{-5} mbar range by Mertens et al., but the emphasis in these experiments was less on the complicated mechanistic aspects of the oscillations, but more on the unusual chemical wave patterns in this reaction (see section VI.C.2).[153,154]

D. The H_2 + O_2 Reaction on Pt

Kinetic oscillations in the H_2 + O_2 reaction on Pt had already been observed quite early on at high pressure.[20,106-108] Detailed investigations of these nonisothermal oscillations were then conducted by Kasemo et al., at ~100 mbar and $T \approx 400$ K.[289] In a recent study by Gimzewski et al., a micromechanical device, based on the principle of a bimetallic strip, served to detect the extremely small variations in the reaction heat of a few milliwatts, which are generated by the oscillatory H_2 + O_2 reaction on Pt at 10^{-2} mbar.[290] Although these oscillations involve heat and mass transfer, these limitations do not explain the time scale of the oscillations. It was shown, however, that the formulation of a mathematical model based on an oxidation/reduction process, similar to that for catalytic CO oxidation, reproduces rather well the experimental findings.[291]

In single crystal studies of hydrogen oxidation, so far no oscillations have been observed, but only stationary patterns in Pt(100)/O_2 + H_2.[111] Surprisingly, however, in FIM experiments with Pt field emitter tips, oscillatory behavior was observed, even with orientations such as Pt(100), which displayed simple bistable kinetics in experiments with a plane Pt(100) single crystal.[110,111] The differences seen in the behavior with field emitter tips and with single crystal surfaces, have led to the conclusion, that the oscillations seen in the former experiments are

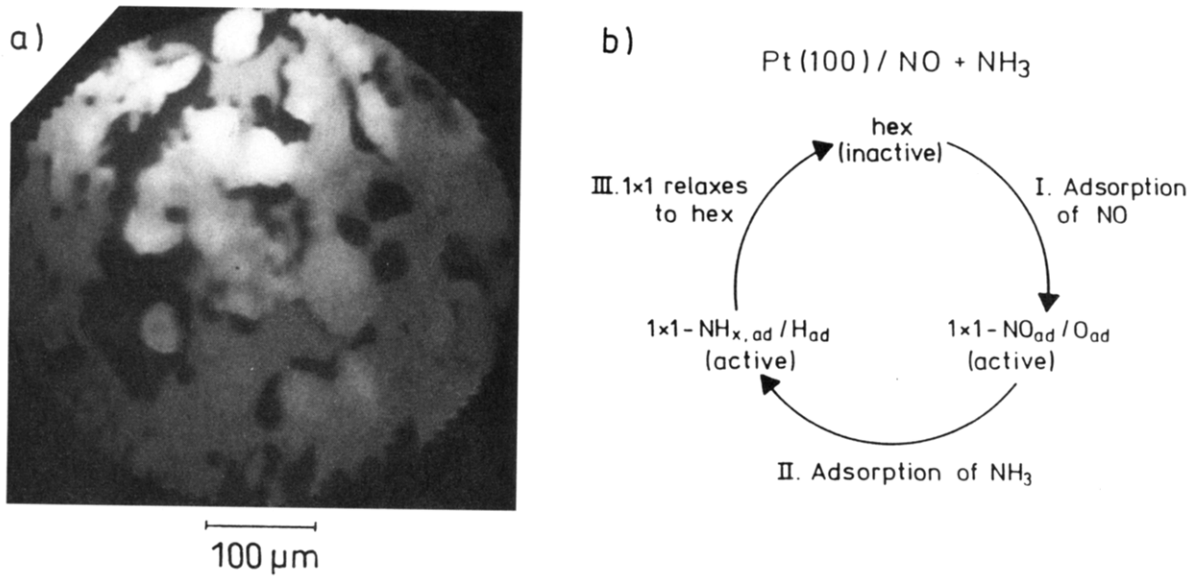

Figure 18. PEEM image showing the formation of fluctuating adsorbate islands during kinetic oscillations in the NO + NH_3 reaction on Pt(100): (a) Experimental conditions: $p_{NO} = 1.3 \times 10^{-6}$ mbar, $p_{NH_3} = 2.1 \times 10^{-6}$ mbar, and $T = 438$ K. The different gray levels are assigned to the following phases: medium gray, adsorbate free hex surface; dark area, NO_{ad}/O_{ad} covered 1×1 surface; bright area, NH_x ($x = 1-3$) covered 1×1 area. The scheme in b shows the mechanistic interpretation of the cyclic transformations the three identifiable surface phases undergo in PEEM. (Reprinted from ref 159. Copyright 1992 J. C. Baltzer AG.)

essentially caused by the coupling between different crystal planes.

VI. Spatiotemporal Pattern Formation

A. Introduction

In an oscillatory surface reaction, some kind of synchronization mechanism has to exist in order to generate macroscopic rate variations. Due to inevitable spatial nonuniformities, the contributions of different local oscillators would otherwise average out to a stationary reaction rate. In principle, three possible mechanisms are available for synchronization, namely coupling via heat transfer, via partial pressure variations in the gas phase (gas-phase coupling), and via surface diffusion of a mobile adsorbate. While heat transfer undoubtedly represents the dominant coupling mode in the nonisothermal experiments conducted at high pressure ($p > 1$ mbar), only surface diffusion and gas-phase coupling are relevant in the single crystal studies ($p < 10^{-3}$ mbar).

The types of pattern which are generated if only diffusional coupling is present, have been analyzed extensively, since such a situation is also realized in fluid-phase chemical reaction systems.[192,292-294] Typically, target patterns and rotating spiral waves are observed in such reaction systems. The basic phenomenon underlying these patterns is that of a chemical wave which can be defined as a steep concentration gradient traveling with constant velocity in space. It was already recognized by Luther in 1906, that chemical waves can arise if an autocatalytic reaction is involved, i.e., a reaction of the type

$$A + mX \rightarrow nX \qquad \text{with} \qquad n > m$$

and if the autocatalytic component X is allowed to diffuse.[296] The velocity, c_f, of a chemical wave or reaction front is given by

$$c_f \approx \sqrt{D_X K}$$

in which K represent a pseudo-first-order reaction constant, and D_X is the diffusion constant of X. Chemical waves may appear as simple reaction fronts, or they may form pulses, spirals, target patterns, or even more complex forms including chemical turbulence. Besides these spatiotemporal patterns, another kind of pattern formation is possible in reaction–diffusion (RD) systems, which are so-called Turing structures, named after A. M. Turing who first proposed their existence in a pioneering paper in 1952.[297] Turing structures are stationary concentration patterns, which can arise in a RD system, if the homogeneous state is unstable with respect to a perturbation of the homogeneity by diffusion.[192,293] This type of pattern has been found in surface reactions as well.

Although reactions on surfaces and reactions in fluid phase both represent reaction–diffusion systems, the two systems exhibit some basic differences. As a consequence of the fixed substrate geometry on which the adsorbed particles move, surface diffusion is in general anisotropic.[298,299] This not only causes an elliptical deformation of otherwise circular patterns, but the anisotropy may also generate completely new phenomena, which are unknown in isotropic media.[153,154,300] A second important difference is that on surfaces, attractive or repulsive interactions exist, leading to coverage dependent diffusion coefficients, which cause a sharpening or widening of reaction fronts.[72,301] Such effects are particularly important as one looks at pattern formation on a microscopic scale, as is the case in experiments with field electron or field ion microscopy.

Probably the most important difference to reactions in liquid phase is that surface reactions exhibit the

possibility of global synchronization via the gas phase.[78] Under isothermal conditions such a global coupling mode is given by the partial pressure variations of the educts that arise due to mass balance in the reaction. Under typical experimental conditions, these variations are only of the order of less than a few percent, but if no local pressure gradients exist, these variations affect all parts of the surface in the same way and practically without any delay (i.e. with a relaxation time < 1 ms). One may thus obtain a uniformly oscillating surface, but besides this trivial solution, a number of new interesting phenomena may occur as will be discussed further below. In the high-pressure experiments conducted with electrically heated wires, global coupling exists as well, since there a global constraint is introduced by the control mode, which can be either constant current, constant voltage, or constant resistance.[302]

Catalytic surfaces are in general nonuniform and for the interpretation of spatiotemporal patterns this property represents a serious problem, since it is not evident whether an observed pattern is due to such defects, or whether it is caused by a genuine symmetry breaking. Furthermore, if a surface is nonuniform, the different parts may couple together such that the coupling gives rise to new types of dynamical behavior, different from the properties of each of the isolated subsystems.[196,197] The analysis of spatiotemporal patterns may for such realistic systems therefore become quite complicated, and one relies on methods that allow one to extract the relevant aspects and to simplify the dynamics. One such method is the Karhunen-Loève decomposition into an optimal set of eigenfunctions, also known as proper orthogonal decomposition (POD).[303] This method, which had initially been used to identify coherent structures in turbulent hydrodynamics, has in the meantime also successfully been applied to catalytic surface reactions.[92,144,304]

B. Nonisothermal Systems

1. Supported Catalysts

In strongly nonisothermal reactions heat transfer is usually much faster than diffusional coupling and because of the exponential dependence of rate expressions on temperature, thermal coupling is usually the dominant coupling mode in the high-pressure experiments. In oscillatory reactions at atmospheric pressure, temperature variations of several tens of degrees are frequently found.[305] Thermal conductivity is a decisive factor in these experiments and therefore it is important to distinguish between monolithic catalysts in the form of disks, rings, ribbons, wires, etc., and supported catalysts. Local variations in temperature can be measured either by simultaneous use of several thermocouples or, more conveniently, by infrared thermography, as first introduced by Barelko.[179,306]

Local temperature variations in catalytic CO oxidation on supported catalysts were followed by Wolf and co-workers,[44,45,307,308] Onken and Wicke,[309,310] and in the group of Jaeger and Plath.[311] These experiments demonstrated that the local behavior can deviate quite substantially from integral rate measurements and that the strength of thermal coupling can determine the dynamical behavior of a catalyst. By varying the thermal contact between individual pellets, it was shown that different levels of synchronization can be obtained, ranging from the limiting case where the individual pellets oscillate independently of each other, to complete synchronization.[40,310,311] Traveling heat waves in fixed-bed reactors have been detected by several groups.[26,309,312] Not always, however, is heat transfer the dominant coupling mode, as was demonstrated by Svensson et al., who showed that small amplitude p_{CO} variations suffice to synchronize the local oscillators in a Pd/zeolite catalyst.[275,311]

IR thermography has been applied to reactions on catalytic wafers by Wolf et al.[44,45,308,313] In catalytic CO oxidation on Rh/SiO_2, they observed moving hot spots, but a Karhunen Loève decomposition demonstrated that the underlying dynamics are actually low dimensional.[45] Following the method originally proposed by Ott, Grebogi, and Yorke ("controlling chaos"),[314] Wolf et al. showed that they could stabilize the reaction on the reactive branch by using a video-feedback system to control the CO inlet pressure.[45]

2. Monolithic Catalysts

Depending on the geometry of the catalyst the experiments can be divided into two groups: 1D-like systems such as wires, ribbons, or thin rings, and 2D-like systems on disks, foils, and plates. Typically the catalytic wires and ribbons are electrically heated, while the heating in the case of disks, foils, etc. is provided externally by an oven and/or internally by the reaction heat itself. Instead of using massive metallic catalysts, one can also evaporate a metallic film onto a nonmetallic substrate, as was done by Dath et al., who studied wave propagation in catalytic CO oxidation on a Pt film they had evaporated onto a sapphire substrate.[41]

An experiment that illustrated the effect of coupling on the dynamical behavior was conducted by Tsai et al., who studied rate oscillations in catalytic CO oxidation on a Pt wire heated solely by the exothermicity of the reaction.[39] They showed, by cutting a Pt wire loop into two halves, that the oscillations on the two parts were strongly different from the oscillations on the intact loop. Catalytic reactions on electrically heated wires were investigated in the group of Barelko, who studied the oxidation of NH_3 and ethylene on a Pt wire.[306] They first reported the existence of standing and travelling waves in systems of this kind. Similar studies with improved experimental setups were then continued in the groups of Luss and Schmidt.[316-321] An array of laser diodes was applied to detect thermal fronts in catalytic reactions on a Pt wire.[171] Figure 19 shows the formation of standing wave fronts, which occur in NH_3 oxidation under the constraint of a fixed average temperature.[317] The same group also investigated the endothermic decomposition of CH_3NH_2 on a Pt wire and found traveling waves, as well as independently oscillating segments.[171]

It was pointed out by Sheintuch that conditions of constant voltage or constant average temperature

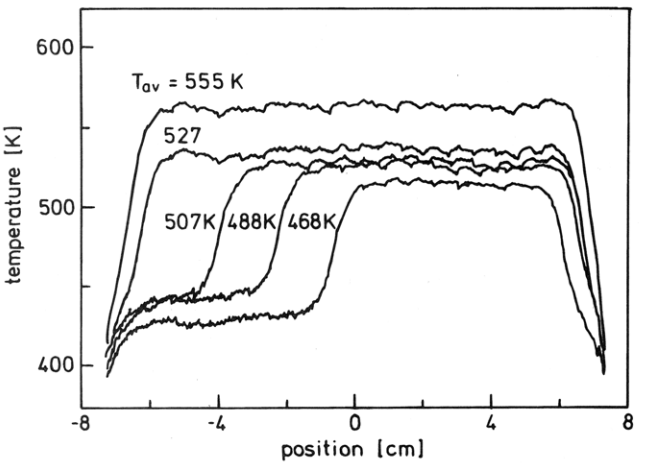

Figure 19. Temperature profiles of a thin Pt ribbon during the air oxidation of ammonia. For fixed average temperature, T_{av}, standing fronts are observed. (Reprinted from ref 317. Copyright 1989 American Chemical Society.)

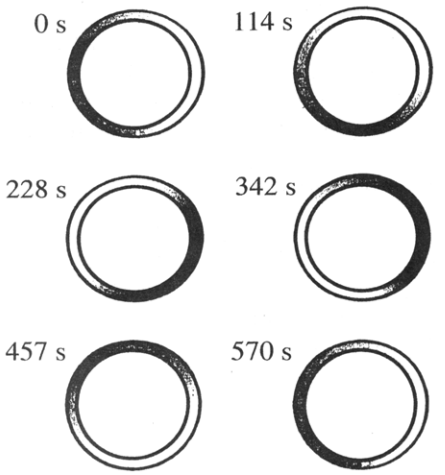

Figure 20. Periodically rotating temperature pulse during H_2 oxidation on a Ni ring of 3.5 cm diameter. The transition from white to black corresponds to a temperature range from 660 to 500 K. (Reprinted from ref 321. Copyright 1993 American Institute of Physics.)

(constant average resistance) represent a global constraint and hence symmetry breaking occurs, leading to spatiotemporal pattern formation.[322,323] The bifurcation diagrams that can be found under different control modes have been established by Luss and coworkers, who studied propylene and ammonia oxidation on an electrically heated Pt ribbon.[317–320] They found stationary patterns, as well as moving fronts, with the latter corresponding to macroscopic rate oscillations. In another experiment in which hydrogen was catalytically oxidized on a nonelectrically heated Ni ring, Luss et al. observed a periodically rotating temperature pulse of ~100 K amplitude.[321,324] As shown in Figure 20, depending on the angular position, the pulse changes its velocity and shape. This change is reflected by macroscopic oscillations in the reaction rate.

In 2D systems the resulting spatiotemporal patterns are in general more complex than in 1D. D'Netto and Schmitz used IR thermography to image the $H_2 + O_2$ reaction on a Pt foil, and they observed centers of activity, as well as the spreading of reaction zones.[325,326] Complex patterns were also found in the $H_2 + O_2$ reaction on a Ni disk by Luss et al.[304] Applying a Karhunen–Loève decomposition to the measured patterns, they were able to identify two pacemakers in the edge zone of the disk.

3. Thermokinetic Models

The analysis of pattern formation in nonisothermal systems is usually based on so-called thermokinetic models.[302,327–330] These models rely on the assumption that the dominant effects are caused by the exothermicity of the reaction and by heat diffusion. Consequently, the chemistry of the reaction is reduced to a single variable and surface diffusion of adsorbates is neglected. The basic equations have the form

$$\epsilon\frac{\partial T}{\partial t} - \frac{\partial^2 T}{\partial x^2} = f(T,\theta,I) = Q_R - Q_{Ex} + Q_H(I)$$

$$\frac{d\theta}{dt} = g(\theta,T)$$

In the term $f(T,\theta,I)$ which describes the heat balance, Q_R is the heat generated by the reaction, Q_{Ex} is the energy exchange with the surroundings and $Q_H(I)$ represents the heat generated by electric heating with current I. The term $g(\theta,T)$ describes the chemistry of the surface reaction, which usually only incorporates the most important effects such as, for example, the blocking of reactive sites by a slowly desorbing species.

A general analysis of the bifurcation diagrams in exothermic reactions with a simple unimolecular step has been conducted by Vance and Ross.[331] Various forms of the thermokinetic model depicted above have been analyzed by Barelko et al.[329,330] and by Sheintuch, Luss, and co-workers.[302,327,328] The latter group performed extensive numerical simulations of the type of patterns one obtains in electrically heated wires or ribbons. A large variety of solutions was found, including stationary fronts, oscillating fronts that move unidirectionally or in a back-and-forth motion, breathing pulses, and irregular patterns, with the latter corresponding to chaotic time series.

C. Chemical Wave Patterns on Single Crystal Surfaces

1. Catalytic CO Oxidation

The first spatially resolved experiments that demonstrated the existence of propagating reaction fronts in an isothermal oscillatory reaction on a single crystal surface were conducted with the so-called scanning LEED technique in Pt(100)/CO + O_2.[56,57] Subsequently, experiments with two Kelvin probes were also conducted to demonstrate coupling effects between different regions of an oscillating single crystal surface.[49,81,96] All these experiments had in common a rather poor spatial resolution of around 1 mm. The breakthrough in the study of pattern formation on single crystal surface came with the introduction of photoemission electron microscopy (PEEM), yielding a spatial resolution of about 0.2 μm and the temporal resolution of video images (40 ms).[180]

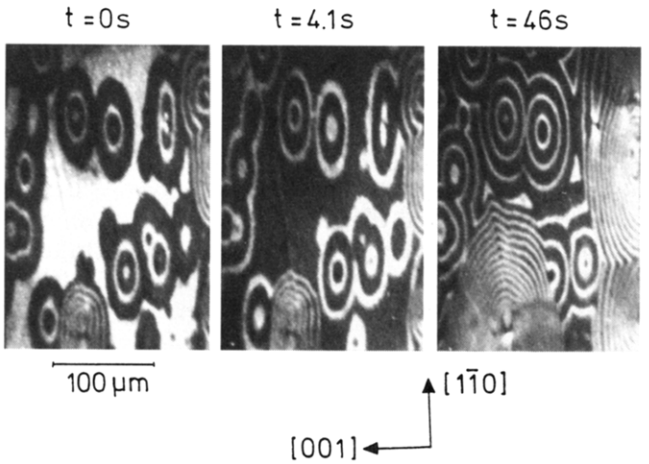

Figure 21. PEEM images showing the development of target patterns with different trigger frequencies during kinetic oscillations in CO oxidation on Pt(110). The experimental conditions are $T = 427$ K, $p_{CO} = 3 \times 10^{-5}$ mbar, and $p_{O_2} = 3.2 \times 10^{-4}$ mbar. Dark areas in the image correspond to an oxygen covered; bright areas, to a CO covered or bare surface. (Reprinted from ref 82. Copyright 1990 American Institute of Physics.)

Nearly all Pt and Pd single crystal reaction systems that exhibit rate oscillations have since then also been investigated with PEEM. The result was that all oscillatory systems exhibit spatiotemporal pattern formation, but with a strongly varying degree of regularity. The regularity in the patterns is reflected in the regularity of the rate oscillations. The latter is mainly determined by the efficiency of gas-phase coupling, since this coupling mode is responsible for the long-range synchronization of an oscillating surface.

By far the richest variety of spatiotemporal patterns has been found in catalytic CO oxidation on Pt(110).[13,82–84,91,92] Here target patterns, rotating spiral waves, solitary oxygen pulses, standing waves, and chemical turbulence have been found. A series of PEEM images showing target patterns in this reaction system is displayed in Figure 21. Several pacemakers, which periodically emanate waves with different frequencies, are seen surrounded by a homogeneously oscillating background. The contrast in these images is due to the high work function difference of ~300−500 meV, between a CO covered (bright) and an oxygen covered (dark) surface. The elliptical shape of the target patterns reflects the anisotropy in the surface diffusion of CO, which is fast along the (110)-oriented troughs and slow perpendicular to them (see Figure 5).[299]

The uniformly oscillating background seen in Figure 21 reflects the synchronizing effect of gas-phase coupling. At higher temperature ($T > 500$ K), one finds a new type of pattern, which has to be attributed to the dominance of gas-phase coupling, namely the occurrence of standing wave patterns, as displayed in Figure 22.[82,84] In this figure the waves have the form of stripes, but the dynamical dislocations separating different regions of coherent dynamical behavior can also grow together, such that a 2D rhombic pattern is generated.

In contrast to Pt(110), no regular patterns are found on Pt(100).[59,65] Gas-phase coupling apparently plays no role for the oscillations on this surface, and

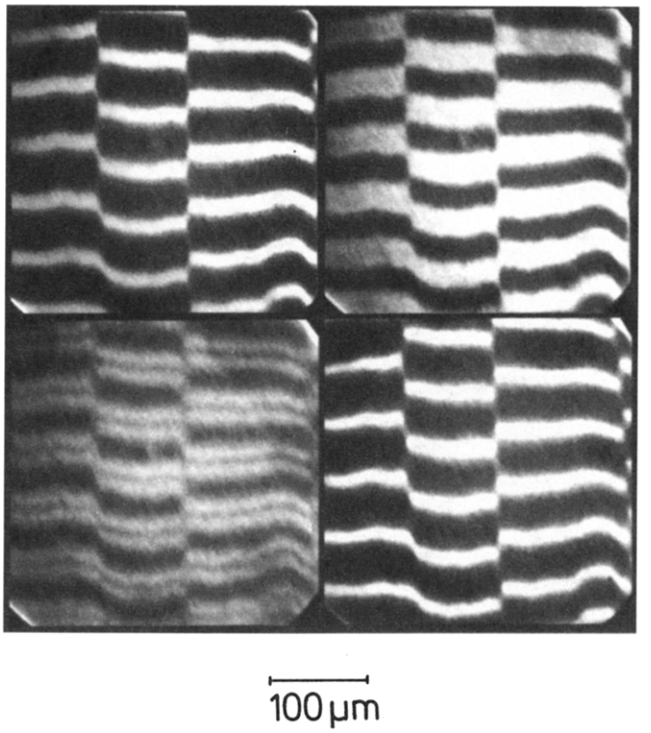

Figure 22. Standing wave patterns accompanying rapid kinetic oscillations in CO oxidation on a Pt(110) surface. The PEEM images which represent an area of 0.3 × 0.5 mm^2 were recorded at intervals of 0.5 s. Experimental conditions: $T = 550$ K, $p_{O_2} = 4.1 \times 10^{-4}$ mbar, $p_{CO} = 1.75 \times 10^{-4}$ mbar. (Reprinted from ref 82. Copyright 1990 American Institute of Physics.)

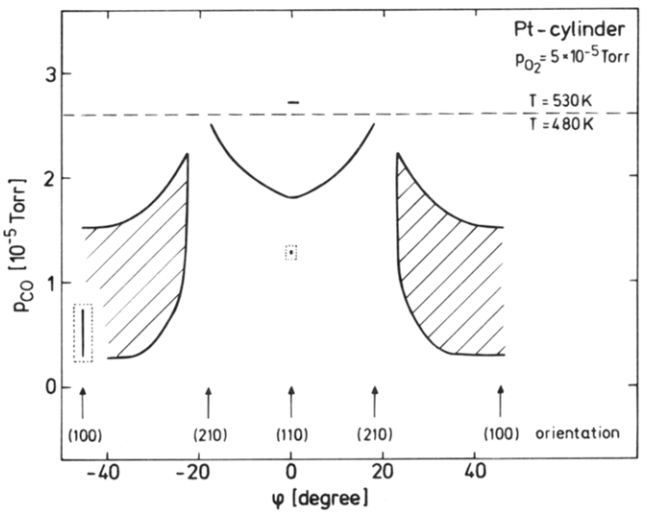

Figure 23. Orientational dependence of the existence range of kinetic oscillations (shaded area) in catalytic CO oxidation on the cylindrical Pt surface at $T = 480$ K and $p_{O_2} = 5 \times 10^{-5}$ Torr. Due to the narrowness of the existence range (in p_{CO}) in between (110) and (210), the width had to be represented by a single line in the plot. The bars encircled by dotted lines represent the existence range for oscillations on plane single crystal surfaces. (Reprinted from ref 96. Copyright 1992 American Institute of Physics.)

the reason is easily seen in the much wider existence range for oscillations shown in Figure 8, which makes the surface less sensitive to small partial pressure variations.[78] The aperiodic oscillations seen typically on Pt(100) are a consequence of this lack of synchronization. In catalytic CO oxidation on Pd(110), synchronization via gas-phase coupling has been

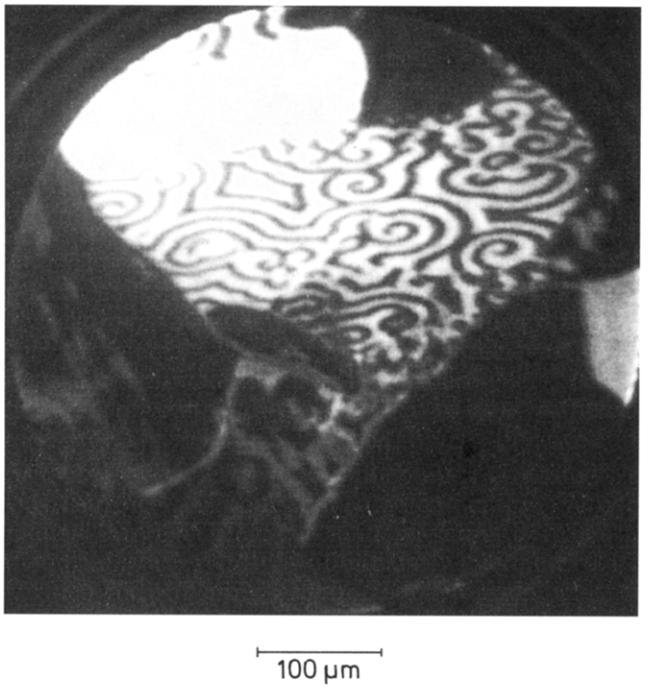

Figure 24. PEEM image from a polycrystalline Pt sample showing different types of behavior for different grains in catalytic CO oxidation. Some type of spiral turbulence is found on (110) grains, while other grains simply display steady-state behavior, i.e. they are either CO covered or oxygen covered. Experimental conditions: $T = 419$ K, $p_{O_2} = 4 \times 10^{-4}$ mbar, $p_{CO} = 2.43 \times 10^{-5}$ mbar. (Reprinted from ref 174. Copyright 1993 Elsevier Science Publishers B.V.)

demonstrated by cutting the crystal into two parts and following the oscillations on the two parts separately.[49]

Coupling effects and spatiotemporal pattern formation have also been investigated on structurally inhomogeneous surfaces. The competition between gas-phase coupling and diffusive coupling via reaction fronts was studied on the cylindrical Pt sample, which exhibited all orientations of the [001] zone, by means of two rotateable Kelvin probes and by PEEM.[96,97] It was found that oscillations in the less reactive region around (100), were initiated by waves, which were triggered at the more reactive zone around (210) and then traveled toward (100). As can be seen from Figure 23, this coupling effect caused a substantial broadening of the existence range for oscillations (in parameter space), as compared to a flat Pt(100) sample. In PEEM experiments with a polycrystalline Pt foil, different grain orientations corresponding to three low-index planes of Pt could be identified from their reactivity and from the characteristics of spatiotemporal pattern formation, known from single crystal studies.[174,175] A PEEM image showing spiral formation on a (110) grain is displayed in Figure 24.

Details of front propagation on Pt(100) have been made visible in the group of Bradshaw, using a combination of PEEM, LEEM, MEM and small-area LEED (sampled area 18 μm diameter) measurements.[69-72] If a CO-saturated layer is titrated with oxygen, the reaction fronts slow down at step edges, while the propagation is fast on terraces, resulting in a kind of stop-and-go motion. The front profile consists of a sequence of ordered CO overlayers, as shown in Figure 25. The experimental observations can be explained with a slowing down of CO diffusion across steps and with the existence of interactions between the CO adparticles, causing a strong coverage dependence of the CO diffusion constant.[72]

2. Catalytic NO Reduction

a. NO Reduction on Pt(100). Pattern formation in the NO + CO reaction on Pt has been investigated by Veser et al. with PEEM, on a plane Pt(100) surface and on a cylindrically shaped Pt single crystal surface (axis II [001]).[136,140-144] On the cylindrical Pt surface, dynamical patterns and hence oscillatory behavior were found to be restricted to a narrow orientational range around (100) and thus very similar to Pt(100).[136,141] In the lower lying of the two T windows for oscillations (see Figure 16), one observes periodic wave trains of the type depicted in Figure 26a, as well as spiral waves. Apparently no long-range synchronization and hence no rate oscillations exist.

A characteristic feature of the NO + CO reaction on Pt is its strong structural sensitivity. This property is also reflected in the chemical wave

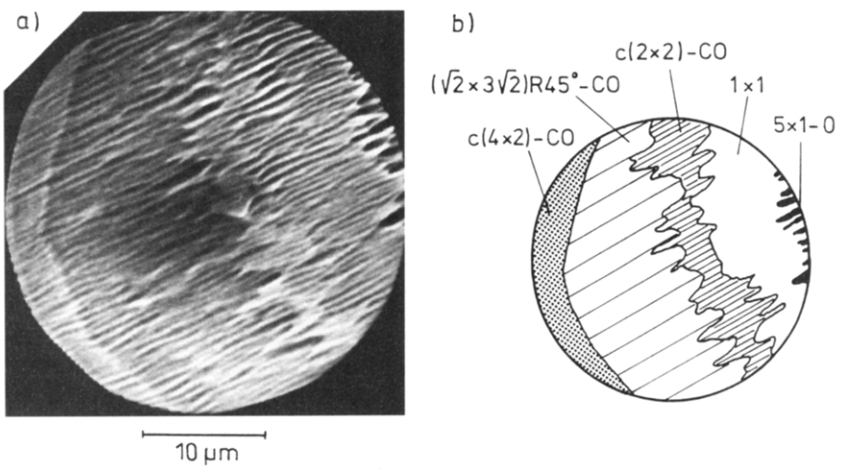

Figure 25. Mirror electron microscopy (MEM) image showing various adsorbate phases in the front profile as a CO adlayer in Pt(100) is reactively removed by oxygen ($p_{O_2} = 2 \times 10^{-6}$ mbar). The different gray levels in a correspond to various adsorbate phases as is indicated schematically in b. The surface roughness seen in the image is due to step bunches oriented along the diagonal. (Reprinted from ref 69. Copyright 1993 Elsevier Science Publishers B.V.)

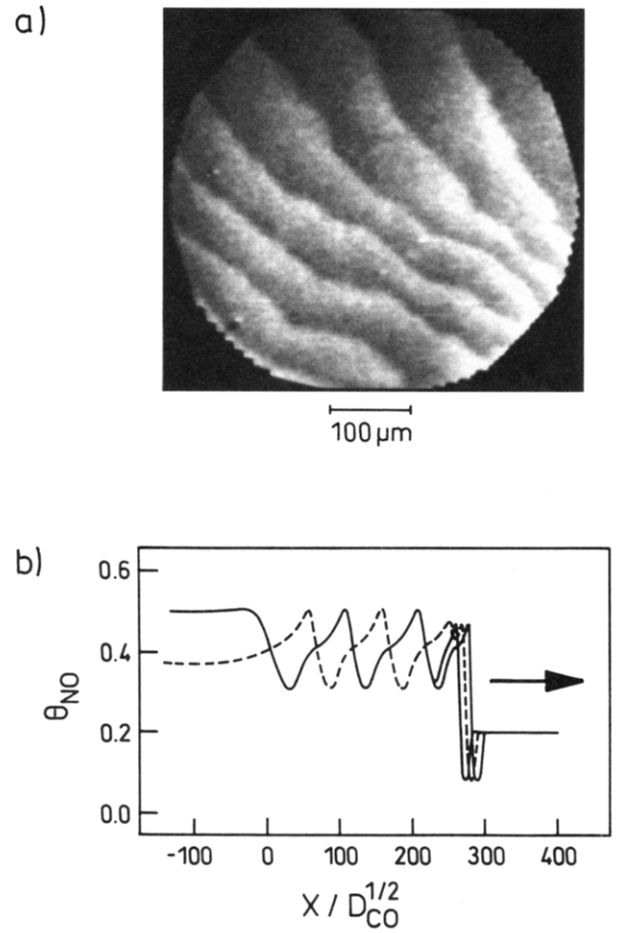

Figure 26. Chemical waves in the NO + CO reaction on Pt(100)−1 × 1: (a) Experiment. PEEM image showing the formation of periodic wave trains propagating with a few micrometers per second. Experimental conditions: $T = 423$ K, $p_{NO} = 4 \times 10^{-6}$ mbar, $p_{CO} = 2 \times 10^{-6}$ mbar. (b) Simulation. The three-variable model for the NO + CO reaction on Pt(100)−1 × 1 was used to simulate the occurrence of periodic wave trains. (a: Reprinted from ref 141. Copyright 1994 American Institute of Physics. b: Reprinted from ref 138. Copyright 1992 American Institute of Physics.)

patterns, because defects often act as trigger centers for waves, or determine the path of propagating reaction fronts. The structural sensitivity of the NO + CO reaction is clearly also the reason why a high degree of irregularity is seen in the patterns on the cylindrical Pt surface.[136] By using a Karhunen−Loève decomposition, it was demonstrated by Graham et al. that the apparently complex patterns on this surface can be decomposed into a small number of modes, i.e. the actual dynamics of the reaction are low dimensional.[144]

Gas-phase coupling apparently plays no role in the lower T window for oscillations, but this mode becomes efficient in the upper T window, leading there to a spatially homogeneous surface (see Figure 17).[140,142] The involvement of the $1 \times 1 \rightleftarrows$ hex phase transition in the oscillation mechanism at higher temperature, was regarded as being decisive for the high efficiency of gas-phase coupling, since the dependence of the phase transition on critical coverages implies a high sensitivity to small partial pressure variations.[257] As shown by Figure 17, with decreasing temperature, the rate oscillations collapse in a discontinuous transition. This transition, which indicates the breakdown of global coupling, takes place as surface defects become supercritical and start to emit waves.[140]

Both the NO + H_2 and the NO + NH_3 reactions on Pt(100) have been the subject of PEEM investigations. Under nonoscillatory conditions, Mundschau and Rausenberger studied front propagation in the NO + H_2 reaction, initiating the reaction fronts by a decrease of p_{NO}.[148] In the NO + NH_3 reaction, one encounters a sequence of different patterns indicating various levels of synchronization, as the temperature window for oscillations is traversed.[159] As indicated in Figure 27 similar to the NO + CO reaction, one finds at high-temperature rate oscillations on a uniformly reacting surface, but with decreasing temperature pattern formation occurs, until finally, the patterns break up into small domains representing a state of chemical turbulence.

b. Rh(110)/NO + H_2. The Rh(110) surface has been the subject of a number of STM studies, owing to the large number of different adsorbate-induced reconstructions one finds on this surface.[332,333] Oscillatory behavior in the NO + H_2 reaction on Rh has been observed in a FEM study by Nieuwenhuys et al.[11,155,161] In a PEEM investigation of this reaction on a Rh(110) surface, rectangularly shaped chemical wave patterns were found—a geometry which so far has not been seen in any other fluid phase or surface reaction system.[153,154] Figure 28 displays the rectangular-shaped target patterns and spiral waves whose sides are oriented along the main crystallographic axes of Rh(110).

While simple anisotropic diffusion, i.e. an anisotropy which can be removed by rescaling the coordinates, just leads to elliptically deformed patterns, the unusual geometries seen here have to be attributed to a state-dependent anisotropy, i.e. an anisotropy that varies along the concentration profile of a chemical wave.[300] In the system Rh(110)/NO + H_2, such a state-dependent anisotropy for surface diffusion is realized by the presence of adsorbate-induced reconstructions with varying substrate geometries. Simulations, which were based on a simple activator−inhibitor model, could reproduce the rectangular shape of the patterns, by taking such a state-dependent anisotropy into account.[154]

D. Analysis of Chemical Wave Patterns

1. Introduction

For classifying different types of chemical wave patterns, it is convenient to distinguish between (i) bistable, (ii) excitable, and (iii) oscillatory media.[293] In bistable media, the transition between two stable steady states may occur via a propagating reaction front, i.e. the interface separating the two states moves such that the less stable state is displaced.

In excitable media, an external perturbation of sufficient amplitude is required in order to stimulate the system to a strong dynamic response.[293−295] After excitation the system returns to its initial state, from where it can be excited again. Pulses and spiral

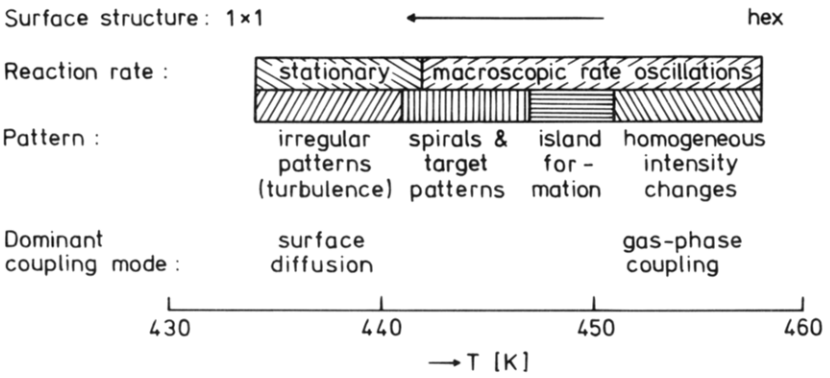

Figure 27. Schematic overview of the temperature ranges in which macroscopic rate oscillations and different types of spatial patterns are observed in the NO + NH_3 reaction on Pt(100). (Reaction conditions: $p_{NO} = 1.1 \times 10^{-6}$ mbar, $p_{NH_3} = 1.6 \times 10^{-6}$ mbar, pumping rate ≈60 L/s). (Reprinted from ref 159. Copyright 1992 J. C. Baltzer AG.)

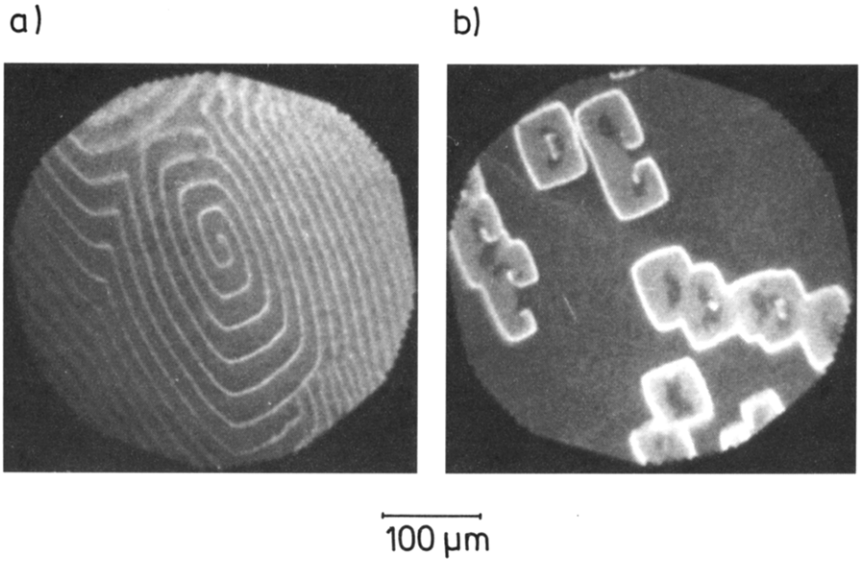

Figure 28. PEEM images showing the formation of rectangularly shaped spiral waves (a) and target patterns (b) in the NO + H_2 reaction on Rh(110). Experimental conditions are $T = 560$ K, $p_{NO} = 1.8 \times 10^{-6}$ mbar, and $p_{H_2} = 5.3 \times 10^{-6}$ mbar for a and $T = 620$ K, $p_{NO} = 1.8 \times 10^{-6}$ mbar and $p_{H_2} = 5 \times 10^{-6}$ mbar for b. (Reprinted from ref 154. Copyright 1994 American Institute of Physics.)

waves are phenomena characteristic for excitable media. In contrast to excitable media, which require an external stimulus, oscillatory media have their own natural frequency, which is the essential experimental criterion for distinction.

For a theoretical description of chemical waves, the kinetic equations have to be complemented by a diffusion term, such that a system of coupled partial differential equations results:

$$\frac{\partial c_i}{\partial t} = F_i(\mathbf{c},p,T) + D_i\frac{\partial^2 c_i}{\partial x^2}$$

For a more realistic description of surface diffusion, the simple Laplacian has to be replaced by $\partial/\partial x[D_i(\mathbf{c})\ \partial c_i/\partial x]$ which takes into account the coverage dependence of D_i. Similarly, for anisotropic diffusion, separate diffusion terms have to be formulated for each direction. To simplify the analysis, the partial pressures, p_i, are often treated as constants, but in order to account for global coupling, the above equations have to be complemented by additional equations for p_i, representing mass balance in the reaction.

In the theoretical description, one can rely on concepts borrowed from the study of oscillatory fluid phase reactions, but anisotropic diffusion, global coupling or coverage dependent diffusion also add some basically novel effects. Pattern formation on single crystal surfaces has been analyzed quite intensely for catalytic CO oxidation on Pt surfaces,[7-10] while catalytic NO reduction on Pt(100) and Rh(110) is treated in only a few papers.[138,139,154] The first simulation of chemical waves on a single crystal system was conducted for Pt(100)/CO + O_2, based on the four-variable model for the kinetics, complemented by a CO diffusion term.[56] These 1D calculations were subsequently continued with 2D simulations by Möller et al. and by Kapral et al.[60,66] Most analyses and simulations, however, focus on catalytic CO oxidation of Pt(110), which is the system where most of the intriguing phenomena have been found.

2. Bistability

In a bistable system both states can coexist only at the equistability point, while at other parameter values, the less stable state is pushed out by a moving interface.[230,293,334] Such a bistable system, for example, is given by catalytic CO oxidation on Pt(111),

where a predominantly oxygen-covered and a predominantly CO-covered surface represent the two stable states. A theoretical analysis for this system yielding the parameter dependence of the front velocity has been conducted by Bär et al., based on the two-variable model for catalytic CO oxidation.[335] Experimentally front propagation in Pt(111)/CO + O_2 was studied by Berdau et al. with PEEM.[336]

On the basis of elementary considerations, it can be be shown that the curvature dependence of front velocity, c_f, obeys the relation $c_f = \overset{\circ}{c}_f \pm D/R$.[293] In this formula $\overset{\circ}{c}_f$ represents the velocity of a plane wave front, D the diffusion constant, and $1/R$ the curvature, with the $\pm$ sign depending on whether the front is concave or convex. From this relation, a property can be deduced, which is crucial for the understanding of pattern formation on surfaces, namely the critical radius, r_c, for front nucleation. r_c can be obtained by setting $c_f = 0$. Using reasonable experimental values for CO diffusion, the critical radius in CO oxidation on Pt can be estimated to be of the order of ~ 1 μm.[335] Accordingly, only macroscopic defects, but not atomic scale defects like steps can initiate reaction fronts.

3. Pulses and Spiral Waves

In an excitable medium the excitation is usually confined to a small region of space propagating with a certain velocity.[293] The 1D solution is denoted a pulse, while in 2D, the excitation region typically expands forming a rotating spiral wave. Both pulses and spiral waves have been found in surface reactions.

Experimentally oxygen pulses were initiated in catalytic CO oxidation on Pt(100), by desorbing locally with a laser pulse some CO from the CO covered surface, such that a reaction nucleus was formed.[63] In catalytic CO oxidation on Pt(110), PEEM measurements showed the existence of both CO and oxygen pulses.[83,91] A theoretical analysis based on the three-variable model demonstrated that pulses exist in the parameter regions adjacent to the oscillatory range.[87]

In catalytic CO oxidation on Pt(110), solitary oxygen pulses, which travel with constant shape and velocity along the [001] direction, were observed.[83] These oxygen pulses exhibit a remarkable behavior, since it was seen that, in some cases, two pulses which collide do not annihilate, but continue their journey with unchanged properties. The pulses thus display soliton-like behavior shown in Figure 29a. The soliton-like behavior was attributed to the influence of surface defects. As demonstrated by Figure 29b, 1D simulations based on the three-variable model could substantiate this interpretation. If two oxygen pulses in the simulation happen to collide near a structural defect, i.e. a region with a higher s_{O_2}, then the excitation survives, generating two new pulses.[88] The stable shape of the oxygen pulses in the experiment which do not form spirals, has been traced back to a state-dependent anisotropy of surface diffusion.[337]

Spiral waves are ubiquitous in reaction−diffusion systems. They are found in the BZ reaction, as well as in cardiac tissue and slime mold aggregation.[292−295]

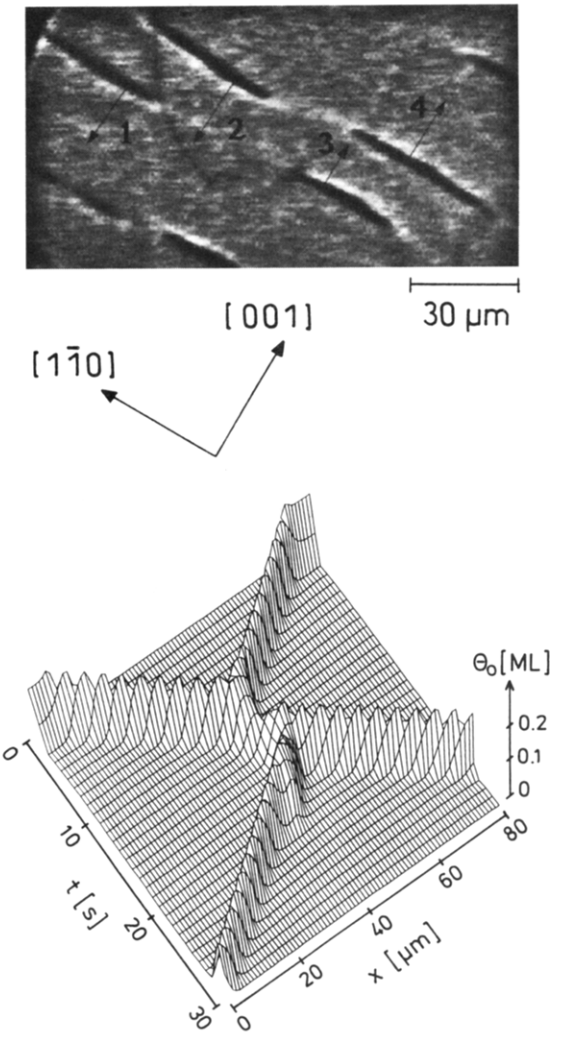

Figure 29. Soliton-like behavior of oxygen pulses during catalytic CO oxidation on a Pt(110) surface: (a) Experimental PEEM image demonstrating the propagation of stable oxygen islands, visible as black elongated bars on a CO-covered surface. The islands propagate with a velocity of ~ 3 μm/s along the (001) direction, as indicted by the arrows. The experimental conditions were $T = 485$ K, $p_{CO} = 1 \times 10^{-4}$ mbar, and $p_{O_2} = 3.5 \times 10^{-4}$ mbar. (b) Model calculations demonstrating the soliton-like behavior that results when two oxygen pulses interact near or at a surface defect. (a: Reprinted from ref 83. Copyright 1990 American Institute of Physics. b: Reprinted from ref 88. Copyright 1992 American Institute of Physics.)

Due to their widespread occurrence, they have also attracted a large amount of theoretical interest. Most of the properties of spiral waves can be rationalized within the so-called kinematic approximation, as worked out by Mikhailov and Zykov and by Keener and Tyson.[338,339]

In nearly all oscillatory surface reactions investigated so far on single crystal surfaces, spiral waves have been found. A typical image showing spirals with different rotation periods in the system Pt(110)/CO + O_2, is displayed in Figure 30.[91] At first sight it seems surprising that spirals in this system do not exhibit equal properties, but the different characteristics are due to the fact that these spirals are not free but pinned to defects.[340] Even on a well-prepared single crystal both microscopic as well as macroscopic structural defects are present. While the former ones are represented by atomic steps and dislocations, the

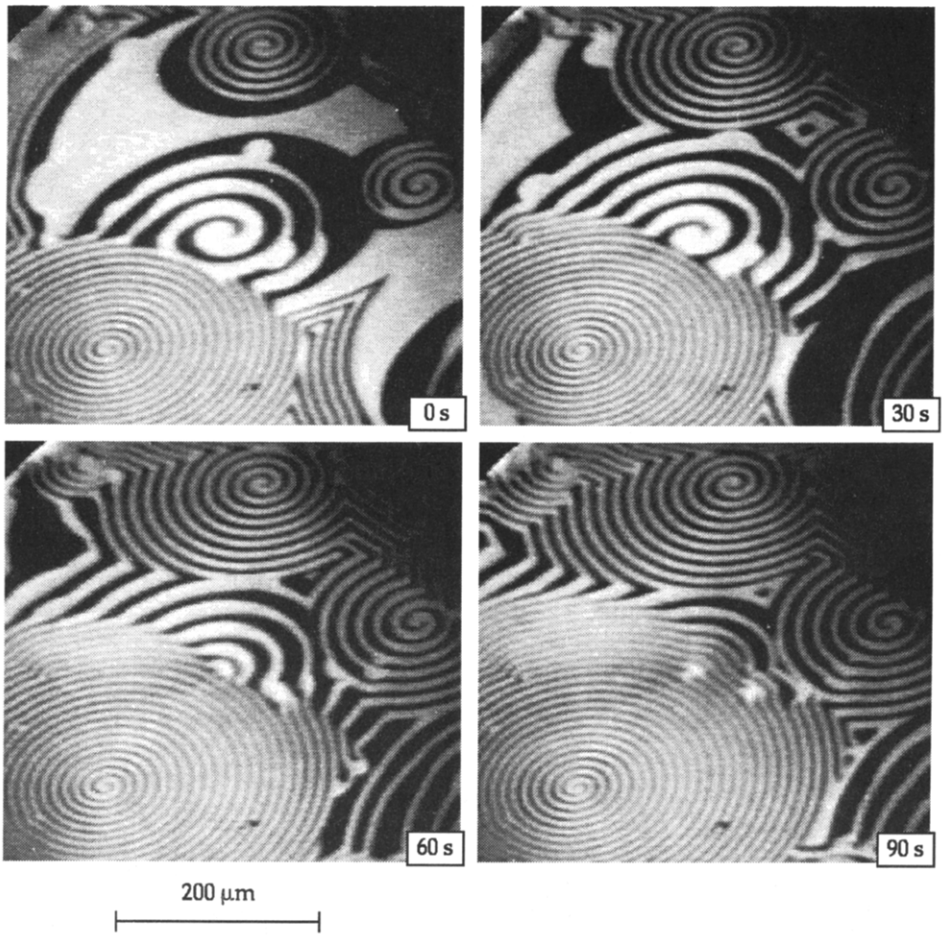

Figure 30. PEEM images demonstrating the temporal evolution of spirals with strongly different rotation periods and wavelengths during CO oxidation on Pt(110): $T = 448$ K, $p_{CO} = 4.3 \times 10^{-5}$ mbar, and $p_{O_2} = 4 \times 10^{-4}$ mbar. The spiral with the largest wavelength rotates around a core of 25×14 μm^2, while the size of the core region for the fast rotating spiral visible in the foreground is only 5×3 μm^2. (Reprinted from ref 91. Copyright 1993 American Institute of Physics.)

latter ones may be simply given by polishing scratches. As far as the nucleation of wave fronts or the pinning of spirals is concerned only the macroscopic defects are of relevance. As has been worked out by Keener and Tyson, the different rotation periods result from differently sized core regions, i.e. defects around which the spirals rotate.[338] Both single-armed, as well as multiarmed spirals, have been observed on surfaces. In a theoretical paper by Bär and Eiswirth, it was shown that, under certain conditions, spiral waves may become unstable.[341,342] The spirals break up into smaller fragments until finally a state of chemical turbulence is reached.

On surfaces the spiral waves are frequently pinned to defects, but one can unpin these spirals by applying a periodic parameter modulation. As predicted by Mikhailov, resonance effects similar to the periodic forcing of an oscillating system occur, and one obtains freely traveling spirals.[293] Experimentally such a depinning has been realized for the spirals in Pt(100)/$CO + O_2$, by applying a small T modulation.[91,340]

4. Global Coupling

In catalytic CO oxidation, gas-phase coupling leads to a synchronized oscillating state, since a positive feedback exists between the transitions in LH kinetics and the concomitant variations in the partial pressures.[343,344] The synchronizing influence of gas-phase coupling is best illustrated by the standing waves found in Pt(110)/$CO + O_2$ (see Figure 22).[82] On the basis of an analysis of the three-variable model, Levine and Zou explained the occurrence of standing waves as being due to parametric resonance.[89] Their simulation can, however, not be considered as fully realistic, since they treated global coupling in the equations in an inadequate way. Simulations in which gas-phase coupling was treated in a realistic way were performed by Falcke et al., and they were able to demonstrate that gas-phase coupling indeed generates standing waves in Pt(110)/$CO + O_2$.[343]

Depending on the kind of feedback that exists between the surface reactions and the gas phase, global coupling may stabilize or destabilize the homogeneously oscillating state. This was first pointed out by Sheintuch, who showed that global coupling may induce symmetry breaking, i.e. generate pattern formation.[345] A systematic analysis of the various generic cases that can occur in an oscillatory medium with global coupling, has been conducted by Mikhailov et al., on the basis of a modified complex Ginzburg–Landau (CGL) equation.[140,346,347]

The CGL equation describes quite generally the behavior of an ensemble of small amplitude harmonic oscillators, independent of the characteristics of a particular model. This condition is fulfilled in the vicinity of a Hopf bifurcation, and therefore, the CGL

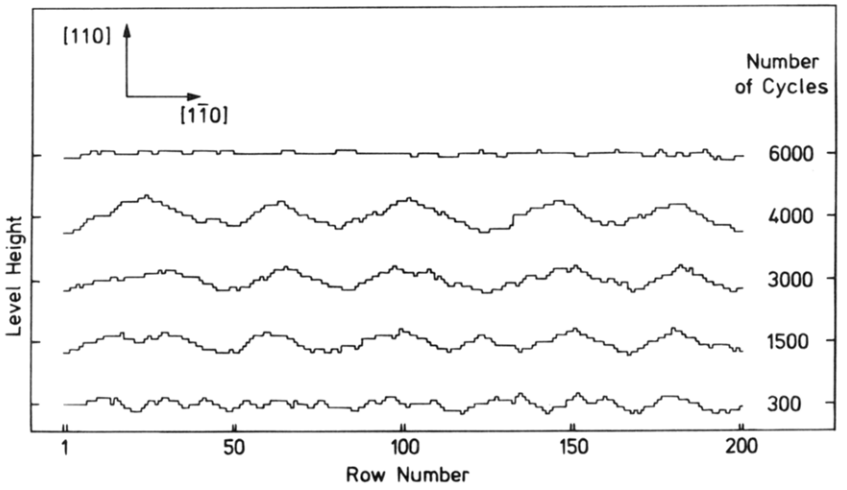

Figure 31. Monte Carlo simulation showing the development of a regular facet structure during catalytic CO oxidation on a Pt(110) surface. The faceting is followed by a restoration of the flat surface after stopping the gas flow after 4000 cycles. (Reprinted from ref 263. Copyright 1991 American Institute of Physics.)

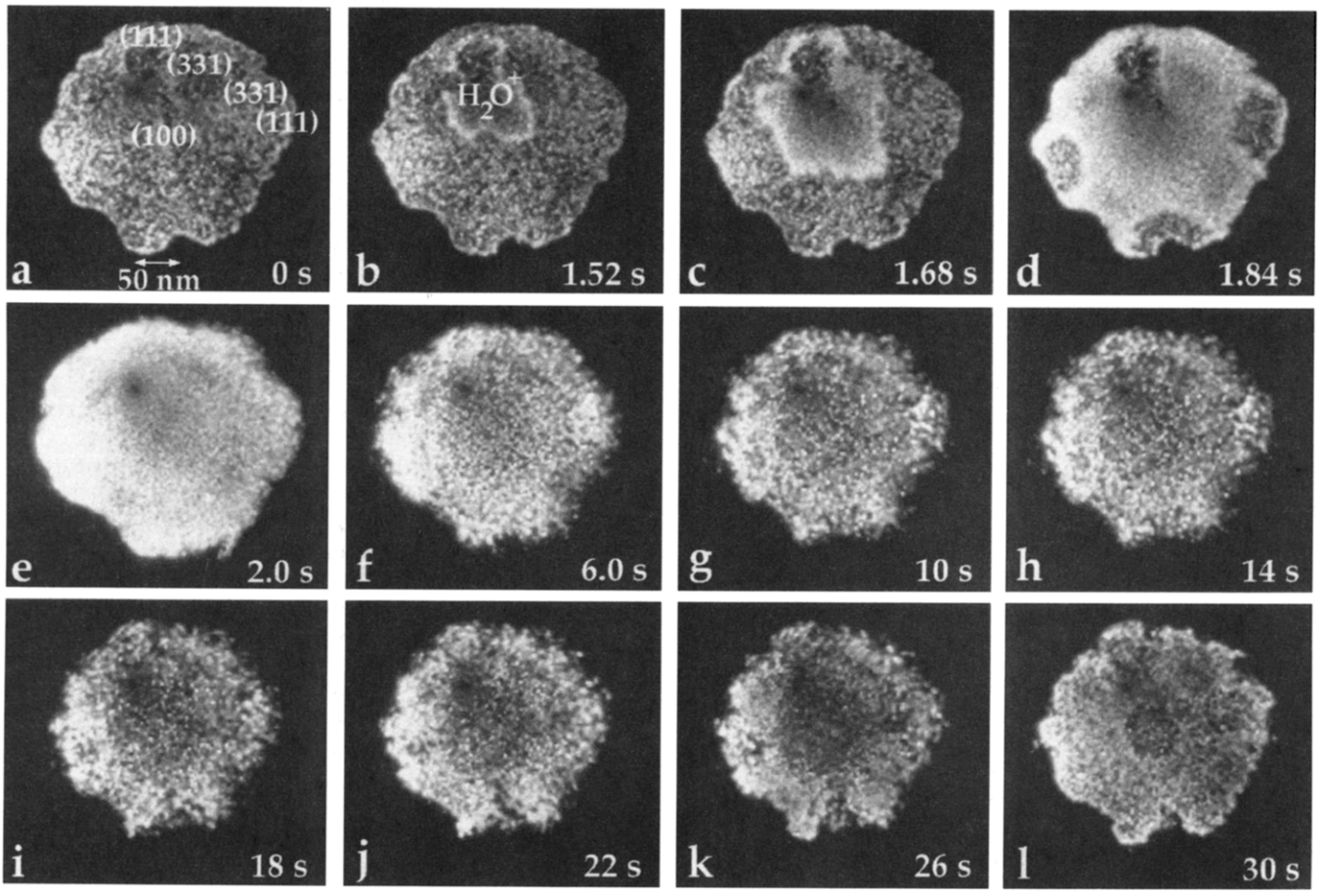

Figure 32. Field ion microscopy (FIM) images from a Pt tip with 180 nm radius under constant conditions of catalytic oxidation of hydrogen: $p_{H_2} = 6 \times 10^{-4}$ mbar. $p_{O_2} = 5 \times 10^{-4}$ mbar. $T = 300$ K. Field strength $F = 1.5 \times 10^8$ V/cm; imaging gases are O_2 and H_2O formed by the reaction. Periodic variation of the local surface composition via propagating concentration waves: (a) At $t = 0$ the surface is uniformly covered by O_{ad}; (b–e) nucleation of a region with high reactivity which rapidly propagates; (f–i) formation of the (inactive) H_{ad} layer; (j–l) restoration of the O_{ad}-covered surface. (Reprinted from ref 111. Copyright 1994 Nature.)

equation exhibits universal validity. It was shown that, if global coupling destabilizes the homogeneous state, the oscillating medium breaks apart into ("Ising-like") domains, that oscillate with opposite phases. Furthermore, if the system without global coupling exhibits turbulence, then global coupling may suppress turbulence, leading to the formation of standing waves or modify the turbulence, such that, for example, spatiotemporal intermittency results.[347]

5. Turing Structures

Stationary concentration patterns in a reaction–diffusion system had been predicted more than 40 years ago by A. M. Turing,[297] but it was only recently that these "Turing structures" could also be identified

in experiment. Clearcut evidence for Turing structures was found in two sets of experiments one being the faceting of Pt(110) in CO + O_2[261] and the other one a BZ-type reaction conducted in a gel reactor.[348] The difficulty in finding such structures in fluid phase reaction systems stems from the very nature of a Turing instability, which is that the diffusion rates of the reacting species have to differ drastically, i.e. typically a fast diffusing inhibitor species has to be present simultaneously with a slow diffusing activator species.[192,293] In liquid phase, however, all substances diffuse about equally fast.

On surfaces the diffusion constants can vary enormously, and Turing instabilities should arise in principle quite readily. So far, only the faceted Pt(110) surface has been identified unambiguously as a dissipative structure of the Turing type. The essential points in classifying the faceted Pt(110) surface as a Turing structure have been that (i) faceting only occurs under reaction conditions and that (ii) the facets are arranged in a regular way forming a sawtooth-like pattern with a lateral periodicity of ~200 Å.[74,261,265] The determination of the periodic structure was the result of a quantitative LEED profile analysis, conducted with a high-resolution instrument of ~2000 Å transfer width.[261]

In order to confirm this interpretation, a Monte Carlo simulation has been conducted, based solely on the LH scheme of catalytic CO oxidation, the properties of the $1 \times 1 \rightleftarrows 1 \times 2$ phase transition, and the enhancement of oxygen adsorption at step sites.[263] As has already been demonstrated by Figure 6, the elementary mechanism in creating steps is the mass transport associated with the phase transition. In the simulation, these processes were implimented by periodically interrupting the surface reaction and rearranging the surface structure according to the local distribution of CO. As demonstrated by Figure 31, the simulation reproduces rather well the formation of facets.

E. Atomic Scale Experiments

While PEEM and related techniques yield only mesoscopic (>1 μm) resolution, field electron microscopy (FEM) and field ion microscopy (FIM), offer the possibility of coming close to atomic resolution. The first experimental demonstrations that FEM can be used as an in situ technique to follow oscillatory surface reactions, were accomplished in the groups of Block and Nieuwenhuys.[11,12] Gorodetskii et al., managed to observe oscillatory behavior in catalytic CO oxidation on a Pt field emitter tip (FET) in the 10^{-4} mbar range.[12] They observed a periodic expansion and concentration of the oxygen and CO covered areas, achieving a lateral resolution of ~20 Å. Similar experiments were conducted in the group of Nieuwenhuys, who used FEM to study oscillatory behavior in the reduction of NO with H_2 and NH_3 on a Rh field emitter tip.[11,155,161]

Again by Gorodetskii et al., it was subsequently shown, that FIM also could be applied, if the reacting gas itself is used to image the surface.[99,100] In a similar manner, NO was used as the imaging gas by Kruse et al. in the oscillatory NO + H_2 reaction on

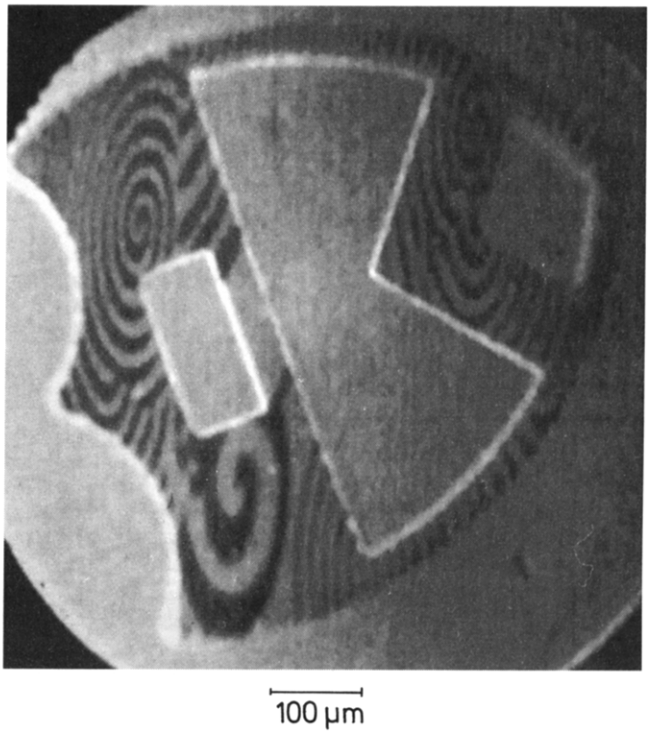

Figure 33. PEEM image showing spiral wave formation on a Pt(110) surface partially covered with a Ti/TiO_2 mask. Pattern formation is only observed in area not covered by the Ti/TiO_2 layer, which in this particular example was given the shape of the Princeton shield. Experimental conditions: T = 440 K, $p_{O_2} = 4 \times 10^{-4}$ mbar, $p_{CO} = 5 \times 10^{-5}$ mbar (unpublished results).

Pt.[152] If not the educt, but the product molecules are the imaging gas, then FIM can be applied to directly image the catalytically active sites. This was demonstrated with the H_2 + O_2 reaction on Pt. Interestingly, here two desorbing species, H_2O^+ and H_3O^+, were identified by mass spectrometry and by the appearance potential for their formation.[110,111,173] Quite remarkably, this reaction only showed oscillatory behavior in the field emitter experiments, while so far no oscillations have been found on macroscopic Pt single crystal planes. In Figure 32a, a sequence of FIM images recorded in situ at 300 K demonstrates the oscillatory expansion and contraction of the reaction zone around the central (100) plane of a field emitter tip.[111] While the Pt(100) orientation displayed oscillatory behavior in the FET experiments, only stationary patterns were found in PEEM experiments under comparable reaction conditions in the 10^{-6}–10^{-4} mbar range.[111] The difference has been attributed to synergetic coupling effects between different orientations present only on the Pt FET.

In comparison to flat single crystal surfaces, the field emitter experiments exhibit a number of important differences which are (i) the influence of the electric field, (ii) the structural heterogeneity of the surface, and (iii) the small size of the system, which implies a strong coupling via diffusion and a possibly strong influence of thermal fluctuations. With respect to the interpretation of the results, the most serious question concerns the influence of the electric field, since it is well-known that a strong field can alter desorption, reaction, diffusion, and the impingement rate of polar gas molecules. An unambigous

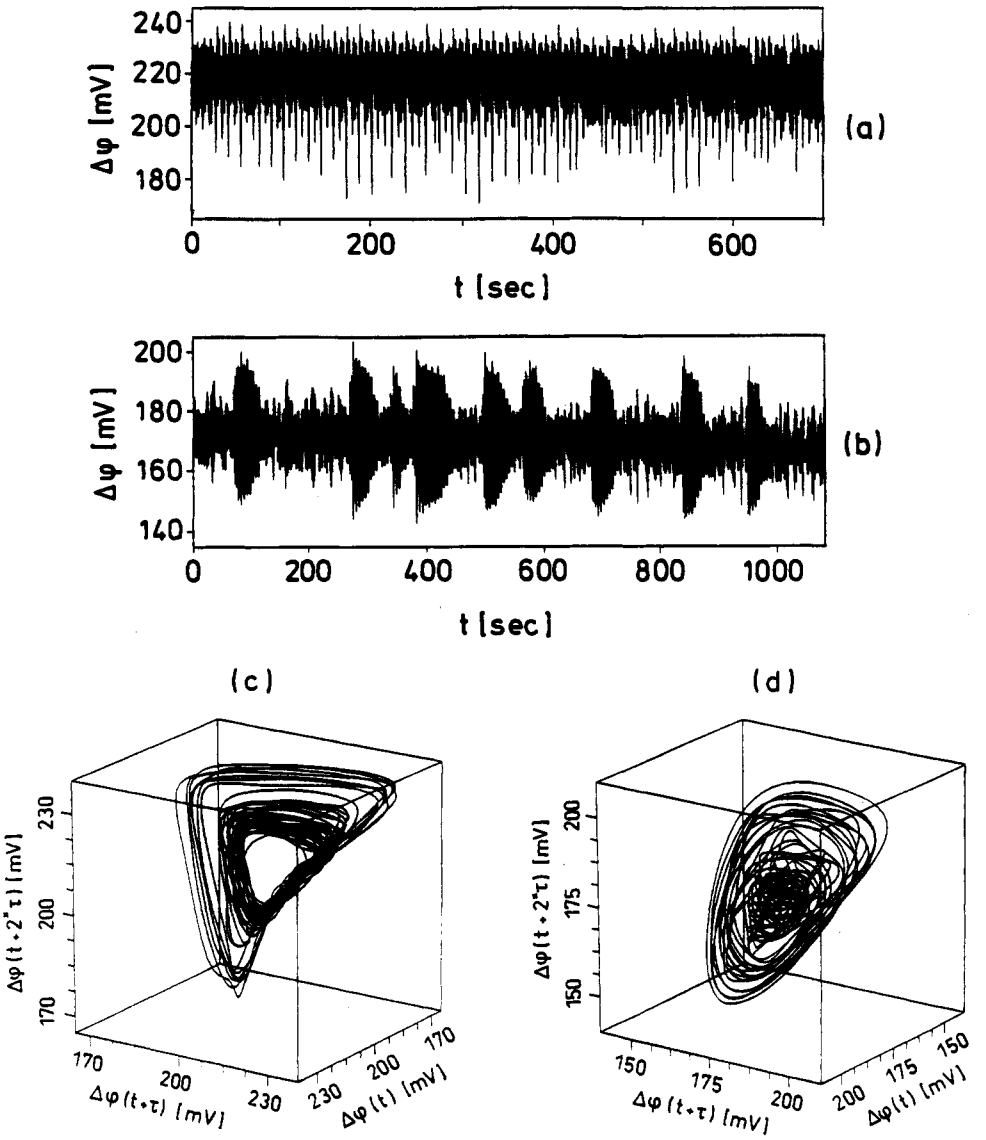

Figure 34. Typical chaotic time series of CO oxidation on Pt(110) recorded (a) close to the accumulation point of a Feigenbaum transition and (b) further inside the chaotic window. The attractors which were reconstructed from the time series shown in a and b are displayed in c and d, respectively. Experimental conditions: $T = 540$ K, $p_{O_2} \approx 1 \times 10^{-4}$ mbar, $p_{CO} \approx 5 \times 10^{-5}$ mbar. (a, c: Reprinted from ref 77. Copyright 1988 Elsevier Science Publishers B.V. b, d: Reprinted from ref 90. Copyright 1992 American Institute of Physics.)

demonstration of the influence of the electric field is the oscillations observed with FIM in the $H_2 + H_2O$ system on Pt, since no net chemical reaction is going on.[173] It was also shown by mathematical modeling that the oscillations in this system are attributed to field effects.[173] However, despite these more spurious effects, there exist several systems for which the influence of the field is of minor importance, or even completely negligible.

With respect to the PEEM results, the field emitter experiments display two significant differences. The front velocity is in most cases considerably smaller, and secondly, the reaction fronts display almost atomically sharp interfaces. The latter observation can only be reconciled with the theory of reaction–diffusion fronts, if attractive/repulsive interactions between the adparticles modify diffusion. Attractive interactions between the adparticles leading to uphill diffusion can account for the formation of near-atomically sharp interfaces in these systems.[301]

F. Microstructures

In hydrodynamic instabilities and similarly, also in reaction–diffusion systems, boundary conditions are known to influence pattern formation markedly.[190] Depending on the size of the system, certain spatiotemporal modes are selected. Furthermore, the propagation of chemical waves can be suppressed through narrow channels and gaps, and obstacles in the path of a chemical wave may alter its behavior.[349–351] By using photolithographic techniques, surface reactions offer a very convenient way to study the behavior of chemical waves in such confined systems. Yet another way to influence pattern formation in a controlled way is to alter the property of the medium itself. On surfaces this possibility can be realized by depositing a metal that alloys with the substrate. Both ways to modify spatiotemporal pattern formation have been demonstrated in a recent set of single crystal experiments.

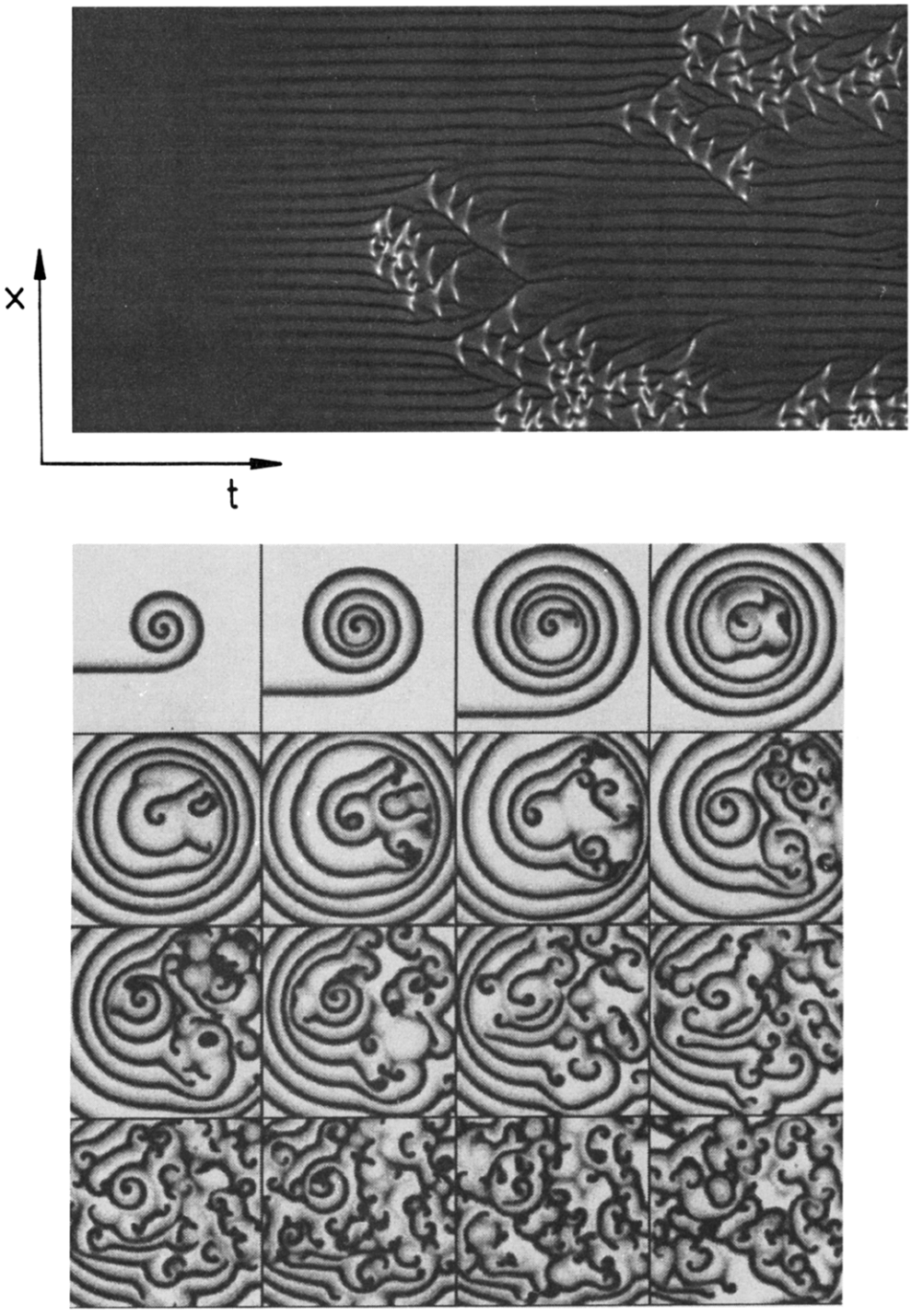

Figure 35. Model calculations showing the development of spatiotemporal turbulence in reaction–diffusion systems. (a) 1D simulation for an oscillating medium showing intermittency, i.e. local outbursts occur in a predominantly laminar regime. The simulation was conducted with the complex Ginzburg–Landau equation, which had been modified to include the effect of global coupling via the gas phase and (b) development of turbulence in an excitable medium via spiral breakup. The FitzHugh–Nagumo equation was used to model the reaction–diffusion system. (a: Reprinted from ref 347. Copyright 1994 American Institute of Physics. b: Reprinted from ref 341. Copyright 1993 American Institute of Physics.)

By depositing a Ti mask with photolithographic techniques onto a Pt(110) surface, one restricts pattern formation in the CO + O_2 reaction to those areas uncovered by Ti, while the Ti film itself is practically inert.[13] As demonstrated by the PEEM images displayed in Figure 33, this technique allows the observation of novel effects not present in a homogeneous medium. In a similar experiment with the NO + CO reaction on Pt(100), it was shown that changes in the size of the active area cause the local oscillation frequency to vary by more than a factor of 2.[143] Experiments in which Pd was deposited on a Pt(110) surface with microlithography demonstrated that the Pd-covered areas can act as a CO supply for the bare Pt(110) surface in catalytic CO oxidation.[353]

By depositing submonolayer coverages of Au onto Pt(110), some properties of the surface, which are

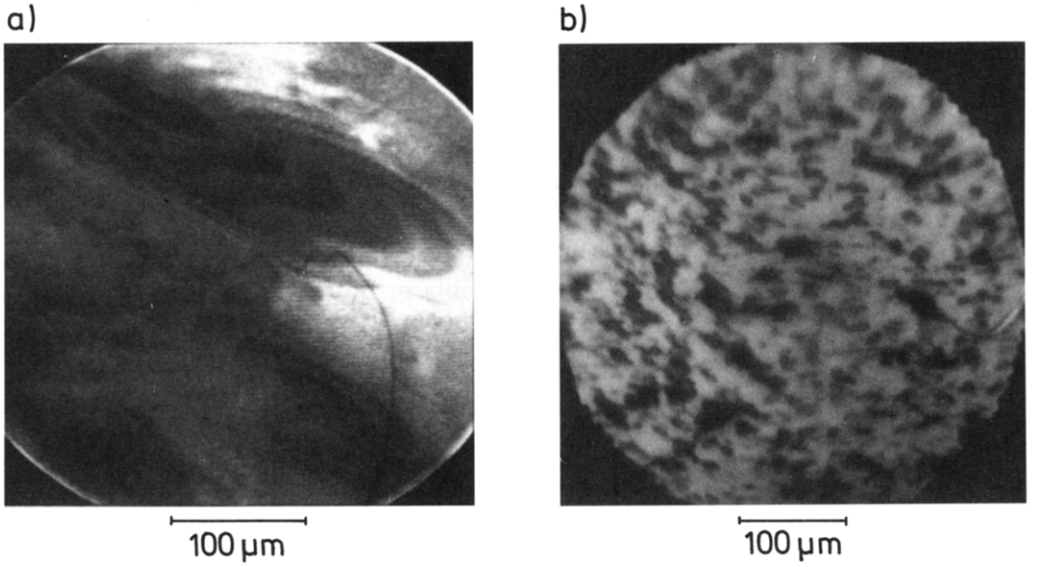

Figure 36. Experimental observations of spatiotemporal turbulence in PEEM measurements: (a) Catalytic CO oxidation on Pt(110). Experimental conditions: $T = 444$ K, $p_{O_2} = 3.1 \times 10^{-4}$ mbar, $p_{CO} = 1.0 \times 10^{-4}$ mbar. (b) NO + NH_3 reaction on Pt(100). Experimental conditions: $T = 432$ K, $p_{NO} = 1.3 \times 10^{-6}$ mbar, $p_{NH_3} = 2.1 \times 10^{-6}$ mbar. (a: Reprinted from ref 82. Copyright 1990 American Institute of Physics. b: Reprinted from ref 159. Copyright 1992 J. C. Baltzer AG.)

relevant for pattern formation in the CO + O_2 reaction, i.e. the oxygen sticking coefficient and the CO diffusion constant, were modified such that patterns with characteristics different from that of an unalloyed Pt(110) surface were observed.[354]

VII. Chaotic Behavior

A. Temporal Chaos

Aperiodic or irregular oscillations are observed quite frequently in catalytic reactions.[23] However, only in very few cases has the existence of deterministic chaos been convincingly demonstrated, and so far no system exists for which the chaotic behavior has been reproduced with a mathematical model. Since chaos in heterogeneously catalyzed reactions was recently reviewed by Eiswirth,[23] this subject is only briefly discussed here.

The main problem in identifying deterministic chaos is to discriminate truly low-dimensional chaotic dynamics from experimental irregularities and noise. For this purpose a number of methods have been developed that allow one to classify a system as chaotic from the analysis of the time series only, i.e. without knowing the underlying equations of motion.[188,190] In order to represent deterministic chaos, a number of criteria have to be fulfilled: the existence of at least one positive Liapunov exponent (LE), a so-called strange attractor characterized by a fractal dimension, a continuous Fourier spectrum, a rapidly decaying autocorrelation function, etc.

In heterogeneous catalysis, deterministic chaos was first proven in high-pressure experiments of catalytic CO oxidation by Razon and Schmitz.[36] Similar studies were conducted by Onken and Wicke,[37] Kapicka and Marek,[355] and by Jaeger et al.[29] In single crystal studies, deterministic chaos has been demonstrated for three systems: Pt(110)/CO + O_2,[77,90] Pt(100)/NO + H_2,[150] and Pt(100)/NO + CO.[140,142] Remarkably, all three systems exhibit a transition from regular to chaotic oscillation via a Feigenbaum scenario, i.e., a sequence of period-doublings.

The best characterized of these chaotic systems is Pt(110)/CO + O_2, for which an extensive data analysis was conducted by Eiswirth et al.[77,90] An embedding dimension of five was determined, i.e. the minimum number of variables to describe the dynamics is five.[77] While this analysis yielded only one positive LE, subsequently a second analysis for conditions further inside the chaotic window was performed.[90] This analysis showed two positive LE's, thus characterizing a state, which has been termed "hyperchaos". The time series and the attractors that correspond to these two differently chaotic states are shown in Figure 34.

For the NO + H_2 reaction on Pt(100), a similar analysis was conducted by Nieuwenhuys et al.[150] The chaotic behavior in this system arises under very similar conditions to Pt(100)/NO + CO (see Figure 17), since the oscillations in both systems occur on a largely hex-reconstructed surface. On the basis of the assumption that the oscillatory surface is synchronized in both systems via a critical dependence of the $1 \times 1 \rightleftarrows$ hex phase transition on partial pressure variations, a model has been proposed, which explains the occurrence of chaos as being due to a transition from synchronized to unsynchronized behavior.[142,356]

B. Spatiotemporal Chaos

Compared to temporal chaos, which does not involve spatial degrees of freedom, the understanding of spatiotemporal chaos is still relatively poor as far as reaction–diffusion systems are concerned. Most of the work in this field focuses still on the development of theoretical concepts, such as phase turbulence,[357] or defect-mediated turbulence[358] in oscillatory media, and turbulence via spiral break-up in excitable media.[341,342] These concepts are usually developed on the basis of general theoretical models, i.e. the complex Ginzburg Landau (CGL) equation for

oscillatory media and the FitzHugh–Nagumo equation for excitable media.

Some connections between these very general equations and surface reactions have been drawn already. With a modified CGL equation, the influence of gas-phase coupling on turbulent states was investigated[346,347] and the spiral breakup scenario in the FitzHugh–Nagumo equation was mapped onto the three-variable model for catalytic CO oxidation on Pt(110).[341,342] Simulations showing different types of turbulence are displayed in Figure 35. How chaos can arise in a heterogeneous catalytic reaction, in which individual pellets are coupled together thermally, has been demonstrated by Schüth et al.[359]

In heterogeneous catalysis, irregular dynamic patterns, that could possibly represent chemical turbulence, are found quite often. In the high-pressure experiments, the irregular nonisothermal patterns imaged by infrared thermography are candidates for such a state.[45,328] In the isothermal single crystal experiments, the concentration patterns seen with PEEM in catalytic CO oxidation on Pt(110) or in the NO reduction with NH_3 on Pt(100), are likely to represent chemical turbulence.[82,159] The corresponding PEEM images are displayed in Figure 36.

The problem in classifying patterns of the type displayed in Figure 36 is that, different from temporal chaos, no well-established methods exist, with which one can analyze and distinctly characterize spatiotemporal chaos. The development of such methods is, however, in progress and one can expect that in the near future similar progress is achieved in this field as was the case with temporal chaos.[360]

VIII. Outlook

When systematic mechanistic studies of oscillatory surface reactions were started more than 10 years ago, little was known about these systems except that, under certain conditions, periodic variations of the reaction rate occurred. In the meantime, detailed insights into the microscopic mechanisms were obtained, and an unexpected variety of new and interesting physical effects has been discovered. The field is far from being mature and it is safe to expect further exciting observations in the near future. Further progress in the development of experimental techniques will allow one to probe smaller and smaller length scales, reaching finally atomic dimensions. Thermal fluctuations and interactions between the reacting particles will become important on the microscopic level. One can anticipate that the need to correctly take these effects into account will also stimulate the further development of theoretical methods.

Another aspect, which is likely to gain further importance and where first experiments have also just begun is that of designing microcatalysts in order to control pattern formation. At present this can be done in the micrometer range with photolithographic techniques, but in the near future this should also become possible on the nanometer scale. Apart from the theoretical interest and the possibility of observing new phenomena, there is also a very practical aspect: since all real catalysts are composite materials. The insights one obtains from such artificial model catalysts can help to achieve a better understanding of the operation and possible improvement of real catalysts.

Acknowledgments

The authors are indebted to S. Rastomjee for carefully correcting the English of this manuscript.

References

(1) Nicolis, G.; Prigogine, I. *Self-Organization in Nonequilibrium Systems*; Wiley: New York, 1977.
(2) Fechner, G. Th.; Schweigg, J. *J. Chem. Phys.* **1828**, *53*, 61.
(3) Hugo, P. *Ber. Bunsen-Ges. Phys. Chem.* **1970**, *74*, 121.
(4) Beusch, H.; Fieguth, D.; Wicke, E. *Chem. Eng. Tech.* **1972**, *44*, 445.
(5) Field, R. J., Burger, M., Eds.; *Oscillations and Traveling Waves in Chemical Systems*; Wiley: New York, 1985.
(6) Razón, L. F.; Schmitz, R. A. *Catal. Rev. Sci. Eng.* **1986**, *28*, 89.
(7) Ertl, G. *Adv. Catal.* **1990**, *37*, 213.
(8) Imbihl, R. *Prog. Surf. Sci.* **1993**, *44*, 185.
(9) Ertl, G. *Science* **1991**, *254*, 1756.
(10) Eiswirth, M.; Ertl, G. *Chemical Waves and Patterns*; Kapral R., Showalter, K., Eds.; Kluwer: Dordrecht, 1994.
(11) van Tol, M. F. H.; Gielbert, A.; Nieuwenhuys, B. E. *Catal. Lett.* **1992**, *16*, 297.
(12) Gorodetskii, V.; Block, J. H.; Drachsel, W.; Ehsasi, M. *Appl. Surf. Sci.* **1993**, *67*, 198.
(13) Graham, M. D.; Kevrekidis, I. G.; Asakura, K.; Lauterbach, J.; Krischer, K.; Rotermund, H. H.; Ertl, G. *Science* **1994**, *264*, 80.
(14) Hegedus, L. L.; Chang, C. C.; McEwen, D. J.; Sloan, E. M. *Ind. Eng. Chem. Fundam.* **1980**, *19*, 367.
(15) Cutlip, M. B.; Hawkins, C. J.; Mukesh, D.; Morton, W.; Kenney, C. N. *Chem. Eng. Commun.* **1983**, *22*, 329.
(16) Vaporciyan, G.; Annapragada, A.; Gulari, E. *Chem. Eng. Sci.* **1988**, *43*, 2957.
(17) For more references on the influence of periodic forcing on the yield and selectivity of catalytic reaction, see, for example: refs 8–20 in ref 19.
(18) Slinko, M. M.; Jaeger, N. *Oscillatory Heterogeneous Catalytic Systems, Studies in Surface Science and Catalysis*; Elsevier: Amsterdam, 1994; Vol. 86.
(19) Schüth, F.; Henry, B. E.; Schmidt, L. D. *Adv. Catal.* **1993**, *39*, 51.
(20) Slinko, M. G.; Slinko, M. M. *Catal. Rev. Sci. Eng.* **1978**, *17*, 119.
(21) Sheintuch, M.; Schmitz, R. A. *Catal. Rev.–Sci. Eng.* **1977**, *15*, 107.
(22) Imbihl, R. *Optimal Structures in Heterogeneous Reaction Systems*; Plath, P. J., Ed.; Springer: Heidelberg, 1989.
(23) Eiswirth, M. *Chaos in Chemistry and Biochemistry*; Fields, R. J., Györgyi, L., Eds.; World Scientific: Singapore, 1993.
(24) Turner, J. E.; Sales, B. C.; Maple, M. B. *Surf. Sci.* **1981**, *109*, 591.
(25) Schüth, F.; Wicke, E. *Ber. Bunsen-Ges. Phys. Chem.* **1989**, *93*, 491.
(26) Böcker, D.; Wicke, E. *Ber. Bunsen-Ges. Phys. Chem.* **1985**, *89*, 629.
(27) Plath, P. J.; Möller, K.; Jaeger, N. I. *J. Chem. Soc., Faraday Trans. 1* **1988**, *84*, 1751.
(28) Jaeger, N. I.; Möller, K.; Plath, P. J. *J. Chem. Soc., Faraday Trans. 1* **1986**, *82*, 3315.
(29) Slinko, M. M.; Jaeger, N. I.; Svensson, P. *J. Catal.* **1989**, *118*, 349.
(30) For a full list of the numerous papers on oscillations in catalytic CO oxidation on polycrystalline Pt catalysts, see the reviews by Razon and Schmitz[6] and by Schüth, Henry, and Schmidt.[19] Here only a few representative examples are given.
(31) Wicke, E.; Kummann, P.; Keil, W.; Schiefler, J. *Ber. Bunsen-Ges. Phys. Chem.* **1980**, *84*, 315.
(32) Turner, J. E.; Sales, B. C.; Maple, M. B. *Surf. Sci.* **1981**, *103*, 54.
(33) Lynch, D. T.; Wanke, S. E. *J. Catal.* **1984**, *88*, 333.
(34) Kaul, D. J.; Wolf, E. E. *J. Catal.* **1985**, *91*, 216.
(35) Lindstrom, T. H.; Tsotsis, T. T. *Surf. Sci.* **1985**, *150*, 487.
(36) Razón, L. F.; Chang, S.-M.; Schmitz, R. A. *Chem. Eng. Sci.* **1986**, *41*, 1561.
(37) Onken, H. U.; Wicke, E. *Ber. Bunsen-Ges. Phys. Chem.* **1986**, *90*, 976.
(38) Burrows, V. A.; Sundaresan, S.; Chabal, Y. J.; Christmann, S. B. *Surf. Sci.* **1985**, *160*, 122.
(39) Tsai, P. K.; Maple, M. B.; Herz, R. K. *J. Catal.* **1988**, *113*, 453.
(40) Kapicka, J.; Marek, M. *J. Catal.* **1989**, *119*, 508.
(41) Dath, J.-P.; Dauchot, J.-P. *J. Catal.* **1989**, *115*, 593.
(42) Schüth, F.; Wicke, E. *Ber. Bunsen-Ges. Phys. Chem.* **1989**, *93*, 191.
(43) Hartmann, N.; Imbihl, R.; Vogel, W. *Catal. Lett.* **1994**, *28*, 373.

(44) Kellow, J. C.; Wolf, E. E. *Chem. Eng. Sci.* **1990**, *45*, 2597.
(45) Qin, F.; Wolf, E. E.; Chang, H.-C. *Phys. Rev. Lett.* **1994**, *72*, 1459.
(46) Eckart, E.; Hlavacek, V.; Marek, M. *Chem. Eng. Commun.* **1973**, *1*, 95.
(47) Ehsasi, M.; Seidel, C.; Ruppender, H.; Drachsel, W.; Block, J. H.; Christmann, K. *Surf. Sci.* **1989**, *210*, L198.
(48) Ladas, S.; Imbihl, R.; Ertl, G. *Surf. Sci.* **1989**, *219*, 88.
(49) Ehsasi, M.; Frank, O.; Block, J. H.; Christmann, K. *Chem. Phys. Lett.* **1990**, *165*, 115.
(50) Bassett, M. R.; Imbihl, R. *J. Chem. Phys.* **1990**, *93*, 811.
(51) Yamamoto, T.; Kasai, H.; Okiji, A. *J. Phys. Soc. Jpn.* **1991**, *60*, 982.
(52) Ehsasi, M.; Berdau, M.; Rebitzki, T.; Charlé, K.-P.; Christmann, K.; Block, J. H. *J. Chem. Phys.* **1993**, *98*, 9177.
(53) (a) Hartmann, N.; Krischer, K.; Imbihl, R. *J. Chem. Phys.* **1994**, *101*, 6717. (b) Yelenin, G. G.; Kurkina, E. S.; Makeev, A. G. *Math. Modeling*, in press (Russian).
(54) Berdau, M.; Ehsasi, M.; Karpowics, A.; Engel, W.; Christmann, K.; Block, J. H. *Vacuum* **1994**, *45*, 271.
(55) Hammoudeh, A.; Ehsasi, M.; Block, J. H.; Christmann, K. *Verh. Dtsch. Phys. Ges.* **1992**.
(56) Imbihl, R.; Cox, M. P.; Ertl, G.; Müller, H.; Brenig, W. *J. Chem. Phys.* **1985**, *83*, 1578.
(57) Cox, M. P.; Ertl, G.; Imbihl, R. *Phys. Rev. Lett.* **1985**, *54*, 1725.
(58) Eiswirth, M.; Schwankner, R. J.; Ertl, G. *Z. Phys. Chem. NF* **1985**, *144*, 59.
(59) Imbihl, R.; Cox, M. P.; Ertl, G. *J. Chem. Phys.* **1986**, *84*, 3519.
(60) Möller, P.; Wetzl, K.; Eiswirth, M.; Ertl, G. *J. Chem. Phys.* **1986**, *85*, 5328.
(61) Schwankner, R. J.; Eiswirth, M.; Möller, P.; Wetzl, K.; Ertl, G. *J. Chem. Phys.* **1987**, *87*, 742.
(62) (a) Andradé, R. F. S.; Dewel, G.; Borckmans, P. *J. Chem. Phys.* **1989**, *91*, 2675. (b) Andradé, R. F. S.; Lima, D.; Dewel, G.; Borckmans, P. *J. Chem. Phys.* **1994**, *100*.
(63) Fink, T.; Imbihl, R.; Ertl, G. *J. Chem. Phys.* **1989**, *91*, 5002.
(64) Rotermund, H. H.; Engel, W.; Kordesch, M. E.; Ertl, G. *Nature* **1990**, *343*, 399.
(65) Rotermund, H. H.; Jakubith, S.; von Oertzen, A.; Ertl, G. *J. Chem. Phys.* **1989**, *91*, 4942.
(66) Wu, X.-G.; Kapral, R. *Physica A* **1992**, *188*, 284.
(67) Rotermund, H. H.; Lauterbach, J.; Haas, G. *Appl. Phys.* **1993**, *A57*, 507.
(68) Lauterbach, J.; Asakura, K.; Rotermund, H. H. *Surf. Sci.* **1994**, *313*, 52.
(69) Swiech, S.; Rausenberger, B.; Engel, W.; Bradshaw, A. M.; Zeitler, E. *Surf. Sci.* **1993**, *294*, 297.
(70) Rausenberger, B.; Swiech, W.; Engel, W.; Bradshaw, A. M.; Zeitler, E. *Surf. Sci.* **1993**, *287/288*, 235.
(71) Rausenberger, B.; Swiech, W.; Rastomjee, C. S.; Mundschau, M.; Engel, W.; Zeitler, E.; Bradshaw, A. M. *Chem. Phys. Lett.* **1993**, *215*, 109.
(72) Swiech, W.; Rastomjee, C. S.; Imbihl, R.; Evans, J. W.; Rausenberger, B.; Engel, W.; Schmidt, A. K.; Bradshaw, A. M.; Zeitler, E. *Surf. Sci.* **1994**, *307*, 138.
(73) Eiswirth, M.; Ertl, G. *Surf. Sci.* **1986**, *177*, 90.
(74) Ladas, S.; Imbihl, R.; Ertl, G. *Surf. Sci.* **1988**, *197*, 153.
(75) Ladas, S.; Imbihl, R.; Ertl, G. *Surf. Sci.* **1988**, *198*, 42.
(76) Eiswirth, M.; Ertl, G. *Phys. Rev. Lett.* **1988**, *60*, 1526.
(77) Eiswirth, M.; Krischer, K.; Ertl, G. *Surf. Sci.* **1988**, *202*, 565.
(78) Eiswirth, M.; Möller, P.; Wetzl, K.; Imbihl, R.; Ertl, G. *J. Chem. Phys.* **1989**, *90*, 510.
(79) Eiswirth, M.; Möller, P.; Ertl, G. *Surf. Sci.* **1989**, *208*, 13.
(80) Vishnevskii, A. L.; Savchenko, V. I. *React. Kinet. Catal. Lett.* **1989**, *38*, 187.
(81) Imbihl, R.; Ladas, S.; Ertl, G. *Surf. Sci.* **1989**, *215*, L307.
(82) Jakubith, S.; Rotermund, H. H.; Engel, W.; von Oertzen, A.; Ertl, G. *Phys. Rev. Lett.* **1990**, *65*, 3013.
(83) Rotermund, H. H.; Jakubith, S.; von Oertzen, A.; Ertl, G. *Phys. Rev. Lett.* **1990**, *66*, 3083.
(84) Rotermund, H. H.; Engel, W.; Jakubith, S.; von Oertzen, A.; Ertl, G. *Ultramicroscopy* **1991**, *36*, 164.
(85) Krischer, K.; Eiswirth, M.; Ertl, G. *J. Chem. Phys.* **1992**, *96*, 9161.
(86) Krischer, K.; Eiswirth, M.; Ertl, G. *J. Chem. Phys.* **1992**, *97*, 307.
(87) Falcke, M.; Bär, M.; Engel, H.; Eiswirth, M. *J. Chem. Phys.* **1992**, *97*, 4555.
(88) Bär, M.; Eiswirth, M.; Rotermund, H. H.; Ertl, G. *Phys. Rev. Lett.* **1992**, *69*, 945.
(89) Levine, H.; Zou, X. *Phys. Rev. Lett.* **1992**, *69*, 204; *Phys. Rev. E* **1993**, *48*, 50.
(90) Eiswirth, M.; Kruel, T.-M.; Ertl, G.; Schneider, F. W. *Chem. Phys. Lett.* **1992**, *193*, 305.
(91) Nettesheim, S.; von Oertzen, A.; Rotermund, H. H.; Ertl, G. *J. Chem. Phys.* **1993**, *98*, 9977.
(92) Krischer, K.; Rico-Martínez, R.; Kevrekidis, I. G.; Rotermund, H. H.; Ertl, G.; Hudson, J. L. *AIChE J.* **1993**, *39*, 89.
(93) Bär, M.; Nettesheim, S.; Rotermund, H.-H.; Eiswirth, M.; Ertl, G.; *Phys. Rev. Lett.* **1995**, *94*, 1246.
(94) Ehsasi, M.; Rezaie-Serej, S.; Block, J. H.; Christmann, K. *J. Chem. Phys.* **1990**, *92*, 7596.
(95) Sander, M.; Imbihl, R.; Ertl, G. *J. Chem. Phys.* **1991**, *95*, 6162.
(96) Sander, M.; Imbihl, R.; Ertl, G. *J. Chem. Phys.* **1992**, *97*, 5193.
(97) Sander, M.; Veser, G.; Imbihl, R. *J. Vac. Sci. Technol. A* **1992**, *10*, 2495.
(98) Yeates, R. C.; Turner, J. E.; Gellman, A. J.; Somorjai, G. A. *Surf. Sci.* **1985**, *149*, 175.
(99) Gorodetskii, V.; Drachsel, W.; Block, J. H. *Catal. Lett.* **1993**, *19*, 223.
(100) Gorodetskii, V.; Drachsel, W.; Ehsasi, M.; Block, J. H. *J. Chem. Phys.* **1994**, *100*, 6915.
(101) Belyaev, V. D.; Slin'ko, M. M.; Timoshenko, V. I.; Slin'ko, M. G. *Kinet. Katal.* **1973**, *14*, 810.
(102) Kurtanjek, Z.; Sheintuch, M.; Luss, D. *J. Catal.* **1980**, *66*, 11.
(103) Sault, A. G.; Masel, R. I. *J. Catal.* **1982**, *73*, 294.
(104) Tsitsopoulos, L. T.; Tsotsis, T. T. *Surf. Sci.* **1987**, *187*, 165.
(105) Rajagopalan, K.; Luss, D. *Chem. Eng. Sci.* **1983**, *38*, 473.
(106) Zuniga, J. E.; Luss, D. *J. Catal.* **1978**, *53*, 312.
(107) Volodin, Y. E.; Barelko, V. V.; Khail'zov, P. I. *Kinet. Katal.* **1982**, *23*, 1240.
(108) Keck, K. E.; Kasemo, B. *Surf. Sci.* **1986**, *167*, 313.
(109) Li, Y. E.; Gonzalez, R. D. *Catal. Lett.* **1988**, *1*, 229.
(110) Gorodetskii, V.; Block, J. H.; Drachsel, W. *Appl. Surf. Sci.* **1994**, *76/77*, 129.
(111) Gorodetskii, V.; Lauterbach, J.; Rotermund, H. H.; Block, J. H.; Ertl, G. *Nature* **1994**, *370*, 277.
(112) Wojnowski, A.; Barcicki, J. *J. Therm. Anal.* **1980**, *19*, 449.
(113) Flytzani-Stephanopoulos; Schmidt, L. D.; Caretta, R. *J. Catal.* **1980**, *64*, 346.
(114) Sheintuch, M.; Schmidt, J. *J. Phys. Chem.* **1988**, *92*, 3404.
(115) Stoukides, M.; Vayenas, C. G. *J. Catal.* **1982**, *74*, 266.
(116) Arsalane, S.; Brochu, R.; Ziyad, M. C. R. *Acad. Sci. Paris. Ser. 2* **1990**, *311*, 1303.
(117) Shaprinskaya, T. M. *Teor. Eksp. Khim* **1988**, *24*, 107.
(118) Zhukov, S. A.; Barelko, V. V. *Khim. Fiz.* **1982**, *4*, 516.
(119) Vayenas, C. G.; Lee, B.; Michaels, J. *J. Catal.* **1980**, *66*, 36.
(120) Onken, H. U.; Wolf, E. E. *Chem. Eng. Sci.* **1988**, *43*, 2551.
(121) Amariglio, A.; Benali, O.; Amariglio, H. *J. Catal.* **1989**, *118*, 164.
(122) Slin'ko, M. M.; Ukharskii, A. A. *Proc. 8th Int. Congr. Catal.* **1984**, *3*, 243.
(123) Choudhary, V. R.; Chaudhari, S. T.; Rajput, A. M.; Rane, V. H. *J. Chem. Soc., Chem. Commun.* **1989**, *10*, 605.
(124) Jaeger, N. I.; Ottensmeyer, R.; Plath, P. J. *Ber. Bunsen-Ges. Phys. Chem.* **1986**, *90*, 1075.
(125) Ionescu, N. I.; Chirca, M. S.; Marchidan, D. I. *React. Kinet. Catal. Lett.* **1989**, *38*, 249.
(126) Jaeger, N. I.; Ottensmeyer, R.; Plath, P. J. *Chem. Eng. Sci.* **1990**, *45*, 947.
(127) Ionescu, N. I.; Chirca, M. S.; Marchidan, D. I. *Rev. Roum. Chim.* **1986**, *31*, 671.
(128) Mukesh, D.; Narasimhan, C. S. *Heterog. Catal.* **1987**, *6*, Part 1, p 31.
(129) Huang, Z.; Yao, D.; Pang, X. *Huaxue Fanying Gongcheng Yu Gongyi* **1987**, *3*, 1.
(130) Adlhoch, W.; Lintz, H.-G.; Weisker, T. *Surf. Sci.* **1981**, *103*, 576.
(131) Singh-Boparai, S. P.; King, D. A. *Proc. 4th Int. Congr. Surf. Sci.* **1980**, 403.
(132) Schwartz, S. B.; Schmidt, L. D. *Surf. Sci.* **1987**, *183*, L269.
(133) Schwartz, S. B.; Schmidt, L. D. *Surf. Sci.* **1988**, *206*, 169.
(134) Fink, T.; Dath, J.-P.; Imbihl, R.; Ertl, G. *J. Chem. Phys.* **1991**, *95*, 2109.
(135) Dath, J.-P.; Fink, T.; Imbihl, R.; Ertl, G. *J. Chem. Phys.* **1992**, *96*, 1582.
(136) Veser, G.; Imbihl, R. *J. Chem. Phys.* **1992**, *96*, 7155.
(137) Imbihl, R.; Fink, T.; Krischer, K. *J. Chem. Phys.* **1992**, *96*, 6236.
(138) Evans, J. W.; Madden, H. H.; Imbihl, R. *J. Chem. Phys.* **1992**, *96*, 4805.
(139) Yelenin, G. G.; Makeev, A. G. *Math. Modeling* **1992**, *4*, 5 (Russian).
(140) Veser, G.; Mertens, F.; Mikhailov, A. S.; Imbihl, R. *Phys. Rev. Lett.* **1993**, *71*, 935.
(141) Veser, G.; Imbihl, R. *J. Chem. Phys.* **1994**, *100*, 8483.
(142) Veser, G.; Imbihl, R. *J. Chem. Phys.* **1994**, *100*, 8492.
(143) Hartmann, N.; Bär, M.; Krischer, K.; Kevrekidis, I. G.; Imbihl, R. Manuscript in preparation.
(144) Graham, M. D.; Kevrekidis, I. G.; Hudson, J. L.; Veser, G.; Krischer, K.; Imbihl, R. *Chaos, Solitons Fractals*, in press.
(145) Schmatloch, V.; Kruse, N. *Surf. Sci.* **1992**, *269/270*, 488.
(146) Madden, H. H.; Imbihl, R. *Appl. Surf. Sci.* **1991**, *48/49*, 130.
(147) Siera, J.; Cobden, P.; Tanaka, K.; Nieuwenhuys, B. E. *Catal. Lett.* **1991**, *10*, 335.
(148) Mundschau, M.; Rausenberger, B. *Platinum Met. Rev.* **1991**, *35*, 188.
(149) Slinko, M.; Fink, T.; Löher, T.; Madden, H. H.; Lombardo, S. J.; Imbihl, R.; Ertl, G. *Surf. Sci.* **1992**, *264*, 157.
(150) Cobden, P. D.; Siera, J.; Nieuwenhuys, B. E. *J. Vac. Sci. Technol. A* **1992**, *10*, 2487.
(151) Lombardo, S. J.; Fink, T.; Imbihl, R. *J. Chem. Phys.* **1993**, *98*, 5526.
(152) Voss, C.; Kruse, N. Manuscript in preparation.
(153) Mertens, F.; Imbihl, R. *Nature* **1994**, *370*, 124.

(154) Gottschalk, N.; Mertens, F.; Eiswirth, M.; Imbihl, R. *Phys. Rev. Lett.* **1994**, *73*, 3483.
(155) van Tol, M. F. H.; Gielbert, A.; Nieuwenhuys, B. E. *Appl. Surf. Sci.* **1993**, *67*, 179.
(156) Takoudis, C. G.; Schmidt, L. D. *J. Phys. Chem.* **1983**, *87*, 958; **1983**, *87*, 964.
(157) Katona, T.; Somorjai, G. A. *J. Phys. Chem.* **1992**, *96*, 5465.
(158) Lombardo, S. J.; Esch, F.; Imbihl, R. *Surf. Sci.* **1992**, *271*, L367.
(159) Veser, G.; Esch, F.; Imbihl, R. *Catal. Lett.* **1992**, *13*, 371.
(160) van Tol, M. F. H.; Siera, J.; Cobden, P. D.; Nieuwenhuys, B. E. *Surf. Sci.* **1992**, *274*, 63.
(161) van Tol, M. F. H.; de Maaijer-Gielbert, J.; Nieuwenhuys, B. E. *Chem. Phys. Lett.* **1993**, *205*, 207.
(162) Kobayashi, M.; Takeda, H.; Kanno, T. *J. Chem. Soc., Chem. Commun.* **1987**, *11*, 825.
(163) Tsotsis, T. T.; Rao, V. U. S.; Polinski, L. M. *AIChE J* **1982**, *28*, 847.
(164) Caldwell, L. *Inst. Chem. Eng. Symp. Ser.* **1984**, *87* (Chem. React. Eng.), 151.
(165) Pyatnitskii, Y. I.; Filonenko, G. V.; Stasevich, V. P.; Shaprinskaya, T. M.; Gritsenko, V. I. *Unsteady State Processes in Catalysis*; Matros, Y. S., Ed.; Utrecht: 1990; p 40.
(166) Niiyama, H.; Suzuki, Y. *Chem. Eng. Commun.* **1982**, *14*, 145.
(167) Bos, A. N. R.; Westerterp, K. R. *Unsteady State Processes in Catalysis*; Matros, Y. S., Ed.; Utrecht: 1990; p 593.
(168) Hesse, D. *Hung. J. Ind. Chem.* **1988**, *16*, 1.
(169) Petrov, L.; Vladov, C.; Eliyas, A.; Kirkov, N.; Tenchev, K.; Bonev, C.; Filkova, D.; Prahov, L. *J. Mol. Catal.* **1989**, *54*, 237.
(170) Yang, Y.; Lai, G.; Luo, R. *Ranliao Huaxue Xuebao* **1985**, *13*, 343.
(171) Cordonier, G. A.; Schüth, F.; Schmidt, L. D. *J. Chem. Phys.* **1989**, *91*, 5374.
(172) Hwang, S. Y.; Schmidt, L. D. *J. Catal.* **1988**, *114*, 230.
(173) Ernst, N.; Bozdech, G.; Gorodetskii, V.; Kreuzer, H.-J.; Wang, R. I. C.; Block, J. H. *Surf. Sci.* **1994**, *318*, L1211.
(174) Lauterbach, J.; Haas, G.; Rotermund, H. H.; Ertl, G. *Surf. Sci.* **1993**, *294*, 116.
(175) Lauterbach, J.; Rotermund, H. H. *Catal. Lett.* **1994**, *27*, 27.
(176) A list of references for the application of different experimental techniques to study oscillatory surface reactions is given in the review article by Schüth et al. in ref 19.
(177) Gardner, P. et al. Private communication.
(178) Block, J. H. Private communication.
(179) Barelko, V. V.; Volodin, Y. E. *Kinetika: Kataliz* **1976**, *17*, 112.
(180) Engel, W.; Kordesch, M. E.; Rotermund, H. H.; Kubala, S.; von Oertzen, A. *Ultramicroscopy* **1991**, *36*, 148.
(181) Telieps, W.; Bauer, E. *Ultramicroscopy* **1985**, *17*, 57.
(182) For an overview of different microscopic techniques related to photoemission electron microscopy and low energy electron microscopy, see: *Ultramicroscopy* **1991**, *36*.
(183) Uchida, Y.; Lehmpfuhl, G.; Jäger, J. *Ultramicroscopy* **1984**, *15*, 119.
(184) Uchida, Y.; Lehmpfuhl, G.; Imbihl, R. *Surf. Sci.* **1990**, *234*, 27.
(185) Uchida, Y.; Imbihl, R.; Lehmpfuhl, G. *Surf. Sci.* **1992**, *275*, 253.
(186) Sander, M.; Imbihl, R.; Schuster, R.; Barth, J. V.; Ertl, G. *Surf. Sci.* **1992**, *281*, 159.
(187) Guckenheimer, J.; Holmes, P. *Nonlinear Dynamics, Dynamical Systems, and Bifurcations of Vector Fields*; Springer: Berlin, 1986.
(188) Thompson, J. M. T.; Stewart, H. B. *Nonlinear Dynamics and Chaos*; Wiley: New York, 1987.
(189) Haken, H. *Synergetics*; Springer: Berlin, 1978.
(190) Manneville, P. *Dissipative Structures and Weak Turbulence*; Academic Press: London, 1990.
(191) Golubitsky, M.; Schaeffer, D. G. *Singularities and Groups in Bifurcation Theory, Applied Mathematical Sciences*; Springer: New York, 1984; Vol. 51.
(192) Murray, J. D. *Mathematical Biology*; Springer: Berlin, 1990.
(193) Evans, J. W. *Langmuir* **1991**, *7*, 2514.
(194) Kreuzer, H. J. *Langmuir* **1992**, *8*, 774.
(195) Wierzbicke, A.; Kreuzer, H. J. *Surf. Sci.* **1991**, *257*, 417.
(196) Taylor, M. A.; Kevrekidis, I. G. *Chem. Eng. Sci.* **1993**, *48*, 2129.
(197) Matthews, P. C.; Strogatz, S. H. *Phys. Rev. Lett.* **1990**, *65*, 1701.
(198) Sheintuch, M. *J. Catal.* **1985**, *96*, 326.
(199) Eigenberger, G. *Chem. Eng. Sci.* **1978**, *33*, 1263.
(200) Sales, B. C.; Turner, J. E.; Maple, M. B. *Surf. Sci.* **1982**, *114*, 381.
(201) Sheintuch, M. *Chem. Eng. Sci.* **1980**, *35*, 877.
(202) Belyaev, V. D.; Slin'ko, M. M.; Slinko, M. G. *Proc. Int. Congr. Catal., 6th* **1977**, *2*, 758.
(203) Pikios, C. A.; Luss, D. *Chem. Eng. Sci.* **1977**, *32*, 191.
(204) Tambe, S. S.; Kumar, V. R.; Ponnani, K. N.; Kulkarni, B. D. *Chem. Eng. J.* **1987**, *34*, 143.
(205) Ivanov, E. A.; Chumakov, G. A.; Slin'ko, M. G.; Bruns, D. D.; Luss, D. *Chem. Eng. Sci.* **1980**, *35*, 795.
(206) Kevrekidis, I.; Schmidt, L. D.; Aris, R. *Surf. Sci.* **1984**, *137*, 151.
(207) Vlachos, D. G.; Schmidt, L. D.; Aris, R. *J. Chem. Phys.* **1990**, *93*, 8306.
(208) Takoudis, C. G.; Schmidt, L. D.; Aris, R. *Surf. Sci.* **1981**, *105*, 325.
(209) McKarnin, M. A.; Aris, R.; Schmidt, L. D. *Proc. R. Soc. Lond. A* **1988**, *415*, 363.
(210) Mukesh, D.; Norton, W.; Kennedy, C. N.; Cutlip, M. B. *Surf. Sci.* **1984**, *138*, 237.
(211) Clarke, B. L. *Adv. Chem. Phys.* **1980**, *43*, 1.
(212) Eiswirth, M.; Freund, A.; Ross, J. *Adv. Chem. Phys.* **1991**, *80*, 127; *J. Phys. Chem.* **1991**, *95*, 1294.
(213) Morton, W.; Goodman, M. G. *Trans. Inst. Chem. Eng.* **1981**, *59*, 253.
(214) Hugo, P. *Eur. Symp. Chem. React. Eng.* **1971**, *4*, 459 (Brussels 1968).
(215) Dagonnier, R.; Dumont, M.; Nuyts, J. *J. Catal.* **1980**, *66*, 130.
(216) Ray, W. H.; Hastings, S. P. *Chem. Eng. Sci.* **1980**, *35*, 589.
(217) Jensen, K. F.; Ray, W. H. *Chem. Eng. Sci.* **1980**, *35*, 241.
(218) Jensen, K. F.; Ray, W. H. *Chem. Eng. Sci.* **1980**, *35*, 2439.
(219) Chang, H. C.; Aluko, M. *Chem. Eng. Sci.* **1984**, *39*, 36.
(220) Aluko, M.; Chang, H. C. *Chem. Eng. Sci.* **1984**, *39*, 51.
(221) Aluko, M.; Chang, H. C. *Chem. Eng. Sci.* **1986**, *41*, 317.
(222) Harold, M. P.; Sheintuch, M.; Luss, D. *Ind. Eng. Chem. Res.* **1987**, *26*, 786.
(223) Harold, M. P.; Sheintuch, M.; Luss, D. *Ind. Eng. Chem. Res.* **1987**, *26*, 794.
(224) Harold, M. P.; Sheintuch, M.; Luss, D. *Ind. Eng. Chem. Res.* **1987**, *26*, 1616.
(225) Ziff, R. M.; Gulari, E.; Barshed, Y. *Phys. Rev. Lett.* **1986**, *56*, 2553.
(226) Yelenin, G. *Mathematical Modeling* **1982**, *4*, 106 (Russian).
(227) Langmuir, I. *Trans. Faraday Soc.* **1921**, *17*, 607.
(228) Langmuir, I. *Trans. Faraday Soc.* **1922**, *17*, 672.
(229) Engel, T.; Ertl, G. *Adv. Catal.* **1979**, *28*, 1.
(230) Zhdanov, V. P.; Kasemo, B. *Surf. Sci. Rep.* **1994**, *20*, 113.
(231) Ehsasi, M.; Matloch, M.; Frank, O.; Block, J. H.; Christmann, K.; Rys, F. S.; Hirschwald, W. *J. Chem. Phys.* **1989**, *91*, 4949.
(232) Burrows, V. A.; Sundaresan, S.; Chabal, Y. J.; Christman, S. B. *Surf. Sci.* **1987**, *180*, 110.
(233) Turner, J. E.; Maple, M. B. *Surf. Sci.* **1984**, *147*, 647.
(234) Yentekakis, I. V.; Vayenas, C. G. *J. Catal.* **1989**, *111*, 170.
(235) Ladas, S.; Poppa, H.; Boudart, M. *Surf. Sci.* **1981**, *102*, 151.
(236) Bonzel, H. P.; Franken, A. M.; Pirug, G. *Surf. Sci.* **1981**, *104*, 625.
(237) Heilmann, P.; Heinz, K.; Müller, K. *Surf. Sci.* **1979**, *83*, 487.
(238) Van Hove, M. A.; Koestner, R. J.; Stair, P. C.; Biberian, J. P.; Kesmodel, L. L.; Bartos, I.; Somorjai, G. A. *Surf. Sci.* **1981**, *103*, 189 (I); 218 (II).
(239) Norton, P. R.; Davies, J. A.; Creber, D. K.; Sitter, C. W.; Jackman, T. E. *Surf. Sci.* **1981**, *108*, 205.
(240) Behm, R. J.; Hösler, W.; Ritter, E.; Binnig, G. *Phys. Rev. Lett.* **1986**, *56*, 228.
(241) Jackman, T. E.; Davies, J. A.; Jackson, D. P.; Unertl, W. N.; Norton, P. R. *Surf. Sci.* **1982**, *120*, 389.
(242) Niehus, H. *Surf. Sci.* **1984**, *145*, 407.
(243) Kellog, G. L. *Phys. Rev. Lett.* **1985**, *55*, 2168.
(244) Fery, P.; Moritz, W.; Wolf, D. *Phys. Rev. B* **1988**, *38*, 7275.
(245) Fenter, P.; Gustafsson, T. *Phys. Rev. B* **1988**, *38*, 10197.
(246) Behm, R. J.; Thiel, P. A.; Norton, P. R.; Ertl, G. *J. Chem. Phys.* **1983**, *78*, 7438 (I); 7448 (II).
(247) Heinz, K.; Lang, E.; Strauss, K.; Müller, K. *Appl. Surf. Sci.* **1982**, *11/12*, 611.
(248) Freyer, N.; Kiskinova, M.; Pirug, G.; Bonzel, H. P. *Appl. Phys. A* **1986**, *39*, 209.
(249) Jackman, T. E.; Griffiths, K.; Davies, J. A.; Norton, P. R. *J. Chem. Phys.* **1984**, *79*, 3529.
(250) Griffiths, K.; Jackman, T. E.; Davies, J. A.; Norton, P. R. *Surf. Sci.* **1984**, *138*, 113.
(251) Hoffman, P.; Bare, S. R.; King, D. A. *Surf. Sci.* **1982**, *117*, 245 (I); **1984**, *144*, 347 (II).
(252) Gardner, P.; Martin, R.; Tüshaus, M.; Bradshaw, A. M. *J. Electr. Spectr. Relat. Phenom.* **1990**, *54/55*, 619.
(253) Ritter, E.; Behm, R. J.; Pötschke, G.; Wintterlin, J. *Surf. Sci.* **1987**, *181*, 403.
(254) Borg, A.; Hilmen, A.-M.; Bergene, E. *Surf. Sci.* **1994**, *306*, 10.
(255) Gritsch, T.; Coulman, D.; Behm, R. J.; Ertl, G. *Phys. Rev. Lett.* **1989**, *63*, 1086.
(256) Hopkinson, A.; Guo, X.-C.; Bradley, J. M.; King, D. A. *J. Chem. Phys.* **1993**, *99*.
(257) Hopkinson, A.; Bradley, J. M.; Guo, X.-C.; King, D. A. *Phys. Rev. Lett.* **1993**, *71*, 1597.
(258) Norton, P. R.; Griffiths, K.; Bindner, P. E. *Surf. Sci.* **1984**, *138*, 125.
(259) Guo, X.-C.; Pasteur, A. T.; King, D. A. *Surf. Sci.*, in press.
(260) Freyer, N.; Kiskinova, M.; Pirug, G.; Bonzel, H. P. *Surf. Sci.* **1986**, *166*, 206.
(261) Falta, J.; Imbihl, R.; Henzler, M. *Phys. Rev. Lett.* **1990**, *64*, 1409.
(262) Imbihl, R.; Sander, M.; Ertl, G. *Surf. Sci.* **1988**, *204*, L701.
(263) Imbihl, R.; Reynolds, A. E.; Kaletta, D. *Phys. Rev. Lett.* **1991**, *67*, 275.
(264) Sander, M.; Imbihl, R. *Surf. Sci.* **1991**, *255*, 61.
(265) Imbihl, R. *Modern Phys. Lett. B* **1992**, *6*, 493.
(266) Falta, J.; Imbihl, R.; Sander, M.; Henzler, M. *Phys. Rev. B* **1992**, *45*, 6858.

(267) Berry, R. J. *Surf. Sci.* **1978**, *76*, 415.
(268) Rosé, H.; Hempel, H.; Schimansky-Geyer, L. *Stat. Phy. A* **1994**, *206*, 421.
(269) Yablonskii, G. S.; Elokhin, V. I. *Perspectives in Catalysis*; Thomas, J. A., Zamaraev, K. I., Eds.; Blackwell Scientific Publications: Boston, 1994.
(270) Vishnevskii, A. L.; Elokhin, V. I. *Unsteady State Processes in Catalysis*; Matros, Y. S., Ed.; VSP-III: Utrecht, 1990; p 437.
(271) Rehmus, P.; Ross, J. *Oscillations and Traveling Waves in Chemical Systems*; Field, R., Burger, M., Eds.; Wiley: New York, 1985.
(272) Vance, W.; Tsarouhas, G. E.; Ross, J. *Progr. Theor. Phys.* **1989**, *99*, 331.
(273) Tsarouhas, G. E.; Ross, J. *J. Chem. Phys.* **1987**, *87*, 6538; **1989**, *89*, 5715; *J. Phys. Chem.* **1989**, *93*, 2833.
(274) Marek, M. *Temporal Order*; Rensing, L., Jaeger, N. I., Eds.; Springer: Heidelberg, 1985.
(275) Svensson, P.; Jaeger, N. I.; Plath, P. J. *J. Phys. Chem.* **1988**, *92*, 1882.
(276) Raval, R.; Haq, S.; Harrison, M. A.; Blyholder, G.; King, D. A. *Chem. Phys. Lett.* **1990**, *167*, 391.
(277) Gaussmann, A.; Kruse, N. *Catal. Lett.* **1991**, *1*, 305.
(278) He, J.-W.; Memmert, U.; Griffiths, K.; Norton, P. R. *J. Chem. Phys.* **1989**, *90*, 5082.
(279) He, J.-W.; Memmert, U.; Norton, P. R. *J. Chem. Phys.* **1989**, *90*, 5088.
(280) Milun, M.; Pervan, P.; Vajic, M.; Wandelt, K. *Surf. Sci.* **1989**, *211/212*, 887.
(281) Rebholz, M.; Prins, P.; Kruse, N. *Surf. Sci.* **1992**, *269/270*, 293.
(282) Egelhoff, W. F., Jr. The Chemical Physics of Solid Surfaces and Heterogeneous Catalysis. *Fundamental Studies of Heterogeneous Catalysis*; King, D. A., Woodruff, D. P., Eds.; Elsevier: Amsterdam, 1982; Vol. 4.
(283) Gorte, R. J.; Schmidt, L. D.; Gland, J. L. *Surf. Sci.* **1981**, *109*, 367.
(284) Banholzer, W. F.; Park, Y. O.; Mak, K. M.; Masel, R. I. *Surf. Sci.* **1983**, *128*, 176.
(285) Gohndrone, J. M.; Masel, R. I. *Surf. Sci.* **1989**, *209*, 44.
(286) Lesley, M. W.; Schmidt, L. D. *Surf. Sci.* **1985**, *155*, 215.
(287) Fink, T.; Dath, J.-P.; Bassett, M. R.; Imbihl, R.; Ertl, G. *Surf. Sci.* **1991**, *245*, 96.
(288) Hopkins, A.; King, D. A. *Chem. Phys.* **1993**, *177*, 433.
(289) Hellsing, B.; Kasemo, B.; Zhdanov, V. P. *J. Catal.* **1991**, *132*, 210.
(290) Gimzewskii, J. K.; Gerber, Ch.; Meyer, E.; Schittler, R. R. *Chem. Phys. Lett.* **1994**, *217*, 589.
(291) Zhdanov, V. P. *Surf. Sci.* **1993**, *296*, 261.
(292) Winfree, A. *When Time Breaks Down*; Princeton University Press: Princeton, 1987.
(293) Mikhailov, A. S. *Foundations of Synergetics I*; Springer: Berlin, 1994.
(294) Swinney, H., Krinsky, V. I., Eds. *Wave Patterns in Chemical and Biological Systems, Phys. D* **1991**, *49*, Vol. 1.
(295) Holden, A. V., Markus, M., Othmer, H. G., Eds. *Nonlinear Wave Processes in Excitable Media*; Plenum Press: New York, 1991.
(296) Luther, R. *Z. Elektrochem.* **1906**, *12*, 596. For an English translation of this paper, see: Arnold, R.; Showalter, K.; Tyson, J. *J. Chem. Educ.* **1987**, *64*, 740.
(297) Turing, A. M. *Philos. Trans. R. Soc. London B* **1952**, *237*, 37.
(298) von Oertzen, A.; Rotermund, H. H.; Nettesheim, S. *Chem. Phys. Lett.* **1992**, *199*, 131.
(299) von Oertzen, A.; Rotermund, H. H.; Nettesheim, S. *Surf. Sci.* **1994**, *331*, 322.
(300) Mikhailov, A. *Phys. Rev. E* **1994**, *49*, 5875.
(301) Mikhailov, A.; Ertl, G. *Chem. Phys. Lett.*, in press.
(302) Middya, O.; Graham, M. D.; Luss, D.; Sheintuch, M. *J. Chem. Phys.* **1993**, *98*, 2823.
(303) Lumley, J. L. *Stochastic Tools in Turbulence*; Academic Press: New York, 1970.
(304) Graham, M. D.; Lane, S. L.; Luss, D. *J. Phys. Chem.* **1993**, *97*, 889.
(305) For more references on nonisothermal effects in oscillating surface reactions, see the review article by Eiswirth and Ertl in ref 10.
(306) Barelko, V.; Kurachka, I. I.; Merzhanao, A. G.; Shkadinskii, K. G. *Chem. Eng. Sci.* **1978**, *33*, 805.
(307) Sant, R.; Wolf, E. E. *J. Catal.* **1988**, *110*, 249.
(308) Chen, C. C.; Wolf, E. E.; Chang, H.-C. *J. Phys. Chem.* **1993**, *97*, 1055.
(309) Wicke, E.; Onken, H. U. *Chem. Eng. Sci.* **1988**, *43*, 2289.
(310) Onken, H. U.; Wicke, E. *Z. Phys. Chem. NF* **1989**, *165*, 23.
(311) Jaeger, N. I.; Liauw, M.; Plath, P. J.; Svensson, P. *Unsteady State Processes in Catalysis*; Matros, Y. S., Ed.; VPS: Utrecht, 1990; p 343.
(312) Puszynski, J.; Hlavacek, V. *Chem. Eng. Sci.* **1984**, *39*, 681.
(313) Kellow, J. C.; Wolf, E. E. *AIChE J.* **1991**, *37*, 1844.
(314) Ott, E.; Grebogi, C.; Yorke, J. A. *Phys. Rev. Lett.* **1990**, *64*, 1196.
(315) Silverberg, M.; Ben-Shaul, A. *Surf. Sci.* **1989**, *214*, 17.
(316) Lobban, L.; Luss, D. *J. Phys. Chem.* **1989**, *93*, 6530.
(317) Lobban, L.; Philippou, G.; Luss, D. *J. Phys. Chem.* **1989**, *93*, 733.
(318) Philippou, G.; Schultz, F.; Luss, D. *J. Phys. Chem.* **1991**, *95*, 3224.
(319) Philippou, G.; Luss, D. *J. Phys. Chem.* **1992**, *96*, 6651.
(320) Philippou, G.; Luss, D. *Chem. Eng. Sci.* **1993**, *48*, 2313.
(321) Lane, S. L.; Luss, D. *Phys. Rev. Lett.* **1993**, *70*, 830.
(322) Sheintuch, M. *J. Phys. Chem.* **1990**, *94*, 5889.
(323) Sheintuch, M. *Chem. Eng. Sci.* **1989**, *44*, 1081.
(324) Graham, M. D.; Lane, S. L.; Luss, D. *J. Chem. Phys.* **1993**, *97*, 7564.
(325) Schmitz, R. A.; D'Netto, G. A.; Razon, L. F.; Brown, J. R. *Chemical Instabilities*; Nicolis, G., Baras, F., Eds.; Dordrecht, 1984.
(326) Pawlicki, P. C.; Schmidt, R. A. *Chem. Eng. Prog.* **1987**, *83*, 40.
(327) Middya, U.; Sheintuch, M.; Graham, M. D.; Luss, D. *Physica D* **1993**, *63*, 393.
(328) Middya, U.; Luss, D.; Sheintuch, M. *J. Chem. Phys.* **1994**, *100*, 3568.
(329) Zhukov, S. A.; Barelko, V. V. *Dokl. Akad. Nauk SSSR* **1978**, *238*, 135.
(330) Volodin, Yu. E.; Zuyagin, V. N.; Ivanova, A. N.; Barelko, V. V. *Adv. Chem. Phys.* **1990**, *77*, 551.
(331) Vance, W.; Ross, J. *J. Chem. Phys.* **1988**, *88*, 5536.
(332) Leibsle, F. M.; Murray, P. W.; Francis, S. M.; Thorton, G.; Bowker, M. *Nature* **1993**, *363*, 706.
(333) Murray, P. W.; Thornton, G.; Bowker, M.; Dhanak, V. R.; Baraldi, A.; Kiskinova, H. *Phys. Rev. Lett.* **1993**, *71*, 4369.
(334) Evans, J. W. *J. Chem. Phys.* **1992**, *97*, 572.
(335) Bär, M.; Zülicke, C.; Eiswirth, M.; Ertl, G. *J. Chem. Phys.* **1992**, *96*, 8595.
(336) Block, J.-H. Private communication.
(337) Mertens, F.; Gottschalk, N.; Bär, M.; Eiswirth, M.; Mikhailov, A.; Imbihl, R. Manuscript submitted to *Phys. Rev. E*.
(338) Keener, J. P.; Tyson, J. J. *Physica D* **1986**, *21*, 300.
(339) Mikhailov, A. S.; Zykov, V. S. *Physica D* **1991**, *52*, 379.
(340) Bär, M.; Gottschalk, N.; Eiswirth, M.; Ertl, G. *J. Chem. Phys.* **1994**, *100*, 1202.
(341) Bär, M.; Eiswirth, M. *Phys. Rev. E.* **1993**, *48*, R1635.
(342) Bär, M.; Gottschalk, N.; Hildebrandt, M.; Eiswirth, M. Manuscript submitted for publication.
(343) Falcke, M.; Engel, H. *J. Chem. Phys.* **1994**, *101*, 6255; *Phys. Rev. B* **1994**, *50*, 1353.
(344) Imbihl, R.; Veser, G. *J. Vac. Sci. Technol.* **1994**, *A12*, 2170.
(345) Sheintuch, M. *Chem. Eng. Sci.* **1981**, *36*, 893.
(346) Mertens, F.; Imbihl, R.; Mikhailov, A. *J. Chem. Phys.* **1993**, *99*, 8668.
(347) Mertens, F.; Imbihl, R.; Mikhailov, A. S. *J. Chem. Phys.* **1994**, *101*, 9903.
(348) Castets, V.; Dulos, E.; Boissonade, J.; De Kepper, P. *Phys. Rev. Lett.* **1990**, *64*, 2953.
(349) Babloyantz, A.; Sepulchre, J. A. *Physica D* **1991**, *49*, 52.
(350) Enderlein, J. *Phys. Lett.* **1991**, *156A*, 429.
(351) Mornev, O. A.; Engel, H.; Enderlin, J.; Linde, H.; Krinsky, V. I. *Physica D*, in press.
(352) Asakura, K.; Lauterbach, J.; Rotermund, H. H.; Ertl, G. *Phys. Rev.* **1994**, *B50*, 8043.
(353) Lauterbach, J.; Asakura, K.; Rasmussen, P. B.; Rotermund, H. H.; Bär, M.; Graham, M. D.; Kevrekidis, I. G.; Ertl, G. Manuscript submitted to *Catal. Lett.*
(354) Asakura, K.; Lauterbach, J.; Rotermund, H. H.; Ertl, G. Manuscript submitted to *J. Chem. Phys.*
(355) Kapicka, J.; Marek, M. *Surf. Sci.* **1989**, *222*, L885.
(356) Khrustova, N.; Veser, G.; Mikhailov, A.; Imbihl, R. Manuscript submitted to *Phys. Rev. Lett.*
(357) Kuramoto, Y. *Chemical Oscillations, Waves and Turbulence*; Springer: Berlin, 1984.
(358) Coullet, P.; Gil, L.; Lega, J. *Phys. Rev. Lett.* **1989**, *62*, 1619.
(359) Schüth, F.; Song, X.; Schmidt, L. D.; Wicke, E. *J. Chem. Phys.* **1990**, *92*, 745.
(360) Hildebrandt, M.; Bär, M.; Eiswirth, M. Manuscript submitted to *Phys. Rev. Lett.*

CR940045G